Fluorescent Detection of Nucleic Acid Using Intelligent Oligonucleotide Probes toward Intracellular RNA Imaging

生細胞内 RNA イメージングを志向した
機能性核酸プローブを用いる核酸分子蛍光検出法の開発

February 2009

早稲田大学大学院　理工学研究科

応用化学専攻　化学工学研究

Kazuhiro FURUKAWA

古川　和寛

JUDGING COMMITTEE

Referee in chief:
Professor Dr. Satoshi Tsuneda
(Dept. of Life science and medical bio-science, Waseda University)
Referees:
Professor Dr. Kiyotaka Sakai
(Dept. of Chemical Engineering, Waseda University)
Professor Dr. Izumi Hirasawa
(Dept. of Chemical Engineering, Waseda University)
Professor Dr. Oliver Seitz
(Dept. of Chemistry, Humboldt-Universität zu Berlin)

Contents

Chapter 1

General Introduction

Chapter 2

Comprehensive analysis of cell wall permeabilizing conditions for highly sensitive fluorescence in situ hybridization

Chapter 3

Reduction-triggered fluorescence probes for sensing nucleic acids

Chapter 4

Reduction-triggered red fluorescent probes for dual-color detection of oligonucleotide sequences

Chapter 5

Intracellular RNA detection with reduction-triggered fluorescence probe in fixed bacterial cells

Chapter 6

Reduction-triggered fluorescence amplifying probe for detection of RNAs in living human cells

Chapter 1

General Introduction

Chapter 1

General Introduction

1

1.1. Background and objectives

Identification and classification of cells in environmental and clinical samples can be critical for determining both prophylactic and curative responses. In dealing with contamination of food or water supplies by microorganisms, bacterial infections in tissues, and cancer-causing mutations in biopsy samples, a rapid diagnosis may be a life or death issue. Standard detection of cells in clinical or environmental samples requires any of a number of methods including culture, antigen detection, serology, nucleic acid amplification, and other biochemical assays [1, 2]. Despite the widespread use of these detection strategies, many can be time-consuming, difficult, and yield inconclusive results. As a result, a great deal of research in clinical and environmental chemistry focuses on developing rapid and specific methods to identify cells and gain information about cell type and characteristics. One of the most promising techniques for doing this is *in situ* detection of nucleic acids.

Fluorescent-labeled oligonucleotides are becoming important tools for detecting oligonucleotide sequences [3, 4]. A possible application is the detection of RNA species in cells by *in situ* hybridization [5-7]. However, standard fluorescent probes require careful handling to avoid nonspecific signals. Fluorogenic probes with a fluorescence on/off mechanism have been developed to avoid this problem [8-15]. Some of these probes have been applied to the detection of RNA in cells [16-19]. Examples are molecular beacon (MB) [17, 18] or target-assisted chemical ligation [16, 20]. Target-dependent fluorescence enhancement of these methods is based on the resonance

energy transfer (RET) mechanism, for which a pair of quencher and fluorescence dyes is normally used. However, higher sensitivity for the detection method is still required to monitor gene expression in cells. Recently, various fluorogenic compounds have been developed for the detection of small biological substances [21-25]. For example, diaminofluorescein when used for the detection of nitric oxide (NO) reacts with NO to yield a fluorescent compound through triazole formation [23]. The boronate fluorescein derivative for detection of hydrogen peroxide (H_2O_2) reacts with H_2O_2 to yield a fluorescent form through cleavage of the carbon–boron bond [22]. In these examples, detection is triggered by a chemical reaction accompanied by transformation of the chemical structure of the fluorogenic compound. Fluorescence modulation is caused by photoinduced electron transfer or absorption change. The signal/background (S/B) ratio of this type of molecule could exceed that of the RET mechanism [26]. However, there are few reports that describe chemical reaction-triggered fluorogenic molecules for oligonucleotide sensing, although this method offers high sensitivity [27]. Here, we report a reduction-triggered fluorescence (RETF) probe that shows a high S/B ratio for sensing oligonucleotides. A new fluorescence molecule, rhodamine azide and fluorescein methylazide, that we designed and synthesized are activated only by a specific reducing reagent on the oligonucleotide target and is very stable under biological conditions, showing little background fluorescence. The probe was applied to the sensing of nucleic acids in vitro and of endogenous RNA in bacterial and native human cells.

1.2. Oligonucleotide probes for intracellular RNA detection

1.2.1. Oligonucleotide Probes

FISH probes several hundreds or thousands of nucleotides long complementary to nearly the entire 16S or 23S rRNA and containing multiple fluorophore labels have long been used to detect microorganisms in environmental samples because such lengthy probes offer reliable hybridization and intense signal. These probes are prepared enzymatically, typically by PCR [28] or *in vitro* transcription [29, 30], at which time multiple fluorophores are incorporated. Although polynucleotide probes allow the visualization of a significantly higher percentage of prokaryotes in a sample compared to

singly labeled oligonucleotide probes [31], polynucleotide probes are only able to discriminate between distantly related groups, such as *Bacteria, Crenarchaeota*, and *Euryarchaeota* [32], because their sensitivity to small sequence differences is very low. Furthermore, long polynucleotide probes must be produced in the laboratory using cost- and labor-intensive protocols. Typical problems encountered include nonspecific binding of probe [32], high autofluorescence vs specific fluorescence [33], poor signal-to-background [34], low cellular detection compared to total cell count [35], and enzymatic degradation *in situ* [36].

More commonly, RNA-targeted FISH probes employ oligonucleotides 15–30 nucleotides long, with a DNA, PNA, or modified nucleic acid backbone, prepared synthetically (Fig. 1.1.A). Fluorescence is typically observed directly, using a fluorophore attached to the 5′-terminus, though in some cases 3′- or internally labeled probes are used. Common fluorophores used in RNA-targeted FISH diagnostics include fluorescein, tetramethylrhodamine (TAMRA), Texas Red, Cy3, and Cy5. Choice of dye is typically determined by its spectral properties and the availability of equipment for imaging. Labeled oligonucleotides are available from a variety of commercial sources, so it is typically not necessary for investigators to synthesize or purify probes.In some applications, indirect sensing is used instead of directly coupling the fluorophore to the probe. Indirect sensing strategies typically involve coupling an enzyme to the oligonucleotide probe, hybridizing to targets, then adding a fluorophore moiety that is recognized by and covalently binds to the enzyme [37]. These approaches can offer the significant advantage of brighter signals, but they tend to have low specificity [38, 39]. The most well-studied approach employs horseradish peroxidase (HRP)-labeled oligonucleotide probes [40-43]. HRP reacts with hydrogen peroxide and tyramide to produce a free radical on the tyramide, which covalently binds to a nearby tyrosine residue (Fig. 1.1.B) [44, 45]. A number of fluorophore-conjugated tyramides are available, thus allowing fluorescence detection of enzymatically deposited tyramide [45].

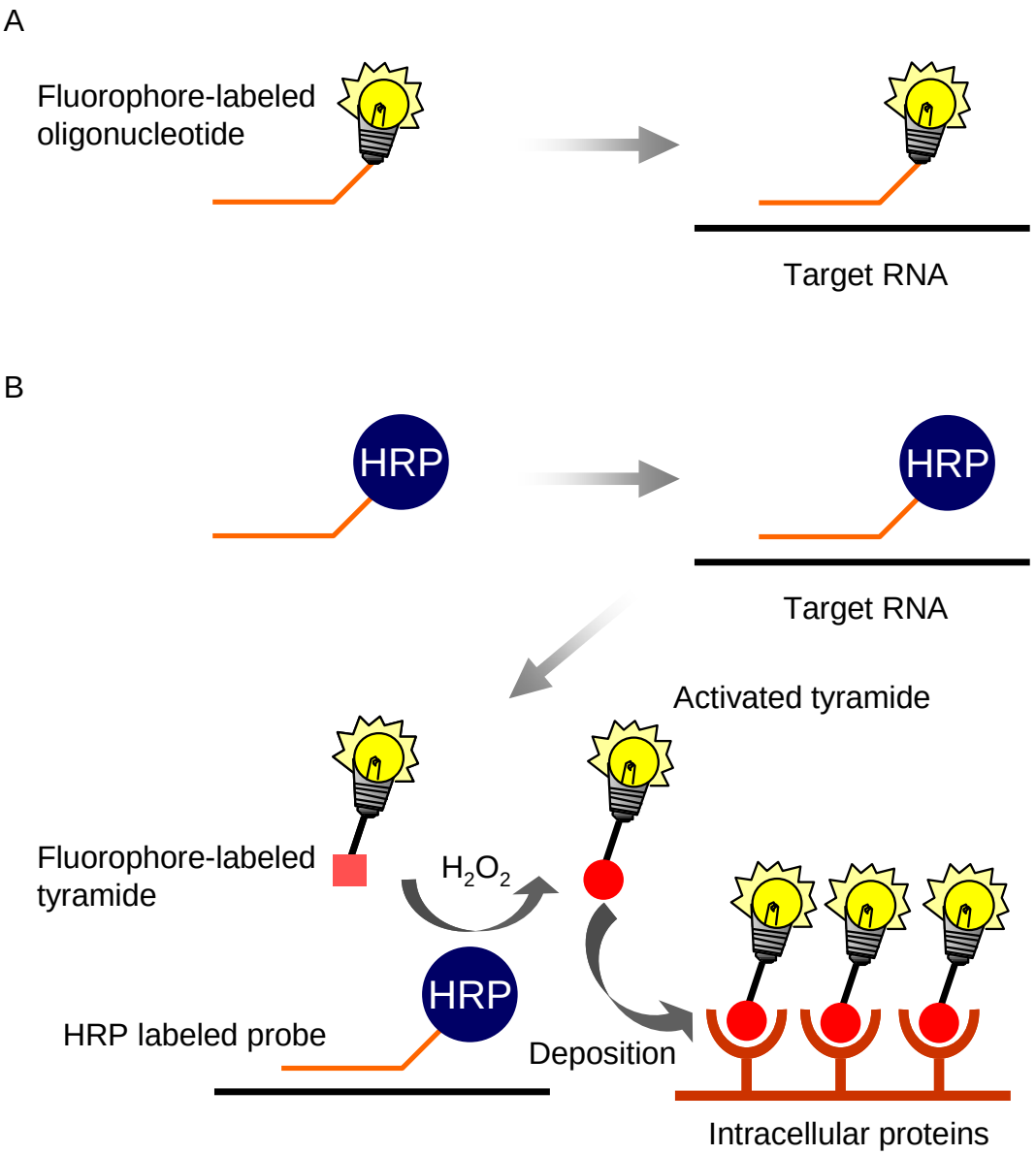

Fig. 1.1 Standard oligonucleotide FISH probes. (A) Standard probe hybridization. (B) Tyramide signal amplification using oligonucleotide FISH probes conjugated to horseradish peroxidase (HRP).

1.2.2. Standard Oligonucleotide FISH Protocols

Standard FISH protocols consist of four steps: (1) fixation and permeabilization of the sample, (2) hybridization of fluorescent probe, (3) washing away unbound probe, and (4) detection of labeled cells by microscopy or flow cytometry [32].

The first issue when setting up an RNA-targeted FISH experiment is getting the probes into the cells. Cells typically must be fixed so that high stringency washing steps may be performed to remove unbound probes. However, it is usually desirable to select fixatives that will disrupt cellular morphology as minimally as possible. The most common fixatives fall into two classes: cross-linking reagents, such as aldehydes, and precipitants such as methanol and ethanol [46]. Cross-linking reagents like formalin and paraformaldehyde are quite commonly used for permeabilization of gram-negative bacteria [47] and human cells [48], but may be ineffective in permeabilizing the cell walls of gram-positive bacteria [49]. Several possibilities exist to permeabilize gram-positive bacteria, and often different procedures are required for different species. Treatment of paraformaldehyde-fixed bacteria with cell wall-lytic enzymes, such as lysozyme or proteinase K, has been shown to increase the cellular permeability of *Lactococci, Enterococci*, and *Streptococci* [50]. Permeabilization by treatment with ethanol/formalin [51], high concentrations of ethanol or methanol [52], or heat [53], also has been successful in many cases.

Hybridization and washing conditions are highly dependent on the probe affinity and T_m and the cell type being examined, and optimal conditions must be determined empirically. Hybridization is performed at a few degrees lower than the probe T_m, typically in the 40–60°C range, in a buffer containing a relatively high salt concentration. For PNA FISH probes, higher hybridization temperatures can be used when the probes have higher T_m's [54]. The advantages to using higher hybridization temperatures are better disruption of target structures and better probe specificity. Washing is carried out in similar temperature ranges, often with the addition of higher concentrations of detergents such as SDS, Triton X, or Tween, or of formamide [32]. More stringent conditions may be required for PNA FISH probes. The washing step is typically difficult to optimize, but the most important in order to minimize false positives from unbound probes.

Insufficiently low signal, on the other hand, can be caused by a number of factors, including low ribosome or mRNA count, poor target accessibility, or impermeability of cells (see above). Low RNA content potentially can be circumvented by using strategies such as tyramide amplification, but this method requires conditions which tend to cause lysis of fixed cells [38, 55]. When target accessibility appears to be an issue, helper probes can be used or a different target site may need to be selected [56]. In some cases, addition of low concentrations of formamide to the hybridization buffer may improve the result, as formamide lowers the T_m of secondary structures (but also lowers the T_m of the probes) [46]. As a result, hybridizations in formamide-containing buffer must be run at lower temperatures.

After washing, cells may be analyzed by fluorescence microscopy or flow cytometry. Microscopy has the advantage of being rapid and simple, but an untrained eye can lead to incorrect reporting of data, and results are usually qualitative. Flow cytometry provides quantitative data on the fluorescence of individual cell populations, but instruments are quite expensive.

The greatest advantages of standard oligonucleotide probes for RNA-targeted diagnostics are that they are commercially available, relatively inexpensive, and well established in the literature for a plethora of applications. However, standard oligonucleotide probes do have several disadvantages. They are typically unable to distinguish related RNA sequences unless there are multiple nucleotide differences [32, 57]. In addition, careful handling is required to avoid nonspecific signals, especially during washing away of unbound probes [58]. The washing step increases the chances of error and nonspecific signal, and prevents application to live cells.

1.2.3. Molecular Beacons

Molecular beacons (MBs) were first developed in 1996 as tools for real-time PCR assays [59, 60]. They have since been developed for multiplex PCR assays [61, 62], solid-phase hybridization assays [63-65], biosensing [66], and FISH applications with both prokaryotic [67] and human cells [68]. Molecular beacons are oligonucleotides, typically with DNA, 2′-OMe RNA, or PNA backbones that have a stem-loop hairpin

conformation in their native state, with a fluorophore and quencher at either end such that the probe is quenched while in the hairpin state [69, 70]. The loop region of the probe, or sometimes the loop and part of the stem [71], is complementary to an RNA target site, and upon binding, the hairpin is disrupted, separating the fluorophore and quencher, enhancing fluorescence signal (Fig. 1.2.A). The quenching efficiencies for several quenchers with many different fluorophores have been examined, allowing for the design of optimal fluorophore–quencher pairs [72].

A careful balance must be reached between the stem length and loop length to design optimal molecular beacons for mismatch discrimination. Solution experiments demonstrated that mismatch discrimination increases as the number of bases in the stem increases [73]. However, if the stem is too long, the kinetics of hybridization to target will be slow [74]. MBs with longer loop lengths tend to have lower hairpin T_m's, and thus increased kinetics of hybridization and decreased specificity, and MBs with very short stem lengths have lower signal-to-background ratios [74]. Design of MBs is substantially simplified by software, typically offered by companies that sell custom MBs.

MBs offer several advantages over standard oligonucleotide probes. Because MBs are quenched, no washing steps are required to remove unbound probe, and they may therefore be applicable to living cells assuming the cells can be permeabilized. Second, MBs have higher mismatch sensitivity than standard oligonucleotide FISH probes as a result of their conformational restraints [73]. The main sources of nonspecific signal in MBs are: (1) incomplete quenching, (2) hairpin–hairpin binding between two beacons, (3) nuclease degradation that separates the quencher and the fluorophore, and (4) nonspecific interactions with proteins and other small molecules within the cell that disrupt the hairpin structure [75]. The last may be the biggest problem in cellular diagnostics, since molecular beacons are known to interact with certain nucleic acid-binding proteins, disrupting the MB secondary structure and giving nonspecific signal [76].

Several new approaches to MBs recently have been developed to improve

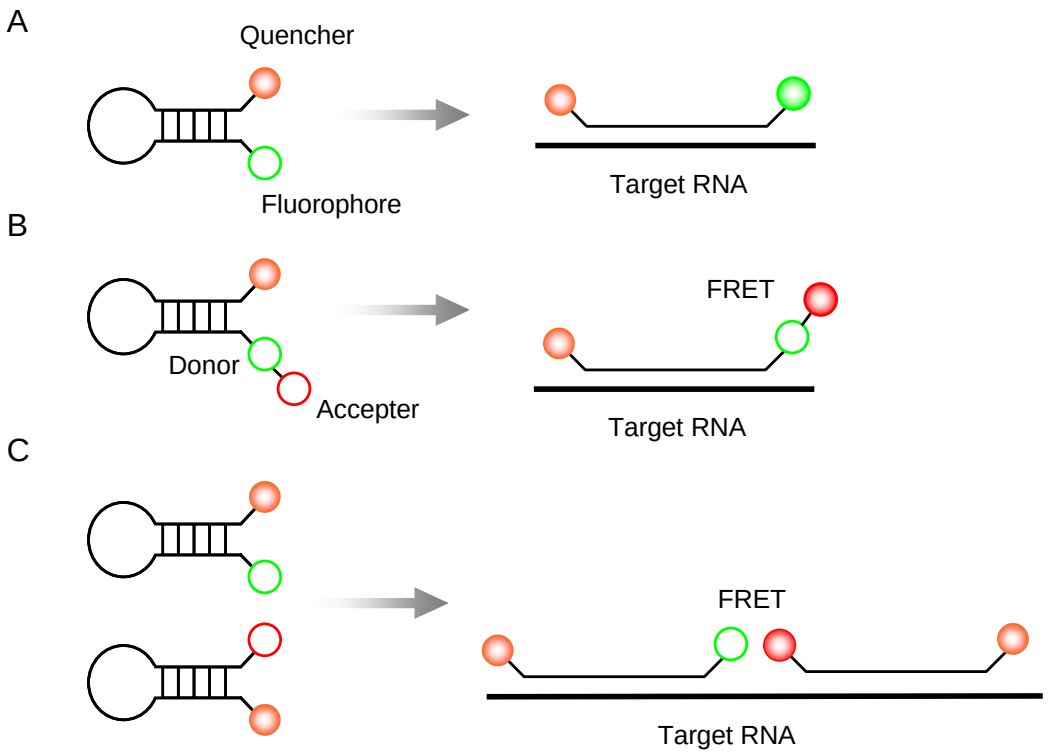

Fig. 1.2 Molecular beacons. (A) Standard MB hybridization. (B) Wavelength-shifting MB. (C) Dual FRET MB.

signal-to-background. Most notably, fluorescence resonance energy transfer (FRET) approaches have the potential to decrease background signal if the spectral overlap between the donor and acceptor is minimal [77]. This approach was first examined with the so-called "wavelength shifting molecular beacons," in which an acceptor fluorophore, such as a rhodamine, was tethered to the fluorescein donor via a linker (Fig. 1.2.B) [78]. Wavelength shifting MBs were found to be useful in multiplex PCR assays, but have not been employed for FISH assays, possibly because the overlap between the donors and acceptors studied is too great to give a substantial signal-to-background advantage. A similar approach uses an acceptor fluorophore instead of a dark quencher, thereby changing the maximum emission wavelength between hairpin and bound states [79]. Going one step further, Bao and coworkers developed "dual FRET MBs," in which two MBs bind side-by-side, with a donor fluorophore on one beacon thereby being brought into proximity with an acceptor fluorophore on the other beacon (Fig. 1.2.C) [80, 81]. Since both donor and acceptor fluorophores are quenched in their native state, and both need to hybridize adjacently in order for FRET to occur, background from nonspecific hairpin opening is substantially reduced.

1.2.4. Quenched Autoligation Probes

Quenched autoligation (QUAL) probes are a relatively new class of *in situ* hybridization probes that were developed for detection of sequences with high specificity [82-84]. Whereas molecular beacons rely on a conformational change to initiate fluorescence signal, QUAL probes utilize a chemical reaction [84]. QUAL probes consist of two oligonucleotide strands, the "dabsyl" probe and the phosphorothioate (thioate) probe (Fig. 1.3). The dabsyl probe is short, typically 7–10 nucleotides, while the thioate probe is longer, around 15–20 nucleotides. The dabsyl probe is modified such that it has a dabsyl group at its 5′-terminus, attached through an electrophilic sulfonate ester linkage, and a fluorescein or other fluorophore internally attached to a uridine base. Dabsyl is a dark quencher that efficiently quenches fluorescein, so the background fluorescence of the dabsyl probe is very low [85]. The thioate probe is modified such that it has a phosphorothioate group at its 3′-terminus. The two probes are

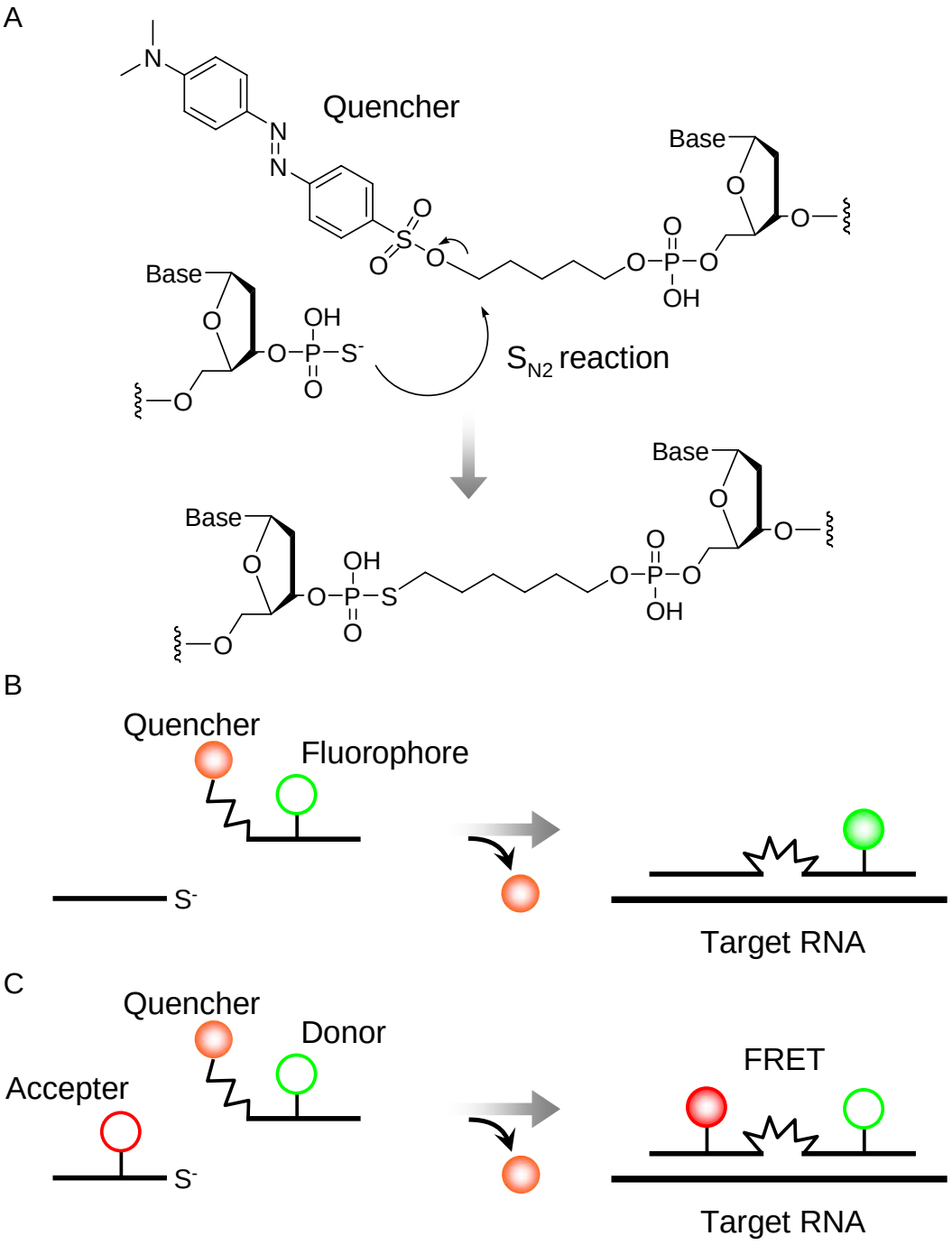

Fig. 1.3 QUAL Probes. (A) Ligation chemistry. (B) QUAL probe hybridization and reaction. (C) FRET–QUAL probes.

designed such that they bind adjacently on their target, bringing the nucleophilic 3′-phosphorothioate close to the electrophilic 5′-dabsyl group. The phosphorothioate reacts to displace the dabsyl group, thereby ligating the two strands and unquenching the fluorophore (Fig. 1.3.A and B). It should be noted that both the 3′-terminal phosphorothioate in the nucleophilic probe and the bridging phosphorothioate linkage formed in the ligation product are quite stable to nucleases and hydrolysis [86]. The 5′-dabsyl group, however, is subject to slow hydrolysis in buffer, particularly in basic conditions or at high temperatures [87].

QUAL probes take advantage of the ability of very short oligonucleotides to sense single nucleotide mismatches while avoiding issues of redundancy and lack of affinity. The highest specificity is achieved when the mismatch is placed in the center of the short probe; substantially less discrimination is observed when the mismatch is at the end of the short probe or in the long probe [82]. Thus, specificity of QUAL probes is determined mostly by binding affinity as opposed to geometry of the reaction site, as mismatches in the center of short probe lead to the greatest T_m difference for binding to a matched vs mismatched target [82, 83]. Naturally, probing for sites with multiple mismatches will increase the specificity of QUAL probes.

When very short probes are used, there is a high probability for sequence redundancy. This issue is made moot in QUAL probes by requiring the two probes that bind adjacently. Thus, even if the short probe represents a sequence that has redundancy in the target RNA, no fluorescence is observed unless the longer probe binds adjacent to it. The lack of affinity of very short probes is dealt with by running the hybridization at relatively low temperatures (37°C or lower) and selecting sequences that have a T_m high enough to hybridize under the desired conditions. Since unbound probes are not fluorescent, no washing steps are required, and ligated fluorescent products are typically 20-mers or longer, which have high affinity for their target.

It should be noted, however, that it is not actually necessary that probes remain bound after ligation occurs in QUAL probes, as ligation permanently switches on fluorescent signal. In fact, if ligated probes dissociate from their target and new probes bind and ligate on the same template, signal amplification may occur [88]. Signal amplification by

turnover is highly desirable for the detection of extremely low abundance targets such as mRNAs. A strategy of using “universal linkers” to attach the quencher to the 5′-terminus of the dabsyl probe yielded turnovers of nearly 100-fold on RNA templates in solution [88], and was used to detect mRNAs in human cells [89]. The product of the ligation reaction using the universal linker is destabilized compared to natural DNA, apparently because the alkane linker adds flexibility to the strand. This decreases product inhibition so that the target RNA can become a catalyst for generating multiple signals per target. Furthermore, the linker has been shown to destabilize the product without destabilizing the transition state of the reaction; in fact, the reaction rate is sped up by a factor of 4–5 [88].

In solution and solid-phase assays, QUAL probes were shown to accurately discriminate between all possible mismatches [84, 87]. QUAL probes offer several advantages over other RNA-targeted diagnostics strategies. Like MBs, unbound probes do not need to be washed out of cells, which reduces experimental time and decreases chances for error. QUAL probes may be less prone to nonspecific signals than MBs because turning on fluorescence requires a chemical reaction; thus, binding to proteins should not lead to nonspecific signals.

Disadvantages of QUAL probes include the slow hydrolysis of quencher leading to nonspecific fluorescence, the requirement that multiple probes be used, and the limited number of systems that they have been applied to thus far. The main sources of nonspecific signal in QUAL probes are: (1) incomplete quenching, (2) nuclease degradation in the 1–3 nucleotides between the fluorophore and quencher, and (3) hydrolysis of the quencher [75]. The last of these appears to be the greatest problem, requiring careful handling and storage of the probe.

Abe and Kool recently described a method to improve signal-to-background by using FRET–QUAL probes (Fig. 1.3.C) [89]. In these specialized QUAL probes, Cy5 was attached internally to the thioate probe. The ligation was monitored by excitation at 488 nm, which gives almost no excitation for Cy5. When the probes ligated, FRET between fluorescein and Cy5 allowed emission to be monitored at 665 nm, beyond the emission wavelength for fluorescein. Thus, background from incomplete quenching or nonspecific

hydrolysis of the quencher was minimized, leading to substantially higher sensitivity.

QUAL probes are not yet commercially available, so they have not yet been adopted wide use in diagnostic settings.

1.3. Fluorogenic molecule for bioimaging

Compared to other technologies, such as radioisotope labeling, MRI, ESR, and electrochemical detection, fluorescence imaging has many advantages, as it enables highly sensitive, non-invasive, and safe detection using readily available instruments. Another advantage of fluorescence imaging we should emphasize here is that the fluorescence signal of a molecule can be drastically modulated, so that sensors relying on 'activation', not just accumulation, can be utilized. Until the 1980s, however, fluorescence imaging was mainly applied to fixed samples owing to the lack of fluorescent chemosensors, or probes, suitable for imaging in living cells. In this review, 'fluorescent probes' are defined as molecules that react specifically with biological molecules to induce a concomitant change of their photochemical properties (fluorescence intensity, excitation/emission wavelength, and so forth). In the past two decades, following pioneering work by Tsien and co-workers on Ca^{2+} probes [90], there has been an explosive increase in the number of fluorescent probes developed [91, 92]. Today, several design strategies for fluorescent probes, including photoinduced electron transfer (PeT) [91, 93], fluorescence resonance energy transfer (FRET) [94], intramolecular charge transfer (ICT) [91 and 93], and spirocyclization [95], are well established and have been applied to many probes. Recent examples, developed in Nagano laboratory (University of Tokyo), are shown in Figure 1.4 [95-98].

In the 1990s, probes based on fluorescent proteins utilizing the FRET mechanism [94, 99] emerged with great success. More recently, probes based on nanoparticles [100, 101] and conjugated polymers [102] have been introduced, and some of them have already been applied to *in vivo* imaging [100]. Although we appreciate the significance of these relatively new scaffolds for fluorescent probes, the scope of this review is limited to recent advances of small-molecular probes in two selected categories owing to limitations of space. For more comprehensive information, readers should consult earlier

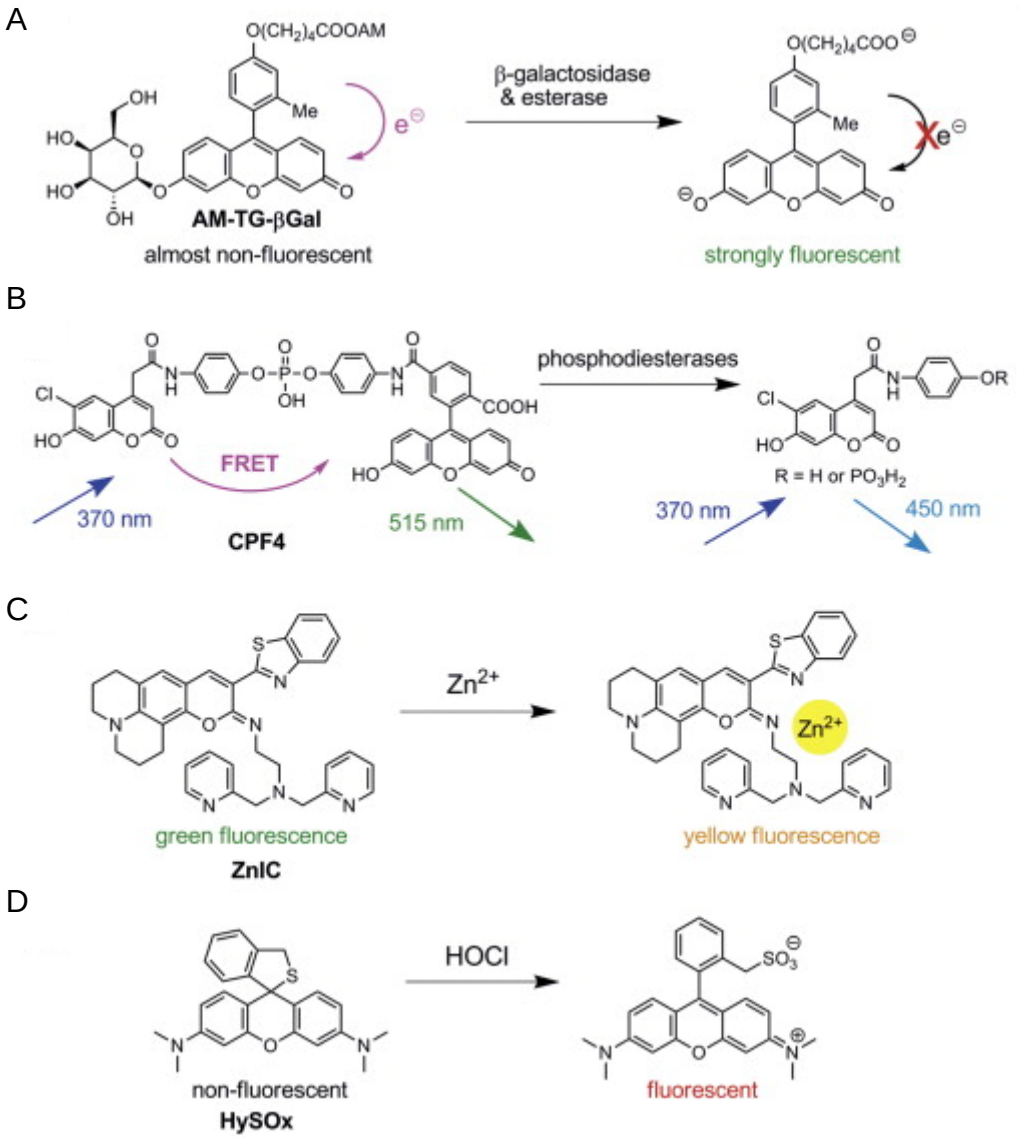

Fig. 1.4 Rational design of fluorescent probes. (A) AM-TG- βGal, a β-galactosidase probe designed to utilize a PeT mechanism [96]. (B) CPF4, a ratiometric phosphodiesterase sensor based on a FRET mechanism [98]. (C) ZnIC, a ratiometric Zn^{2+} sensor utilizing ICT [97]. (D) HySOx, a probe for hypochlorous acid, designed to utilize a spirocyclization strategy [95].

reviews [91, 92, 103] or monographs [104, 105]. In addition, probes for other analytes, including reactive oxygen species (ROS) [106], reactive nitrogen species (RNS) [107], anions [108], and saccharides [109], have recently been reviewed elsewhere, as have probes with near-infrared emission [110].

1.3.1. Fluorescent probes for metal ions

Ever since the advent of fluorescent probes, metal ions have been one of the most fruitful targets. The chemical structures of probes for metal ions can generally be divided into two moieties: chelator and fluorophore. The chelator moiety binds to the metals with a certain dissociation constant (K_d) and induces a change of the spectroscopic properties of the fluorophore. To obtain a large spectroscopic response, the structure of this moiety must be carefully selected, because the K_d value should lie between the concentrations of the monitored ion before and after the stimulus. It should be also noted that intracellular K_d is often different from the value *in vitro* [104]. Up to now, selective chelators for various metal ions, such as BAPTA for Ca^{2+}, TPEN for Zn^{2+}, and APTRA for Mg^{2+} (Fig. 1.5.A), have been developed and incorporated into fluorescent probes. The fluorophore is the moiety that determines the wavelengths of excitation and emission, as well as the mode of spectral change (turn on/off or ratiometric). For cell imaging, fluorophores excited by visible light (fluorescein, rhodamine, BODIPY, etc.) are desirable owing to their brightness and low phototoxicity, but those requiring UV excitation (benzofuran, etc.) are still used because they are suitable for ratiometric measurements. Ratiometric sensors, which exhibit spectral shift upon reaction or binding to the target, have advantages over turn-on/off sensors, because the results of ratiometric measurements are independent of dye concentration, bleaching, and illumination intensity [90].

Although dozens of probes have already been developed for the detection of Ca^{2+} [104, 111], Zn^{2+} [112], and others, improvements are still ongoing. For example, Bradley and co-workers immobilized a Ca^{2+} probe, Indo-1, on polystyrene beads to develop a cell-permeable microsphere-based sensor (Fig. 1.5.B), and succeeded in real-time calcium sensing in living cells [113]. At present, most of the probes for cations must be loaded into cells in the form of their acetoxymethyl (AM) ester [103], which is

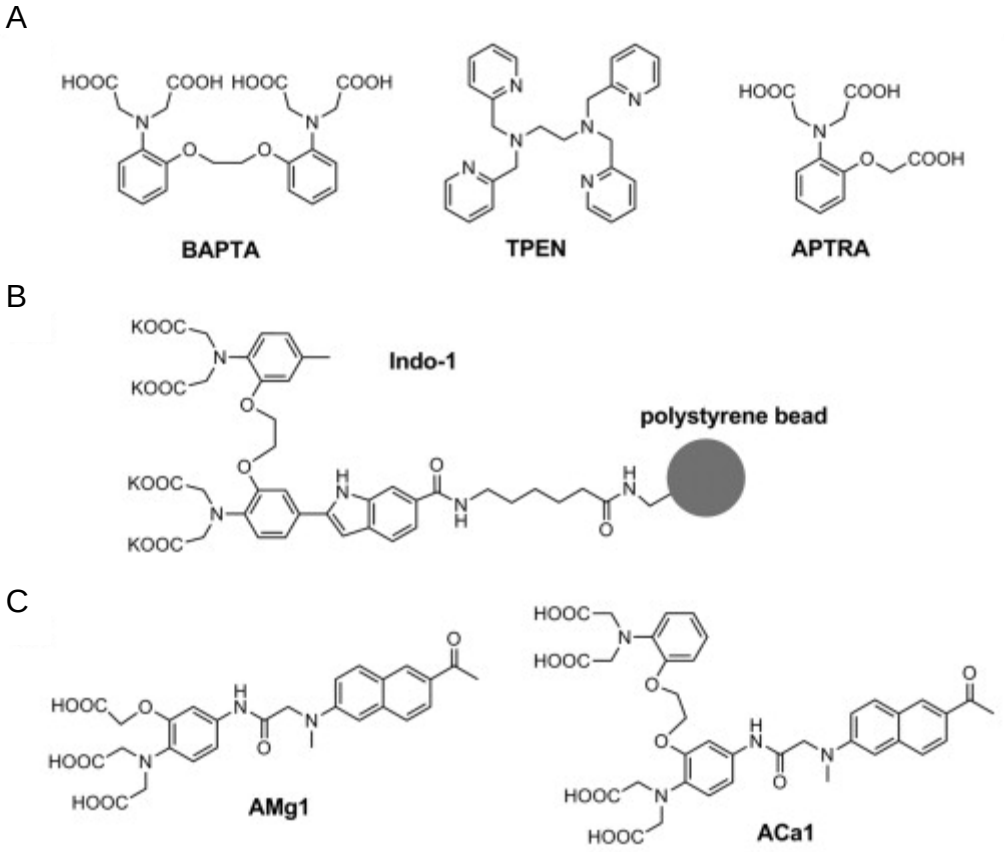

Fig. 1.5 Chemical structures of cation chelators and probes. (A) Selective chelators for metal ions, BAPTA (for Ca^{2+}), TPEN (for Zn^{2+}), and APTRA (for Mg^{2+}). (B) A microsphere-based sensor for Ca^{2+} [113]. (C) Two-photon fluorescent probes for Mg^{2+} and Ca^{2+}, AMg1 [115] and ACa1 [116], respectively. (C)

subsequently hydrolyzed by intracellular esterases, because the probes themselves often contain free acid moieties that impede cell-permeability. This AM strategy has proved to be powerful and versatile, but it has some disadvantages, such as incomplete hydrolysis, compartmentalization, and leakage over time [113]. The microsphere-based probe developed by Bradley *et al*. is cell-permeable in the form of acid salts, and reports calcium concentration at the surface of the beads. While further studies are necessary concerning the mechanism of cellular uptake and the control of intracellular localization of the microspheres, the combination of nano/micro-materials and organic fluorescent sensors is a promising approach.

These days, growing attention is focused on two-photon microscopy (TPM) [114], which allows non-invasive imaging deep (up to 1 mm) within tissues, with high resolution. Although existing one-photon probes can be used for TPM, high laser power is often required to obtain clear images owing to the small two-photon action cross section (Φδ). To address this problem, Cho and co-workers developed two fluorescent probes, AMg1 [115] and ACa1 [116] (Fig. 1.5.C), which are specific to Mg^{2+} and Ca^{2+}, respectively. Both probes contain 2-acetyl-6-(dimethylamino)naphthalene, which was shown previously by the authors to be an efficient polarity-sensitive two-photon fluorophore [117]. One-photon fluorescence of AMg1 and ACa1 exhibited a dramatic (>10 fold) increase upon addition of Mg^{2+} and Ca^{2+}, respectively, presumably as a result of the blocking of PeT upon metal complexation. Two-photon excitation at 780 nm gave similar results, and notably, the probes had Φδ values over 100 GM, more than five fold greater than those of commercial probes (Mag-fura-2 and Oregon Green 488 BAPTA-1) [104]. Interestingly, when the probes were applied to cultured cells via the AM strategy, bright spots with blue-shifted emission were detected in the cells. On the basis of the solvent-dependency of the fluorophore, the authors attributed the spots to membrane-associated organelles, in which uncleaved AM esters accumulated. Hence, the blue-shifted emission was cut off to acquire the ‘true’ signal from the free and metal-bound probes localized in the cytosol. This simple manipulation allowed the precise distributions of the analytes inside the cells to be imaged. To demonstrate the utility of AMg-1, acute hippocampal slices from mice were incubated with the probe. The

TPM images clearly revealed the Mg^{2+} distribution in the pyramidal neuron layer of the CA1 region. ACa-1 was similarly applied to rat hypothalamic slices and spontaneous Ca^{2+} waves were clearly visualized by TPM. The results, taken together, validate the applicability of these probes for two-photon imaging of the analytes in living tissue.

Other recently developed metal ion probes include visible [97] or near-infrared [118] ratiometric fluorescent probes for Zn^{2+} reported by our group, and selective turn-on probes for Cu^{+} [119] and Hg^{2+} [120] developed in Chang's laboratory.

1.3.2. Fluorescent probes for proteolytic enzyme

Proteolytic enzymes, or proteases, are enzymes that catalyze hydrolysis of peptide bonds. They are said to occupy approximately 2% of the whole human genome, and are involved not only in many physiological events, but also in major diseases such as cancer, neurodegeneration, inflammation, and others [121]. Although several analytical methods have been established to investigate the biology of proteases [122], assays using fluorogenic substrates [123] are advantageous as they report not the mere expression, but rather the activity of the target enzymes. Another benefit of these substrate-based probes is that the signal is amplified by the catalytic enzyme reaction. Conventional fluorophores, however, are not optimal for applications using biological samples that have high levels of background signal (serum, urine, etc.). Lanthanide complexes with extraordinarily long-lived luminescence [124, 125] are expected to be advantageous for these applications, because the short-lived background fluorescence can be eliminated by time-resolved luminescence measurements. Recently, we have developed a novel long-lived protease probe by designing a method to modulate the PeT process within a lanthanide complex, and applied it to the diagnosis of cancer [126].

Another approach to elucidate the activities of specific enzymes in complex systems, termed activity-based protein profiling (ABPP), is currently attracting attention [127, 128]. In ABPP, samples are treated with small molecules known as activity-based probes (ABPs), which bind covalently to the active site of the target enzymes, and this is followed by analysis (imaging, SDS-PAGE, etc.) or purification of the target using tags (fluorescent molecules, biotin, etc.) attached to the ABPs. Compared with substrate-based

fluorescent probes, fluorescent ABPs have the advantage that they can provide direct biochemical evidence concerning the enzyme(s) responsible for the signal. Furthermore, the spatial distribution of the target can be precisely visualized with fluorescent ABPs. These features should be particularly advantageous in complicated systems containing various enzymes, such as living tissues. Hydrolytic enzymes, including proteases, are the most common targets of ABPP, which have been used in proteomic profiling of metalloproteases [129] and for the investigation of cysteine protease activity during tumor formation [130].

Although conventional ABPs are powerful tools with diverse applications, they are not suitable for live-cell or *in vivo* imaging owing to the lack of a fluorescence on/off switch. In other words, they are not 'fluorescence probes' in terms of the definition in this review, and extensive washout is necessary before images can be acquired. To overcome this limitation, Bogyo and co-workers developed 'quenched' probes (qABPs), which become fluorescent only after binding to the target [131]. The first qABP they developed (GB117) incorporated an acyloxymethyl ketone (AOMK) reactive moiety that targets cysteine proteases, together with BODIPY-TMR-X as a fluorophore, and QSY 7 as a quencher (Fig. 1.6.A). Before binding covalently to the enzyme, fluorescence of BODIPY-TMR-X was efficiently quenched (>70 fold) presumably via energy transfer to the quencher. When the probe binds to the active site of the enzyme, the quencher moiety is released from the probe, resulting in recovery of fluorescence. After confirming that qABP could successfully label cathepsins *in vitro*, the authors applied it to living cells. While non-specific staining of entire cells was observed with the unquenched ABP, a discrete labeling pattern that matched the distribution of lysosomes was obtained using GB117, without the need for a washing procedure. This result indicates that qABPs can provide a good signal-to-noise ratio, allowing direct imaging of protease activity in living cells. Interestingly, in an experiment using cell culture models, the probe and anti-cathepsin antibody gave different labeling patterns, illustrating the activity-directed nature of ABPs.

Recently, an improved version of GB117, termed GB137, was reported by the same group [132]. GB137, with Cy 5 as a fluorophore, has excitation/emission in the NIR

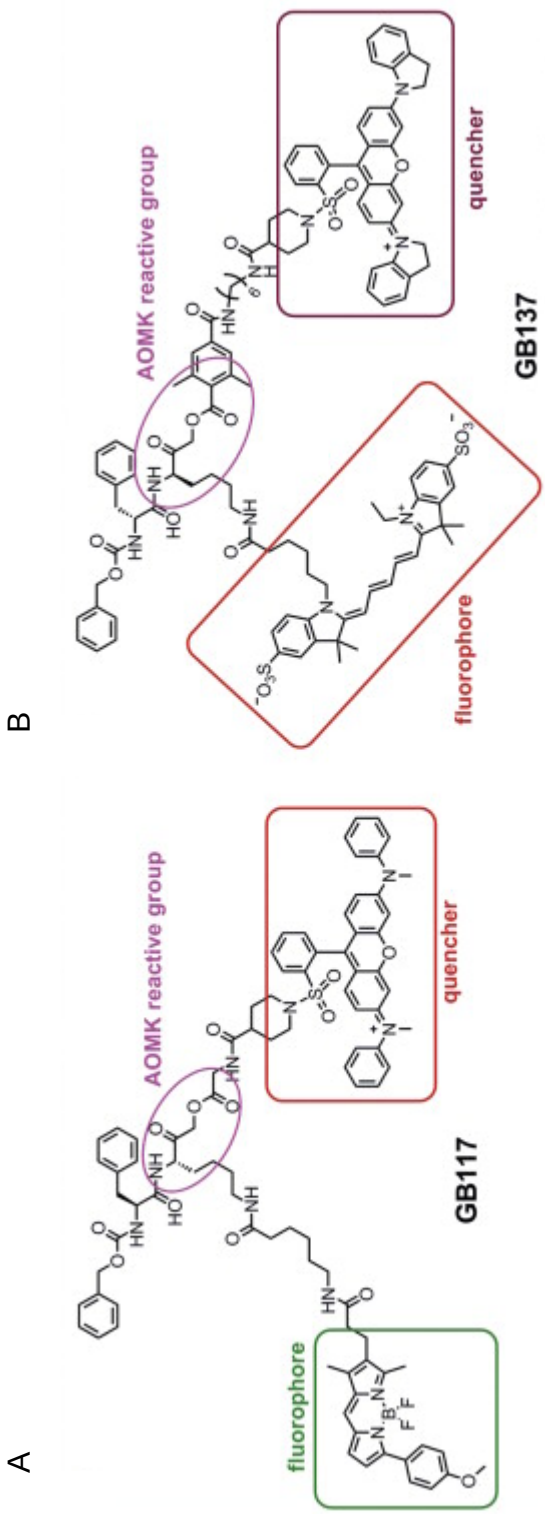

Fig. 1.6 Chemical structures of qABPs developed by Bogyo and co-workers. (A)GB117 [131]; (B) GB137 [].

region, which is favorable for *in vivo* imaging (Fig. 1.6.B). GB137 was found to specifically label active cathepsins in a number of cancer cell lines, while it is insensitive to serum. After confirming *in vivo* that the probe with the AOMK 'warhead' was retained in cancer cells by covalently binding to cathepsins, the authors compared GB137 with the non-quenched counterpart (GB123). The non-quenched probe stained the whole body until unlabeled probe was completely eliminated from the animal. GB137, however, produced a specific and stable signal in tumors from the earliest time point, demonstrating the clear advantage of qABPs. The signal was reduced in mice treated with a cysteine protease inhibitor, K11777, suggesting the potential utility of the probe for the assessment of therapeutic agents that inhibit proteases.

One possible disadvantage of ABPs over substrate-based approaches is the lack of signal amplification by the target enzymes. Although clear images with sufficient signal-to-noise ratios were acquired in the above cases, it remains yet to be seen whether this strategy is applicable to targets with lower expression levels. Another concern for activity-based imaging is that the inhibition of the target by ABPs might lead to undesirable and non-physiological biological responses. Furthermore, it is no less difficult to find specific activity-based inhibitors for the target enzyme, which are necessary to design ABPs, than to find substrates, which are required to develop substrate-based probes. Considering these points, it seems likely that ABPs and traditional probes will play complementary roles in the field of biological imaging.

References

1. Gracias, K. S. and McKillip, J. L. (2004) A review of conventional detection and enumeration methods for pathogenic bacteria in food. *Can. J. Microbiol. 50*, 883-890.
2. Lipski, A., Friedrich, U. and Altendorf, K. (2001) Application of rRNA-targeted oligonucleotide probes in biotechnology. *Appl. Environ. Microbiol. 56*, 40-57.
3. DeLong, E. F., Wickham, G. S., and Pace, N. R. (1989) Phylogenetic stains: ribosomal RNA-based probes for the identification of single cells. *Science 243*, 1360-1363.
4. Levsky, J. M., and Singer, R. H. (2003) Fluorescence in situ hybridization: past, present and future. *J. Cell Sci. 116*, 2833-2838.
5. Amann, R., Fuchs, B. M., and Behrens, S. (2001) The identification of microorganisms by fluorescence in situ hybridisation. *Curr. Opin. Biotechnol. 12*, 231-236.
6. Moter, A., and Gobel, U. B. (2000) Fluorescence in situ hybridization (FISH) for direct visualization of microorganisms. *J. Microbiol. Methods 41*, 85-112.
7. Levsky, J. M., Shenoy, S. M., Pezo, R. C., and Singer, R. H. (2002) Single-cell gene expression profiling. *Science 297*, 836-840.
8. Tyagi, S., and Kramer, F. R. (1996) Molecular beacons: probes that fluoresce upon hybridization.

Nature Biotechnol. 14, 303-308.
9. Sando, S., and Kool, E. T. (2002) Quencher as leaving group: efficient detection of DNA-joining reactions. *J. Am. Chem. Soc. 124*, 2096-2097.
10. Okamoto, A., Tanaka, K., Fukuta, T., and Saito, I. (2003) Design of base-discriminating fluorescent nucleoside and its application to t/c SNP typing. *J. Am. Chem. Soc. 125*, 9296-9297.
11. Babendure, J. R., Adams, S. R., and Tsien, R. Y. (2003) Aptamers switch on fluorescence of triphenylmethane dyes. *J. Am. Chem. Soc. 125*, 14716-14717.
12. Kolpashchikov, D. M. (2006) A binary DNA probe for highly specific nucleic Acid recognition. *J. Am. Chem. Soc. 128*, 10625-10628.
13. Ha, T., Enderle, T., Ogletree, D. F., Chemla, D. S., Selvin, P. R., and Weiss, S. (1996) Probing the interaction between two single molecules: Fluorescence resonance energy transfer between a single donor and a single acceptor. *Proc. Nat. Acad. Sci. USA 93*, 6264-6268.
14. Piatek, A. S., Tyagi, S., Pol, A. C., Telenti, A., Miller, L. P., Kramer, F. R., and Alland, D. (1998) Molecular beacon sequence analysis for detecting drug resistance in Mycobacterium tuberculosis. *Nature Biotechnol. 16*, 359-363.
15. Sando, S., and Kool, E. T. (2002) Imaging of RNA in bacteria with self-ligating quenched probes. *J. Am. Chem. Soc. 124*, 9686-9687.
16. Abe, H., and Kool, E. T. (2006) Flow cytometric detection of specific RNAs in native human cells with quenched autoligating FRET probes. *Proc. Nat. Acad. Sci. USA 103*, 263-268.
17. Sokol, D. L., Zhang, X., Lu, P., and Gewirtz, A. M. (1998) Real time detection of DNA.RNA hybridization in living cells. *Proc. Nat. Acad. Sci. USA 95*, 11538-11543.
18. Bratu, D. P., Cha, B.-j., Mhlanga, M. M., Kramer, F. R., and Tyagi, S. (2003) Visualizing the distribution and transport of mRNAs in living cells. *Proc. Nat. Acad. Sci. USA 100*, 13308-13313.
19. Tsuji, A., Koshimoto, H., Sato, Y., Hirano, M., Sei-Iida, Y., Kondo, S., and Ishibashi, K. (2000) Direct observation of specific messenger RNA in a single living cell under a fluorescence microscope. *Biophys. J. 78*, 3260-3274.
20. Sando, S., Abe, H., and Kool, E. T. (2004) Quenched auto-ligating DNAs: multicolor identification of nucleic acids at single nucleotide resolution. *J. Am. Chem. Soc. 126*, 1081-1087.
21. Maeda, H., Fukuyasu, Y., Yoshida, S., Fukuda, M., Saeki, K., Matsuno, H., Yamauchi, Y., Yoshida, K., Hirata, K., and Miyamoto, K. (2004) Fluorescent probes for hydrogen peroxide based on a non-oxidative mechanism. *Angew. Chem. Int. Ed. Engl. 43*, 2389-2391.
22. Miller, E. W., Tulyathan, O., Isacoff, E. Y., and Chang, C. J. (2007) Molecular imaging of hydrogen peroxide produced for cell signaling. *Nat. Chem. Biol. 3*, 263-267.
23. Kojima, H., Nakatsubo, N., Kikuchi, K., Kawahara, S., Kirino, Y., Nagoshi, H., Hirata, Y., and Nagano, T. (1998) Detection and imaging of nitric oxide with novel fluorescent indicators: Diaminofluoresceins. *Anal. Chem. 70*, 2446-2453.
24. Dale, T. J., and Rebek, J., Jr. (2006) Fluorescent Sensors for Organophosphorus Nerve Agent Mimics. *J. Am. Chem. Soc. 128*, 4500-4501.
25. Lemieux, G. A., de Graffenried, C. L., and Bertozzi, C. R. (2003) A fluorogenic dye activated by the Staudinger ligation. *J. Am. Chem. Soc. 125*, 4708-4709.
26. Marras, S. A., Kramer, F. R., and Tyagi, S. (2002) Efficiencies of fluorescence resonance energy transfer and contact-mediated quenching in oligonucleotide probes. *Nucleic Acids Res. 30*, e122.
27. Cai, J., Li, X., Yue, X., and Taylor, J. S. (2004) Nucleic acid-triggered fluorescent probe activation by the Staudinger reaction. *J. Am. Chem. Soc. 126*, 16324-16325.
28. Zimmermann, J., Ludwig, W., Schleifer, K. H. (2001) DNA polynucleotide probes generated from representatives of the genus Acinetobacter and their application in fluorescence in situ hybridization of environmental samples. *Syst. Appl. Microbiol. 24*, 238–244.
29. DeLong, E. F., Taylor, L. T., Marsh, T. L., Preston, C. M. (1999) Visualization and enumeration of marine planktonic archaea and bacteria by using polyribonucleotide probes and fluorescence in situ hybridization. *Appl. Environ. Microbiol. 65*, 5554–5563.
30. Trebesius, K. H., Amann, R., Ludwig, W., Muhlegger, K., Schleifer, K. H. (1994) Identification of whole fixed bacterial cells with nonradioactive rRNA-targeted transcript probes. *Appl. Environ. Microbiol. 60*, 3228–3235.
31. Pernthaler, A., Preston, C. M., Pernthaler, J., DeLong, E. F., Amann, R. (2002) Comparison of fluorescently labeled oligonucleotide and polynucleotide probes for the detection of pelagic marine bacteria and archaea. *Appl. Environ. Microbiol. 68*, 661–667.
32. Amann, R., Fuchs, B., Behrens, S. (2001) The identification of microorganisms by fluorescence in situ hybridization. *Curr. Opin. Biotechnol. 12*, 231–236.

33. DeLong, E. F., Taylor, L. T., Marsh, T. L., Preston, C. M. (1999) Visualization and enumeration of marine planktonic archaea and bacteria by using polyribonucleotide probes and fluorescent in situ hybridization. *Appl. Environ. Microbiol. 65*, 5554–5563.
34. Alfreider, A., Pernthaler, J., Amann, R., Sattler, B., Glockner, F., Wille, A. (1996) Community analysis of the bacterial assemblages in the winter cover and pelagic layers of a high mountain lake by in situ hybridization. *Appl. Environ. Microbiol. 62*, 2138–2144.
35. Kemp, P. F., Lee, S., LaRoche, J. (1993) Estimating the growth rate of slowly growing marine bacteria from RNA content. *Appl. Environ. Microbiol. 59*, 2594–2601.
36. Wagner, M., Horn, M., Daims, H. (2003) Fluorescent in situ hybridization for the identification and characterization of prokaryotes. *Curr. Opin. Microbiol. 6*, 302–309.
37. Speel, E. J. M, Ramaekers, F. C. S, Hopman, A. H. N. (1997) Sensitive multicolor fluorescence in situ hybridization using caralyzed reporter deposition (CARD) amplification. *J. Histochem. Cytochem. 45*, 1439–1446.
38. Schonhuber, W., Fuchs, B. M., Juretschko, S., Amann, R. (1997) Improved sensitivity of whole-cell hybridization by the combination of horseradish peroxidase-labeled oligonucleotides and tyramide signal amplification. *Appl. Environ. Microbiol. 63*, 3268–3273.
39. Amann, R. I., Zarda, B., Stahl, D. A., Schleifer, K. H. (1992) Identification of individual prokaryotic cells with enzyme-labeled, rRNA-targeted oligonucleotide probes. *Appl. Environ. Microbiol. 58*, 3007–3011.
40. van de Corput, M. P. C., Dirks, R. W., van Gijlswijk, R. P. M., van de Rijke, F. M., Raap, A. K. (1998) Fluorescence in situ hybridization using horseradish peroxidase-labeled oligodeoxynucleotides and tyramide signal amplification for sensitive DNA and mRMA detection. *Histochem. Cell Biol. 110*, 431–437.
41. Schweickert, B., Moter, A., Lefmann, M., Gobel, U. B. (2004) Let them fly or light them up: Matrixassisted laser desorption/ionization time of flight (MALDI-TOF) mass spectrometry and fluorescence in situ hybridization (FISH). *APMIS 112*, 856–885.
42. Jupraputtasri, W., Cheevadhanarak, S., Chaiprasert, P., Tanticharoen, M., Techkarnjanaruk, S. (2004) Use of fluorochrome-labeled rRNA targeted oligonucleotide probe and tyramide signal amplification to improve sensitivity of fluorescence in situ hybridization. *J. Biosci. Bioeng. 98*, 282–286.
43. Pernthaler, A., Amann, R. (2004) Simultaneous fluorescence in situ hybridization of mRNA and rRNA in environmental bacteria. *Appl. Environ. Microbiol. 70*, 5526–5533.
44. van Gijlswijk, R. P. M., van de Corput, M. P. C., Bezrookove, V., Wiegant, J., Tanke, H. J., Raap, A. K. (2000) Synthesis and purification of horseradish peroxidase-labeled oligonucleotides for tyramide-based fluorescence in situ hybridization. *Histochem. Cell Biol. 113*, 175–180.
45. van Gijlswijk, R. P. M., Zijlmans, H. J. M. A. A., Wiegant, J., Bobrow, M. N., Erickson, T. J., Adler, K. E., (1997) Fluorochrome-labeled tyramides: Use in immunocytochemistry and fluorescence in situ hybridization. *J. Histochem. Cytochem. 45*, 375–382.
46. Amann, R. I., Ludwig, W., Schleifer, K. H. (1995) Phylogenetic identification and in situ detection of individual microbial cells without cultivation. *Microbiol. Rev. 59*, 143–169.
47. Amann, R., Krumholz, L., Stahl, D. A. (1990) Fluorescent-oligonucleotide probing of whole cells for determinative, phylogenetic, and environmental studies in microbiology. *J. Bacteriol. 172*, 762–770.
48. Hoetelmans, R. W. M., van Slooten, H. J., Keijzer, R., van de Velde, C. J., Hvan Dierendonck, J. H. (2001) Routine formaldehyde fixation irreversibly reduces immunoreactivity of Bcl-2 in the nuclear compartment of breast cancer cells, but not in the cytoplasm. *Appl. Immunohistochem. Mol. Morphol. 9*, 74–80.
49. Hahn, D., Amann, R. I., Ludwig, W., Akkernans, A. D. L., Schleifer, K. H. (1992) Detection of microorganisms in soil after in situ hybridization with rRNA-targeted, fluorescently labeled oligonucleotides. *J. Gen. Microbiol. 138*, 870–887.
50. Beimfohr, C., Krause, A., Amann, R., Ludwig, W., Schleifer, K. H. (1993) In situ identification of lactococci, enterococci and streptococci. *Syst. Appl. Microbiol. 16*, 450–456.
51. Braun-Howland, E. B., Danielsen, S. A., Nierzwicki-Bauer, S. A. (1992) Development of a rapid method for detecting bacterial cells in situ using 16S rRNA-targeted probes. *BioTechniques 13*, 928–933.
52. Roller, C., Wagner, M., Amann, R., Ludwig, W., Schleifer, K. H. (1994) In situ probing of grampositive bacteria with high DNA G t C content using 23S rRNA-targeted oligonucleotides. *Microbiology 51*, 2849–2858.
53. Jurtshuk, R. J., Blick, M., Bresser, J., Fox, G. E., Jurtshuk, P. (1992) Rapid in situ hybridization technique using 16S rRNA segments for detecting and diVerentiating the closely related gram-positive

organisms Bacillus polymyxa and Bacillus macerans. *Appl. Environ. Microbiol. 58*, 2571–2578.
54. Egholm, M., Buchardt, O., Christensen, L., Behrens, C., Freier, S. M., Driver, D. A. (1993) PNA hybridizes to complementary oligonucleotides obeying the Watson-Crick hydrogenbonding rules. *Nature 365*, 566–568.
55. Pernthaler, A., Pernthaler, J., Amann, R. (2002) Fluorescence in situ hybridization and catalyzed reported deposition for the identification of marine bacteria. *Appl. Environ. Microbiol. 68*, 3094–3101.
56. Fuchs, B. M., Glockner, F. O., Wulf, J., Amann, R. (2000) Unlabeled helper oligonucleotides increase the in situ accessibility to 16S rRNA of fluorescently labeled oligonucleotide probes. *Appl. Environ. Microbiol. 66*, 3603–3607.
57. Manz, W. (1999) In situ analysis of microbial biofilms by rRNA-targeted oligonucleotide probing. *Methods Enzymol. 310*, 79–91.
58. Moter, A., Gobel, U. B. (2000) Fluorescence in situ hybridization (FISH) for direct visualization of microorganisms. *J. Microbiol. Methods 41*, 85–112.
59. Tyagi, S., Kramer, F.R. (1996) Molecular beacons: Probes that fluoresce upon hybridization. *Nat. Biotechnol. 14*, 303–308.
60. Tyagi, S., Bratu, D.P., Kramer, F. R. (1998) Multicolor molecular beacons for allele discrimination. *Nat. Biotechnol. 16*, 49–53.
61. Marras, S. A. E., Kramer, F. R, Tyagi, S. (1999) Multiplex detection of single-nucleotide variations using molecular beacons. *Genet. Anal. 14*, 151–156.
62. Vet, J. A. M., Majithia, A. R, Marras, S. A. E., Tyagi, S., Dube, S., Poiesz, B. J. (1999) Multiplex detection of four pathogenic retroviruses using molecular beacons. *Proc. Natl. Acad. Sci. USA 96*, 6394–6399.
63. Horejsh, D., Martini, F., Poccia, F., Ippolito, G., Di Caro, A., Capobianchi, M. R. (2005) A molecular beacon, bead-based assay for the detection of nucleic acids by flow cytometry. *Nucleic Acids Res. 33*, e13.
64. Yao, G., Tan, W. H. (2004) Molecular-beacon-based array for sensitive DNA analysis. *Anal. Biochem. 331*, 216–223.
65. Yao, G., Fang, X. H., Yokota, H., Yanagida, T., Tan, W. H. (2003) Monitoring molecular beacon DNA probe hybridization at the single-molecule level. *Chem. Eur. J. 9*, 5686–5692.
66. Fang, X. H., Mi, Y. M., Li, J. W. J., Beck, T., Schuster, S., Tan, W. H. (2002) Molecular beacons: Fluorogenic probes for living cell study. *Cell Biochem. Biophys. 37*, 71–81.
67. Xi, C. W., Balberg, M., Boppart, S. A., Raskin, L. (2003) Use of DNA and peptide nucleic acid molecular beacons for detection and quantification of rRNA in solution and in whole cells. *Appl. Environ. Microbiol. 69*, 5673–5678.
68. Tan, W. H., Wang, K. M., Drake, T. J. (2004) Molecular beacons. *Curr. Opin. Chem. Biol. 8*, 547–553.
69. Tsourkas, A., Behlke, M. A., Bao, G. (2002) Hybridization of 2'O-methyl and 2'deoxy molecular beacons to RNA and DNA targets. *Nucleic Acids Res. 30*, 5168–5174.
70. Kuhn, H., Demidov, V. V., Coull, J. M., Fiandaca, M. J., Gildea, B. D., Frank-Kamenetskii, M. D. (2002) Hybridization of DNA and PNA molecular beacons to single-stranded and doublestranded DNA targets. *J. Am. Chem. Soc. 124*, 1097–1103.
71. Tsourkas, A., Behlke, M. A., Bao, G. (2002) Structure-function relationships of shared-stem and conventional molecular beacons. *Nucleic Acids Res. 30*, 4208–4215.
72. Marras, S. A. E., Kramer, F. R, Tyagi, S. (2002) Efficiencies of fluorescence resonance energy transfer and contact-mediated quenching in oligonucleotide probes. *Nucleic Acids Res. 30*, e122.
73. Bonnet, G., Tyagi, S., Libchaber, A., Kramer, F. R. (1999) Thermodynamic basis of the enhanced specificity of structured DNA probes. *Proc. Natl. Acad. Sci. USA 96*, 6171–6176.
74. Tsourkas, A., Behlke, M. A., Rose, S. D., Bao, G. (2003) Hybridization kinetics and thermodynamics of molecular beacons. *Nucleic Acids Res. 31*, 1319–1330.
75. Silverman, A. P., Kool, E. T. (2005) Quenched probes for highly specific detection of cellular RNAs. *Trends Biotechnol. 23*, 225–230.
76. Molenaar, C., Marras, S. A., Slats, J. C. M., TruVert, J. C., Lemaitre, M., Raap, A. K. (2001) Linear 2'O-methyl RNA probes for the visualization of RNA in living cells. *Nucleic Acids Res*. 29, e89.
77. Valeur, B. (2002) Resonance energy transfer and its applications. In: Molecular Fluorescence: Principles and Applications. Weinheim: Wiley-VCH, 247–272.
78. Tyagi, S., Marras, S. A. E., Kramer, F. R. (2000) Wavelength-shifting molecular beacons. *Nat. Biotechnol. 18*, 1191–1196.
79. Zhang, P., Beck, T., Tan, W. H. (2001) Design of a molecular beacon DNA probe with two fluorophores. *Angew. Chem. Int. Ed. Engl. 40*, 402–405.

80. Santangelo, P. J., Nix, B., Tsourkas, A., Bao, G. (2004) Dual FRET molecular beacons for mRNA detection in living cells. *Nucleic Acids Res. 32*, e57.
81. Bao, G., Tsourkas, A., Santangelo, P. (2003) Dual FRET molecular beacons for gene detection in living cells. *Abstracts of Papers of the American Chemical Society 225*, U982.
82. Xu, Y., Kool, E. T. (1999) High sequence fidelity in a non-enzymatic DNA autoligation reaction. *Nucleic Acids Res. 27*, 875–881.
83. Xu, Y. Z., Karalkar, N. B., Kool, E. T. (2001) Nonenzymatic autoligation in direct three-color detection of RNA and DNA point mutations. *Nat. Biotechnol. 19*, 148–152.
84. Sando, S., Kool, E. T. (2002) Quencher as leaving group: Effcient detection of DNA-joining reactions. *J. Am. Chem. Soc. 124*, 2096–2097.
85. Marras, S. A. E., Kramer, F. R., Tyagi, S. (2002) Efficiencies of fluorescence resonance energy transfer and contact-mediated quenching in oligonucleotide probes. *Nucleic Acids Res. 30*, e122.
86. Xu, Y. Z., Kool, E. T. (1998) Chemical and enzymatic properties of bridging 5' -S-phosphorothioester linkages in DNA. *Nucleic Acids Res. 26*, 3159–3164.
87. Sando, S., Abe, H., Kool, E. T. (2004) Quenched auto-ligating DNAs: Multicolor identification of nucleic acids at single nucleotide resolution. *J. Am. Chem. Soc. 126*, 1081–1087.
88. Abe, H., Kool, E. T. (2004) Destabilizing universal linkers for signal amplification in self-ligating probes for RNA. *J. Am. Chem. Soc. 126*, 13980–13986.
89. Abe, H., Kool, E. T. (2006) Flow cytometric detection of specific RNAs in native human cells with quenched autoligating FRET probes. *Proc. Natl. Acad. Sci. USA 103*, 263–268.
90. Grynkiewicz, G., Poenie, M., Tsien, R. Y. (1985) A new generation of Ca2+ indicators with greatly improved fluorescence properties. *J. Biol. Chem. 260*, 3440-3450.
91. deSilva, A. P., Gunaratne, H. Q. N., Gunnlaugsson, T., Huxley, A. J. M., McCoy, C. P., Rademacher, J. T., Rice, T. E. (1997) Signaling recognition events with fluorescent sensors and switches. *Chem. Rev. 97*, 1515-1566.
92. Callan, J. F., de Silva, A. P., Magri, D. C. (2005) Luminescent sensors and switches in the early 21st century. *Tetrahedron 61*, 8551-8588.
93. Valeur, B., Leray, I. (2000) Design principles of fluorescent molecular sensors for cation recognition. *Chem. Rev. 205*, 3-40.
94. Miyawaki, A. (2003) Visualization of the spatial and temporal dynamics of intracellular signaling. *Dev. Cell 4*, 295-305.
95. Kenmoku, S., Urano, Y., Kojima, H., Nagano, T. (2007) Development of a highly specific, rhodamine-based fluorescence probe for hypochlorous acid and its application to real-time imaging of phagocytosis. *J. Am. Chem. Soc., 129*, 7313-7318.
96. Kamiya, M., Kobayashi, H., Hama, Y., Koyama, Y., Bernardo, M., Nagano, T., Choyke, P. L., Urano, Y. (2007) An enzymatically activated fluorescence probe for targeted tumor imaging. *J. Am. Chem. Soc. 129*, 3918-3929.
97. Komatsu, K., Urano, Y., Kojima, H., Nagano, T. (2007) Development of an iminocoumarin-based zinc sensor suitable for ratiometric fluorescence imaging of neuronal zinc. *J. Am. Chem. Soc. 129*, 13447-13454.
98. Takakusa, H., Kikuchi, K., Urano, Y., Sakamoto, S., Yamaguchi, K., Nagano, T. (2002) Design and synthesis of an enzyme-cleavable sensor molecule for phosphodiesterase activity based on fluorescence resonance energy transfer. *J. Am. Chem. Soc. 124*, 1653-1657.
99. Piston, D. W., Kremers, G. J. (2007) Fluorescent protein FRET: the good, the bad and the ugly. *Trends Biochem. Sci. 32*, 407-414.
100. Jamieson, T., Bakhshi, R., Petrova, D., Pocock, R., Imani, M., Seifalian, A. M. (2007) Biological applications of quantum dots. *Biomaterials 28*, 4717-4732.
101. Wang, X., Ruedas-Rama, M. J., Hall, E. A. H. (2007) The emerging use of quantum dots in analysis. *Anal. Lett. 40*, 1497-1520.
102. Herland, A., Inganas, O. (2007) Conjugated polymers as optical probes for protein interactions and protein conformations. *Macromol. Rapid Commun. 28*, 1703-1713.
103. Johnson, I. (1998) Fluorescent probes for living cells. *Histochem. J. 30*, 123-140.
104. Haugland, R. P. (2005) The Handbook—A Guide to Fluorescent Probes and Labeling Technologies, 10th ed. Invitrogen Corp.
105. Lakowicz, J. R. (2006) Principles of Fluorescence Spectroscopy, edn 3 Springer.
106. Soh, N. (2006) Recent advances in fluorescent probes for the detection of reactive oxygen species. *Anal. Bioanal. Chem. 386*, 532-543.
107. Gomes, A., Fernandes, E., Lima, J. L. F. C. (2006) Use of fluorescence probes for detection of reactive

nitrogen species: a review. *J. Fluorescence 16*, 119-139.
108. O'Neil, E. J., Smith, B. D. (2006) Anion recognition using dimetallic coordination complexes. *Chem. Rev. 250*, 3068-3080.
109. Cao, H., Heagy, M. D. (2004) Fluorescent chemosensors for carbohydrates: a decade's worth of bright spies for saccharides in review. *J. Fluorescence 14*, 569-584.
110. Kiyose, K., Kojima, H., Nagano, T. (2008) Functional near-infrared fluorescent probes. *Chem. Asian J. 3*, 506-515.
111. Takahashi, A., Camacho, P., Lechleiter, J. D., Herman, B. (1999) Measurement of intracellular calcium. *Physiol. Rev. 79*, 1089-1125.
112. Kikuchi, K., Komatsu, K., Nagano, T. (2004) Zinc sensing for cellular application. *Curr. Opin. Chem. Biol. 8*, 182-191.
113. Sanchez-Martın, R. M., Cuttle, M., Mittoo, S., Bradley, M. (2006) Microspherebased real-time calcium sensing. *Angew. Chem. Int. Ed. 45*, 5472-5474.
114. Helmchen, F., Denk, W. (2005) Deep tissue two-photon microscopy. *Nat. Methods 2*, 932-940.
115. Kim, H. M., Jung, C., Kim, B. R., Jung, S, Y., Hong, J. H., Ko, Y. G., Lee, K. J., Cho, B. R. (2007) Environment-sensitive two-photon probe for intracellular free magnesium ion in live tissue. *Angew. Chem. Int. Ed. 46*, 3460-3463.
116. Kim, H. M., Kim, B. R., Hong, J. H., Park, J. S., Lee, K. J., Cho, B. R. (2007) A twophoton fluorescent probe for calcium waves in living tissue. *Angew. Chem. Int. Ed. 46*, 7445-7448.
117. Kim, H. M., Choo, H. J., Jung, S. Y., Ko, Y. G., Park, W. H., Jeon, S. J., Kim, C. H., Joo, T., Cho, B. R. (2007) A two-photon fluorescent probe for lipid raft imaging: C-laurdan. *ChemBioChem 8*, 553-559.
118. Kiyose, K., Kojima, H., Urano, Y., Nagano, T. (2006) Development of a ratiometric fluorescent zinc ion probe in near-infrared region, based on tricarbocyanine chromophore. *J. Am. Chem. Soc. 128*, 6548-6549.
119. Zeng, L., Miller, E. W., Pralle, A., Isacoff, E. Y., Chang, C. J. (2006) A selective turn-on fluorescent sensor for imaging copper in living cells. *J. Am. Chem. Soc. 128*, 10-11.
120. Yoon, S., Miller, E. W., He, Q., Do, P. H., Chang, C. J. (2007) A bright and specific fluorescent sensor for mercury in water, cells, and tissue. *Angew. Chem. Int. Ed. 46*, 6658-6661.
121. Turk, B. (2006) Targeting proteases: successes, failures and future prospects. *Nat. Rev. Drug Discov. 5*, 785-799.
122. Lopez-Otın, C., Overall, C. M. (2002) Protease degradomics: a new challenge for proteomics. *Nat. Rev. Mol. Cell Biol. 3*, 509-519.
123. Goddard, J. P., Reymond, J. L. (2004) Enzyme assays for highthroughput screening. *Curr. Opin. Biotechnol. 15*, 314-322.
124. Pandya, S., Yu, J., Parker, D. (2006) Engineering emissive europium and terbium complexes for molecular imaging and sensing. *Dalton Trans*. 2757-2766.
125. Bunzli, J. C. G., Piguet, C. (2005) Taking advantage of luminescent lanthanide ions. *Chem. Soc. Rev. 34*, 1048-1077.
126. Terai, T., Kikuchi, K., Iwasawa, S., Kawabe, T., Hirata, Y., Urano, Y., Nagano, T. (2006) Modulation of luminescence intensity of lanthanide complexes by photoinduced electron transfer and its application to a long-lived protease probe. *J. Am. Chem. Soc. 128*, 6938-6946.
127. Evans, M. J., Cravatt, B. F. (2006) Mechanism-based profiling of enzyme families. *Chem. Rev. 106*, 3279-3301.
128. Sadaghiani, A. M., Verhelst, S. H. L., Bogyo, M. (2007) Tagging and detection strategies for activity-based proteomics. *Curr. Opin. Chem. Biol., 11*, 20-28.
129. Sieber, S. A., Niessen, S., Hoover, H. S., Cravatt, B. F. (2006) Proteomic profiling of metalloprotease activities with cocktails of activesite probes. *Nat. Chem. Biol. 2*, 274-281.
130. Joyce, J. A., Baruch, A., Chehade, K., Meyer-Morse, N., Giraudo, E., Tsai, F. Y., Greenbaum, D. C., Hager, J. H., Bogyo, M., Hanahan, D. (2004) Cathepsin cysteine proteases are effectors of invasive growth and angiogenesis during multistage tumorigenesis. *Cancer Cell 5*, 443-453.
131. Blum, G., Mullins, S. R., Keren, K., Fonovic, M., Jedeszko, C., Rice, M., Sloane, B. F., Bogyo, M. (2005) Dynamic imaging of protease activity with fluorescently quenched activity-based probes. *Nat. Chem. Biol. 1*, 203-209.
132. Blum, G., von Degenfeld, G., Merchant, M. J., Blau, H. M., Bogyo, M. (2007) Noninvasive optical imaging of cysteine protease activity using fluorescently quenched activity-based probes. *Nat. Chem. Biol. 3*, 668-677.

Chapter 2

Comprehensive Analysis of Cell Wall Permeabilizing Conditions for Highly Sensitive Fluorescence In Situ Hybridization

Chapter 2

Comprehensive analysis of cell wall permeabilizing conditions for highly sensitive fluorescence in situ hybridization

2

2.1. Introduction

One of the long-standing goals of environmental microbiology is to simultaneously ascertain the identity, activity, and biogeochemical impact of individual organisms in situ. Fluorescence in situ hybridization (FISH) with a rRNA-targeted oligonucleotide probe is a powerful tool to analyze the structure and dynamics of complex microbial communities in a cultivation-independent way [4, 9, 25]. However, this method relies on the presence of many target sequences within an individual cell. Therefore, this taxonomic identification approach cannot be used to detect the presence of single-copy functional genes or their mRNA expression products at the single-cell level. For the detection of bacteria based on a specific metabolic activity, the development of highly sensitive methods is essential.

To detect bacterial strains on the basis of their activities, several techniques have been developed, such as catalyzed reporter deposition (CARD)-FISH [5, 12, 16, 17, 20, 21, 24], digoxigenin (DIG)-FISH [26], in situ loop-mediated isothermal amplification (LAMP) [15], in situ PCR [10, 11, 23], in situ reverse transcription [8], and recognition of individual genes (RING)-FISH [27]. However, these signal amplification methods require the diffusion of large-molecular-weight molecules such as enzymes, antibodies, or (strept)avidin into fixed whole cells. Therefore, the cell walls must be permeabilized

for probe access to the target molecule, while minimizing the loss of the target molecule and cell morphology. Many such digestion strategies have been employed to permeabilize fixed cells using enzymes such as lysozyme, proteinase K, and/or achromopeptidase [10, 21]. However, this step remains problematic in that each cell wall type requires different digestion conditions to achieve optimal results [20]. This is especially pronounced in Gram-positive bacteria because of their thick cell walls [19-21]. Generally, identical functional genes are possessed by many bacterial strains with different types of cell wall. For example, nitrite reductase genes (*nirK* and *nirS*) have been widely found in the bacterial strains belonging to almost all major physiological groups [7]. Therefore, the ability to estimate the differences in digestion conditions required for various cell wall types and to define the optimal digestion conditions for certain bacterial strains is of considerable significance. However, there are no reports on comprehensive analyses of permeabilization conditions for highly sensitive FISH.

The purpose of the present study is to define the optimal digestion conditions for several bacterial strains belonging to different phylogenetic divisions by permeabilization at different concentrations of lysozyme and/or achromopeptidase solution for conventional FISH, DIG–FISH, and CARD–FISH. In this study, rRNA was targeted instead of mRNA because it enables us to evaluate pretreatment conditions for detecting each cell types that rRNA can be easily detected by FISH. Consequently, the optimal conditions for the detection of the majority of bacterial strains were determined. Furthermore, the problems associated with previously developed signal amplification methods are discussed.

2.2. Materials and Methods

2.2.1. Bacterial strains, cultivation, and cell fixation

The bacterial strains used in this study and their phylogenetic affiliations are listed in Table 2.1. To estimate the permeabilizing conditions for various types of cell walls, the bacterial strains were selected from various phylogenetic groups. The media and cultivation conditions were determined in accordance with the respective catalogs of the bacterial strains. The cells were harvested at the end of their logarithmic growth phase.

Table 2.1 List of strains and their phylogenetic affiliations

Strains	Source or strain no.	Phylogenetic affiliation
Paracoccus denitrificans	IFO 16712	Alpha subclass of *Proteobacteria*
Alcaligenes faecalis	IFO 13111	Beta subclass of *Proteobacteria*
Pseudomonas stutzeri	IFO 14165	Gamma subclass of *Proteobacteria*
Cytophaga hutchinsonii	IFO 15051	*Bacteroidetes*
Flavobacterium columnare	NBRC 100251	*Bacteroidetes*
Enterococcus faecalis	IFO 3971	Gram-positive bacteria with low G+C content of DNA
Bacillus subtilis	NBRC 13719	Gram-positive bacteria with low G+C content of DNA
Corynebacterium glutamicum	NBRC 12153	Gram-positive bacteria with high G+C content of DNA

Samples were fixed in 3% paraformaldehyde for 9 h at 4°C, centrifuged, and washed three times with PBS solution (137 mM NaCl, 8.10 mM $Na_2HPO_4 \cdot 12H_2O$, 2.68 mM KCl, 1.47 mM KH_2PO_4; pH 7.4). Cells were then resuspended in 50% ethanol in PBS and stored at –20°C until further processing.

2.2.2. Permeabilization

Cell walls were permeabilized according to the method described previously [10] with minor modifications. The samples were resuspended in PBS solution. A 10-µl aliquot was spotted onto amino alkylsilane-coated slides (Applied Biosystems, Foster City, CA) and dried in an oven at 46°C. The fixed samples were treated with a lysozyme solution (0, 1, 3, 7, 10, and 20 mg of lysozyme per ml, 100 mM Tris-HCl [pH 8.0], and 50 mM EDTA) for 1 h at 37°C. As a further analysis, *A. faecalis*, *F. columnare*, and *C. glutamicum* were additionally permeabilized with an achromopeptidase solution (0, 25, 50, 100, and 500 units of achromopeptidase per ml, 10 mM Tris-HCl [pH 8.0], and 10 mM EDTA) for 30 min at 37°C after the lysozyme pretreatment (20 mg of lysozyme per ml), as appropriate. For CARD-FISH, the digested samples were incubated in 0.01 M HCl for 10 min at room temperature to inactive endogenous peroxidases. Then, the HCl solution was removed by consecutive washes with distilled deionized water (ddH_2O) and the samples were dehydrated sequentially in 50, 80, and 98% ethanol.

2.2.3. In situ hybridization with oligonucleotide probes

The oligonucleotide probe EUB338 [3] was used in this study. DIG- and tetramethylrhodamine isothiocyanate (TRITC)-labeled oligonucleotides were purchased from Takara Bio (Ohtsu, Japan) and horseradish peroxidase (HRP)-labeled probes were purchased from Greiner Japan (Tokyo, Japan). TRITC- and DIG-labeled probes were hybridized according to the method of Amann [2], which was followed by a stringently washing. HRP-labeled probes were hybridized at 35°C for 2 h to prevent the inactivation of HRP. Then, the slides were washed at 37°C for 20 min and were kept moist until the following step.

2.2.4. Signal detection with tetramethylrhodamine-labeled antidigoxigenin antibody

Samples hybridized with DIG-labeled probes were detected using a tetramethylrhodamine-labeled antidigoxigenin Fab fragment (Roche Diagnostics, Mannheim, Germany). First, 10 µl of blocking buffer (5 mg of bovine serum albumin per ml of PBS solution) was spotted onto the samples and incubated for 30 min at room temperature. Then, 10 µl of tetramethylrhodamine-labeled anti-DIG Fab fragment solution (10 µg of Fab fragment per ml of blocking buffer) was spotted onto the samples and incubated for 1 h at 37°C. Next, the slides were rinsed briefly with a few milliliters of a washing buffer (0.5% Triton X-100 in PBS solution) and then immersed three times in 40 ml of the washing buffer for 15 min at room temperature. The washing buffer was removed by rinsing the slides with ddH_2O. Then, the samples were counterstained with a working solution of SYBR Green I (FMC BioProducts, Rockland, ME) for 5 min. For preparation of the working solution, SYBR Green I was diluted with PBS solution 10,000-fold. After washing, the samples were mounted in FluoroGuard antifade reagent (Bio-Rad, Richmond, CA) for observation under a confocal laser scanning microscope (TCS4D; Leica Lasertchnik, Heidelberg, Germany).

2.2.5. Tyramide signal amplification

The stringently washed slides were rinsed briefly with ddH_2O and equilibrated with TNT buffer (0.1 M Tris-HCl [pH 7.5], 0.15 M NaCl, 0.3% Triton X-100) for 15 min. Excess buffer was removed without drying the slides. Tetramethylrhodamine-labeled tyramide stock solution was diluted 1:50 with amplification diluent to produce the fluorophore tyramide working solution (Dupont, NEN Research Products, Boston, MA). The samples were incubated in tetramethylrhodamine-tyramide working solution. After 10 min at room temperature, the slides were rinsed briefly with a few milliliters of TNT buffer and then immersed three times in 40 ml of the same buffer for 5 min at room temperature. TNT buffer was removed by rinsing the slides with ddH_2O. Then, the samples were counterstained with SYBR Green I, mounted in FluoroGuard antifade reagent for observation under the confocal laser scanning microscope.

2.2.6. Microscopic evaluation and data analysis

After FISH, DIG-FISH, or CARD-FISH, images were recorded using the confocal laser scanning microscope equipped with an Ar-Kr ion laser (488, 568, and 647 nm), and identical scanning parameters were applied for each strain. Parameter settings were such that the brightest cell signals observed did not cause saturation (pixel grey values <255), while low signal intensities were still detectable. To standardize the signal intensities, images of fluorescein isothiocyanate (FITC)-labeled particles (SPHERO™ FITC Particles; Spherotech Inc., Libertyville, IL) were recorded using identical conditions for each strain. The following image analysis was performed using NIH image software. At first, all color information in an image was turned into gray scale values of corresponding intensities. Then, all of the SYBR Green I-stained cells in a microscopic field (between 100 and 300 cells) were counted for each sample. In the same microscopic field, the signal intensities of the cells at an excitation wavelength of 568 nm, visualized using FISH, DIG-FISH, or CARD-FISH, were measured. The measured signal intensities were divided by the signal intensity obtained from FITC-labeled particles; consequently, relative signal intensities were obtained for each sample. FITC-labeled particles generated a weak signal at an excitation wavelength of 568 nm; therefore, a threshold value was determined for the signal intensity of particles (relative signal intensity value = 1.0). The cells with relative signal intensity values above 1.0 were counted, and then, the percentages of positive cell fractions were obtained.

2.3. Results

2.3.1. Differences in detectable conditions using lysozyme pretreatment

The fractions of hybridized cells, which were labeled by FISH, DIG-FISH, and CARD-FISH following incubation with lysozyme at concentrations between 0 and 20 mg/ml, were evaluated (Fig. 2.1).

The tested representatives of the alpha, beta, and gamma subclasses of *Proteobacteria* showed the same pattern, with the exception of *P. denitrificans* (Fig. 2.1A to C). Conventional FISH did not yield sufficient signals with cultures of *P. denitrificans* unless

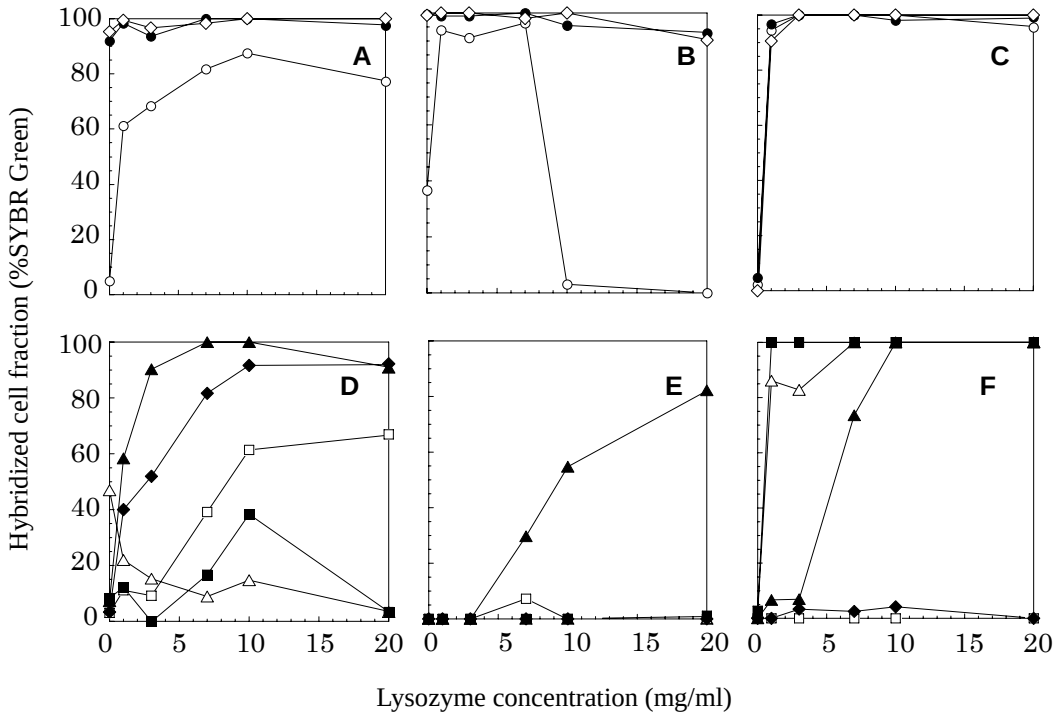

Fig. 2.1 Comparison of detection rates of each strain using FISH (A and D), DIG-FISH (B and E), and CARD-FISH (C and F). Panels A to C: detection rates of *Proteobacteria*. Symbols: open circles, *P. denitrificans*; closed circles, *A. faecalis*; open diamonds, *P. stutzeri*. Panels D to F: detection rates of *Bacteroidetes* and Gram-positive bacteria. Symbols: open triangles, *C. huchinsonii*; open squares, *F. columnare*; closed triangles, *E. faecalis*; closed squares, *B. subtilis*; closed diamonds, *C. glutamicum*.

the lysozyme pretreatment was carried out (Fig. 2.1.A). In contrast, *A. faecalis* and *P. stutzeri* showed homogeneous signals without lysozyme pretreatment. In the case of DIG-FISH, more than 96% of the total cells were detected for each strain with lysozyme pretreatment at 7 mg/ml, and the hybridized cell fraction of only *P. denitrificans* dramatically decreased at lysozyme concentrations higher than 7 mg/ml (Fig. 2.1.B). Following CARD-FISH without lysozyme pretreatment, only a few cells for each strain were visualized; whereas the hybridized cell fractions of the tested *Proteobacteria* strains reached 100% with lysozyme pretreatment at 3 mg/ml (Fig. 2.1.C).

In the case of the two examined *Bacteroidetes* (open symbols in Fig. 2.1.D), the hybridized cell fraction of *C. huchinsonii* decreased from 46% without lysozyme pretreatment to 3% with lysozyme pretreatment at 20 mg/ml, whereas that of *F. columnare* increased from 3% without lysozyme pretreatment to 67% with lysozyme pretreatment at 20 mg/ml (Fig. 2.1.D, open symbols). Neither strain was visualized using DIG-FISH (Fig. 2.1.E, open symbols). *C. huchinsonii* could be detected using CARD-FISH with lysozyme pretreatment, whereas *F. columnare* was not detected using this method (Fig. 2.1.F, open symbols).

It was difficult to detect Gram-positive bacteria using FISH without lysozyme pretreatment (closed symbols in Fig. 2.1.D). The maximum hybridized cell fractions were obtained by FISH with lysozyme pretreatment at 10 mg/ml for *B. subtilis*, 20 mg/ml for *C. glutamicum*, and 10 mg/ml for *E. faecalis* (Fig. 2.1.D, closed symbols). Most Gram-positive bacteria could not be visualized using DIG-FISH except for *E. faecalis* with lysozyme pretreatment (Fig. 2.1.E, closed symbols). In contrast, *E. faecalis* and *B. subtilis* could be detected using CARD-FISH with lysozyme pretreatment at 10 mg/ml and 1 mg/ml, respectively. On the other hand, *C. glutamicum* was not detected using CARD-FISH even with lysozyme pretreatment (Fig. 2.1.F, closed symbols). Thus, six of the eight examined bacterial strains were successfully detected using CARD-FISH with 10 mg/ml of lysozyme pretreatment, suggesting that this pretreatment condition enables the detection of a relatively large fraction of bacterial strains.

2.3.2. Permeabilization with achromopeptidase

Two examined bacterial strains, *C. glutamicum* and *F. columnare*, could not be detected, even using CARD-FISH. Detection of these two bacterial strains was attempted following an additional permeabilization step. In the case of *C. glutamicum*, lysozyme pretreatment (20 mg/ml) followed by the incubation with achromopeptidase at 25 or 50 units/ml (30 min at 37°C) showed a pronounced effect on visualization using CARD-FISH (Fig. 2.2, panel A and B). On the other hand, the probe signal on *A. faecalis* was completely lost using achromopeptidase at above 25 units/ml because of the destruction of cell morphology by excessive permeabilization, although this strain was detected using lysozyme pretreatment (Fig. 2.2, panel C and D). This phenomenon was also observed in the case of the other Proteobacterial strains (data not shown). *F. columnare* cells could not be detected using CARD-FISH even with lysozyme and achromopeptidase treatment (data not shown). Higher achromopeptidase concentrations (>50 units/ml) did not increase the fraction of hybridized cells, but rather caused a visible disintegration of cells (data not shown). Achromopeptidase pretreatment followed by incubation with lysozyme and achromopeptidase pretreatment alone did not increase the fraction of hybridized cells.

2.4. Discussion

To detect bacterial strains on the basis of their functional gene expression products (mRNA) in situ, the simultaneous detection of different bacterial strains carrying a certain functional gene is absolutely imperative. In this study, we analyzed different conditions for the detection of taxonomically diverse bacterial strains by using rRNA-targeted oligonucleotide probe, particularly with highly sensitive FISH.

When a fluorescent signal cannot be obtained using highly sensitive FISH, the following explanations are conceivable:

(1) a low penetrating efficiency of the antibody or enzyme such as anti-DIG antibody and HRP,

(2) a low rRNA content in each cell, and

(3) a mismatch of the oligonucleotide probes.

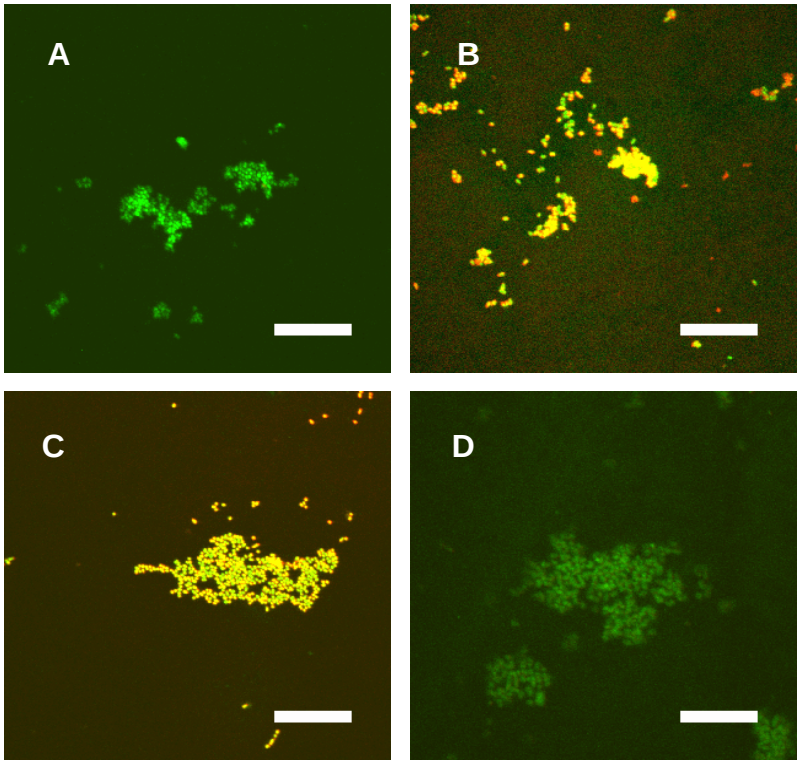

Fig. 2.2 Photomicrograph of CARD-FISH stained *C. glutamicum* (A and B) and *A. faecalis* (C and D) with lysozyme pretreatment alone (A and C) and achromopeptidase followed by lysozyme pretreatment (B and D). Yellow indicates positive cells, while green shows negative cells. Scale bar, 20 µm.

Cases 2 and 3 were inconceivable in this study. As for case 2, all the tested bacterial strains could be visualized using conventional FISH, which indicated that they contained sufficient target molecule for highly-sensitive FISH (Fig. 2.1.A and 2.1.D). Furthermore, the intracellular RNA contents in each bacterial strain were compared using RiboGreen. As shown in Table 2.2, the highest signal intensities were obtained from *C. huchinsonii* and *C. glutamicum* and the lowest signal intensity was obtained from *E. faecalis*. The signal intensities obtained from *C. huchinsonii* and *C. glutamicum* were nearly 1.6 times higher than that of *E. faecalis*, indicating that all the tested bacterial strain contained nearly level of intracellular RNA. Although RiboGreen also binds to DNA, the signal intensities were regarded as intracellular RNA contents because intracellular DNA contents are not varies with the bacterial strains. As for case 3, using the BLAST program[1)], there is no mismatch between the sequence of probe and that of all the examined bacterial strains (data not shown). Consequently, case 1 is the only explanation of why the fluorescent signal was not visualized following highly sensitive FISH.

As shown in Table 2.3, we classified the examined bacterial strains into three types on the basis of detection results obtained from lysozyme pretreatment with various lysozyme concentrations. The bacterial strains belonging to type 1 were successfully detected using both a conventional FISH procedure and highly sensitive FISH. Hence, it is evident that the probe, antibody, or enzyme can easily penetrate the cell walls of these bacterial strains. In contrast, the bacterial strains belonging to type 2 could not be detected using FISH without lysozyme pretreatment. Furthermore, they were not detected using highly sensitive FISH at all. These results suggest that they possess cell walls that do not allow antibody or enzyme to penetrate. The bacterial strains belonging to type 3 were detected using CARD-FISH, although they were poorly detected using conventional FISH, suggesting that their cell walls were more difficult to penetrate than those belonging to type 1. From these results, the classification of the detection patterns is not closely associated with that of phylogenetic affiliation.

As shown in Fig. 2.1, the number of detected bacterial strains using CARD-FISH was larger than that using DIG-FISH. This is most likely to be attributed to the crucial difference in signal amplification efficiencies between DIG-FISH and CARD-FISH. The

Table 2.2. Relative fluorescence signal intensity (%)[a] of all examined strains staining with RiboGreen

Strains	% of relative signal intensity
P. denitrificans	109
A. faecalis	127
P. stutzeri	116
C. hutchinsonii	161
F. columnare	123
E. faecalis	100
B. subtilis	124
C. glutamicum	161

[a]Relative to signal intensity of *E. faecalis*.

Table 2.3. Classification of the detection types[a]

Type	Strain (affiliation[b])	Method		
		FISH	DIG-FISH	CARD-FISH
I	*A. faecalis* (β)	++	++	(++)
	P. stutzeri (γ)	++	++	(++)
II	*C. glutamicum* (HGC)	(++)	–	–
	F. columnare (CFB)	(+)	–	–
III	*B. subtilis* (LGC)	(+)	–	(++)
	C. huchinsonii (CFB)	+	–	(++)
	E. faecalis (LGC)	(++)	(++)	(++)
	P. denitrificans (α)	(+)	(++)	(++)

[a]–, no signals; +, a part of all cells (10–80%) hybridized; ++, almost all cells (>80%) hybridized; sign in brackets, with lysozyme pretreatment.

[b]α, α-*Proteobacteria*; β, β-*Proteobacteria*; γ, γ-*Proteobacteria*; CFB, *Bacteroidetes*; LGC, Gram-positive bacteria with low G+C content of DNA; HGC, Gram-positive bacteria with high G+C content of DNA.

amplification efficiency of CARD-FISH is nearly fivefold higher than that of DIG-FISH [20]. Hence, for CARD-FISH, a small number of penetrated probes would enable successful detection. It should be pointed out that it was difficult to quantify the target RNA in cells because the fluorescence signal was saturated by CARD-FISH.

Schönhuber *et al*. [20] have reported that CARD-FISH was unable to detect Gram-positive bacteria even with lysozyme pretreatment. However, *E. faecalis* and *B. subtilis* (low G+C Gram-positive bacteria) were detected using CARD-FISH with lysozyme pretreatment at 10 and 1 mg/ml, respectively, in our study. This was probably due to the difference in permeabilizing conditions, that is, they carried out cell wall permeabilization with 0.1 mg/ml of lysozyme for 10 min at 0°C. On the other hand, *C. glutamicum* (high G+C Gram-positive bacteria) could not be visualized using CARD-FISH with lysozyme pretreatment in our study. This is likely because of their highly specific cell walls. The main component of their cell wall is the mycolyl-arabinogalactan peptidoglycan complex. This mycolic acid region is poor in proteins; only a small amount of a pore-forming protein with a weak activity has been detected, causing the low penetrability of hydrophilic substances [22]. This hydrophobicity caused difficulties associated with the penetration of hydrophilic substances such as the anti-DIG antibody or tyramide. To improve the permeabilization of mycolic acid-rich bacteria, many techniques have been examined: including reduced fixation time [18], acid hydrolysis [14], and ethanol fixation [19]. Sekar *et al*. [21] demonstrated that incubations with 10 mg/ml of lysozyme followed by 60 units/ml of achromopeptidase can successfully permeabilize the cell walls of this group of bacterial strains for subsequent CARD-FISH. We were also able to detect *C. glutamicum* by using this procedure (Fig. 2.2, panel A and B); however, this procedure resulted in the loss of the target molecule and cell morphology for other bacterial strains (Fig. 2.2, panel C and D). Lan *et al*. [13] reported that microwave oven heating can be used as a substitute for enzymatic cell wall digestion for a wide variety of eukaryotic cells, and the hybridization signal obtained after microwave pretreatment was very uniform in six different tissues. We tried to apply this pretreatment to *C. glutamicum*; however, we were unable to obtain signals using CARD-FISH (data not shown). This is most likely due to the differences in

cell structures between prokaryotic cells and eukaryotic cells. These results imply that it is difficult to find a universal method for permeabilizing all kinds of cell wall.

Surprisingly, for most bacterial strains, except for the two examined *Proteobacteria* strains *A. faecalis* and *P. stutzeri*, conventional FISH without lysozyme pretreatment could not generate a sufficient hybridization signal (Fig. 2.1.A and 2.1.D). These results suggest that well-suited cell wall permeabilization techniques are required for quantitative FISH targeting the *Bacteroidetes* or Gram-positive bacteria. However, it must be noted that all images were obtained using identical conditions in this study; therefore, these results might be improved if photomicroscopic conditions such as laser voltage settings were optimized for each strain. Meanwhile, we must take into account the possibility of underestimating positive cells in the case of using universal probes such as the eubacterial probe EUB338. Bouvier and Giorgio [6] have reported that for cases in which the results are not affected by the contribution of *Archea*, the percentage of cells detected using EUB338 varies from 1 to 100% of the total bacterial count in different published reports, with an average of 56%. Provided that bacterial strains that have unusual cell wall structures, such as mycolic acid-rich cell wall structures, are not dominant species, a more refined quantification could be carried out using CARD-FISH with 10 mg/ml lysozyme pretreatment.

In this study, most bacterial strains were successfully detected using CARD-FISH with 10 mg/ml lysozyme pretreatment. Additionally, achromopeptidase pretreatment was a highly effective means of permeabilizing the bacterial strains that were unable to be detected with lysozyme pretreatment, while it was considered impossible to visualize all bacterial strains by a universal permeabilizing procedure. If highly sensitive FISH methods are applied to well-defined target bacterial strains, permeabilizing conditions should be optimized according to our results. It should be noted that, for environmental samples, there are many variable factors such as the type of ecosystem, bacterial growth rate, and growth phase. Nevertheless, our results will contribute to the optimization of permeabilizing conditions, which is one of the most important factors for the successful application of highly sensitive FISH. It is anticipated that in future studies, a method that is not affected by cell wall structures will be developed, and consequently, this method

will enable us to universalize the highly sensitive FISH procedure.

References

1. Altschul, S. F., Gish, W., Miller, W., Myers, E. W., and Lipman, D. J. (1990) Basic local alignment search tool. *J. Mol. Biol. 215*, 403-410.
2. Amann, R. I. (1995) In situ identification of micro-organism by whole cell hybridization with rRNA-targeted nucleic probes. p. 1-15. In Akkerman, A. D. C., van Elsas, J. D., and de Bruijin, F. J. (ed.), Molecular microbial ecology manual. Kluwer Academic Publishers.
3. Amann, R. I., Binder, B. J., Olson, R. J., Chisholm, S. W., Devereux, R., and Stahl, D. A. (1990) Combination of 16S rRNA-targeted oligonucleotide probes with flow cytometry for analyzing mixed microbial populations. *Appl. Environ. Microbiol. 56*, 1919-1925.
4. Aoi, Y., Miyoshi, T., Okamoto, T., Tsuneda, S., Hirata, A., Kitayama, A., and Nagamune, T. (2000) Microbial ecology of nitrifying bacteria in wastewater treatment process examined by fluorescence in situ hybridization. *J. Biosci. Bioeng. 90*, 234-240.
5. Bakermans, C., and Madsen, E. L. (2002) Detection in coal tar waste-contaminated groundwater of mRNA transcripts related to naphthalene dioxygenase by fluorescent in situ hybridization with tyramide signal amplification. *J. Microbiol. Methods 50*, 75-84.
6. Bouvier, T., and Giorgio P. A. (2003) Factors influencing the detection of bacterial cells using fluorescence in situ hybridization (FISH): A quantitative review of published reports. *FEMS Microbiol. Ecol. 44*, 3-15.
7. Braker, G., Fesefeldt, A., and Witzel., K. P. (1998) Development of PCR primer systems for amplification of nitrite reductase genes (*nirK* and *nirS*) to detect denitrifying bacteria in environmental samples. *Appl. Environ. Microbiol. 64*, 3769-3775.
8. Chen, F., Gonzalez, J. M., Dustman, W. A., Moran, M. A., and Hodson, R. E. (1997) In situ reverse transcription, an approach to characterize genetic diversity and activities of prokaryotes. *Appl. Environ. Microbiol. 63*, 4907-4913.
9. DeLong, E. F., Wickham, G. S., and Pace, N. R. (1989) Phylogenetic stains: ribosomal RNA-based probes for the identification of single cells. *Science 243*, 1360-1363.
10. Hoshino, T., Noda, N., Tsuneda, S., Hirata, A., and Inamori, Y. (2001) Direct detection by in situ PCR of the *amoA* gene in biofilm resulting from a nitrogen removal process. *Appl. Environ. Microbiol. 67*, 5261-5266.
11. Hoshino, T., Tsuneda, S., Hirata, A., and Inamori, Y. (2003) In situ PCR for visualizing distribution of a functional gene "amoA" in a biofilm regardless of activity. *J. Biotechnol. 105*, 33-40.
12. Ishii, K., Mussmann, M., MacGregor, B. J., and Amann, R. (2004) An improved fluorescence in situ hybridization protocol for the identification of bacteria and archaea in marine sediments. *FEMS Microbiol. Ecol. 50*, 203-212.
13. Lan, H. Y., Mu, W., Ng, Y. Y., Nikolic-Paterson, D. J., and Atkins, R. C. (1996) A simple, reliable, and sensitive method for nonratioactive in situ hybridization: use of microwave heating to improve hybridization efficiency and preserve tissue morphology. *J. Histchem. Cytochem. 44*, 281-287.
14. Macnaughton, S. J., O'Donnell, A. G., and Embley, T. M. (1994) Permeabilization of mycolic-acid-containing actinomycetes for in situ hybridization with fluorescently labeled oligonucleotide probes. *Microbiology 140*, 2859-2865.
15. Maruyama, F., Kenzaka, T., Yamaguchi, N., Tani, K., and Nasu, M. (2003) Detection of bacteria carrying the stx_2 gene by in situ loop-mediated isothermal amplification. *Appl. Environ. Microbiol. 69*, 5023-5028.
16. Pernthaler, A., Pernthaler, J., and Amann, R. (2002) Fluorescence in situ hybridization and catalyzed reporter deposition for the identification of marine bacteria. *Appl. Environ. Microbiol. 68*, 3094-3101.
17. Pernthaler, A., and Amann R. (2004) Simultaneous fluorescence in situ hybridization of mRNA and rRNA in environmental bacteria. *Appl. Environ. Microbiol. 70*, 5426-5433.
18. Reyes, F. L., Ritter, W., and Raskin, L. (1997) Group-specific small-subunit rRNA hybridization probes to characterize filamentous foaming in activated sludge systems. *Appl. Environ. Microbiol. 63*, 1107-1117.
19. Roller, C., Wagner, M., Amann, R., Ludwig, W., and Schleifer, K. H. (1994) In situ probing of Gram-positive bacteria with high DNA G+C content using 23S rRNA-targeted oligonucleotides. *Microbiology 140*, 2849-2858.

20. Schönhuber, W., Fuchs, B., Juretschko, S., and Amann, R. (1997) Improved sensitivity of whole-cell hybridization by the combination of horseradish peroxidase-labeled oligonucleotides and tyramide signal amplification. *Appl. Environ. Microbiol. 63*, 3268-3273.
21. Sekar, R., Pernthaler, A., Pernthaler, J., Warnecke, F., Posch, T., and Amann, R. (2003) An improved protocol for quantification of freshwater *Actinobacteria* by fluorescence in situ hybridization. *Appl. Environ. Microbiol. 69*, 2928-2935.
22. Seltmann, G., and Holst, O. (2002) The bacterial cell wall, p. 204-215. Springer-Verlag, Berlin, Germany.
23. Tani, K., Kurokawa, K., and Nasu, M. (1998) Development of a direct in situ PCR method for detection of specific bacteria in natural environments. *Appl. Environ. Microbiol. 64*, 1536-1540.
24. Wagner, M., Schmid, M., Juretschko, S., Trebesius, K. H., Bubert, A., Goebel, W., and Schleifer, K. H. (1998) In situ detection of a virulence factor mRNA and 16S rRNA in *Listeria monocytogenes*. *FEMS Microbiol. Lett. 160*, 159-168.
25. Wagner, M., Erhart, R., Manz, W., Amann, R., Lemmer, H., Wedi, D., and Schleifer, K. H. (1994) Development of an rRNA-targeted oligonucleotide probe specific for the genus *Acinetobacter* and its application for in situ monitoring in activated sludge. *Appl. Environ. Microbiol. 60*, 792-800.
26. Zarda, B., Amann, R., Wallner, G., and Schleifer, K. H. (1991) Identification of single bacterial cells using digoxigenin-labelled, rRNA-targeted oligonucleotides. *J. Gen. Microbiol. 137*, 2823-2830.
27. Zwirglmaier, K., Ludwig, W., and Schleifer, K. H. (2004) Recognition of individual genes in a single bacterial cell by fluorescence in situ hybridization - RING-FISH. *Mol. Microbiol. 51*, 89-96.

Chapter 3

Reduction-triggered fluorescence probes for sensing nucleic acids

Chapter 3

Reduction-triggered fluorescence probes for sensing nucleic acids

3

3.1. Introduction

Fluorescent-labeled oligonucleotides are becoming important tools for detecting oligonucleotide sequences [1, 2]. A possible application is the detection of RNA species in cells by *in situ* hybridization [3-5]. However, standard fluorescent probes require careful handling to avoid nonspecific signals. Fluorogenic probes with a fluorescence on/off mechanism have been developed to avoid this problem [6-13]. Some of these probes have been applied to the detection of RNA in cells [14-17]. Examples are molecular beacon (MB) [15, 16] or target-assisted chemical ligation [14, 18]. Target-dependent fluorescence enhancement of these methods is based on the resonance energy transfer (RET) mechanism, for which a pair of quencher and fluorescence dyes is normally used. However, higher sensitivity for the detection method is still required to monitor gene expression in cells. Recently, various fluorogenic compounds have been developed for the detection of small biological substances [19-23]. For example, diaminofluorescein when used for the detection of nitric oxide (NO) reacts with NO to yield a fluorescent compound through triazole formation [21]. The boronate fluorescein derivative for detection of hydrogen peroxide (H_2O_2) reacts with H_2O_2 to yield a fluorescent form through cleavage of the carbon–boron bond [20]. In these examples, detection is triggered by a chemical reaction accompanied by transformation of the chemical structure of the fluorogenic compound. Fluorescence modulation is caused by

photoinduced electron transfer or absorption change. The signal/background (S/B) ratio of this type of molecule could exceed that of the RET mechanism [24]. However, there are few reports that describe chemical reaction-triggered fluorogenic molecules for oligonucleotide sensing, although this method offers high sensitivity [25]. Here, we report a reduction-triggered fluorescence (RETF) probe that shows a high S/B ratio for sensing oligonucleotides (Figure 3.1). A new fluorescence molecule, rhodamine azide, that we designed and synthesized is activated only by a specific reducing reagent on the oligonucleotide target and is very stable under biological conditions, showing little background fluorescence. The probe was applied to the sensing of nucleic acids *in vitro*.

3.2. Materials and Methods

*3.2.1. t-Boc-rhodamine110 Azide (**2**)*

t-Boc-rhodamine110 (48.0 mg, 0.112 mmol) was dissolved in CH_3CN (8 ml) and CH_2Cl_2 (4 ml) under Ar (g). TFA (12.4 μl, 0.167 mmol) was added followed by addition of isopentyl nitrite (17.8 μl, 0.134 mmol) at 0 °C. After stirring for 2 h at 0 °C, sodium azide (15.0 mg, 0.223 mmol) was added to the resulting solution followed by stirring for 1 h at ambient temperature. The reaction was quenched with saturated aqueous $NaHCO_3$. The aqueous layer was extracted with AcOEt (×2) and the combined organic layers were dried over Na_2SO_4, concentrated, and subjected to flash column chromatography (silica gel, 6:1 hexane:EtOAc) to give azide-Rhodamine110-t-Boc (**2**) as a pale yellow crystalline solid (36.5 mg, 80.0 μmol, 71%). ^{1}H NMR (400 MHz, $CDCl_3$) δ = 1.53 (9H, s), 6.61 (1H, brs), 6.68 (1H, d, J = 3.2 Hz), 6.71 (1H, d, J = 3.2 Hz), 6.77 (1H, d, J = 8.5 Hz), 6.87 (1H, dd, J = 2.2 Hz, 8.8 Hz), 6.93 (1H, d, J = 1.9 Hz), 7.12 (1H, brd, J = 7.3 Hz), 7.56 (1H, brs), 7.62 (1H, dt, J = 1.0 Hz, 7.5 Hz), 7.66 (1H, dt, J = 1.2 Hz, 7.6 Hz), 8.02 (1H, brd, J = 7.3 Hz). ^{13}C NMR (100 MHz, $CDCl_3$) δ 28.36, 81.25, 82.19, 105.97, 107.21, 112.87, 114.26, 114.74, 115.59, 123.70, 125.07, 126.22, 128.45, 129.43, 129.78,

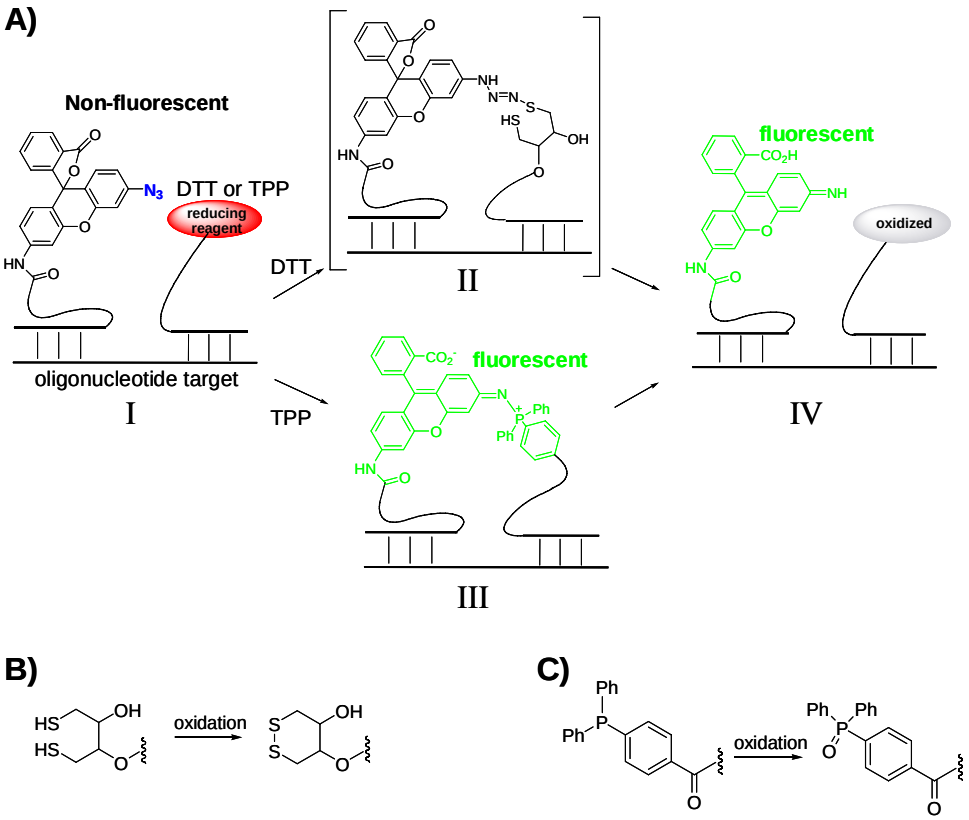

Fig. 3.1 Fluorescence emission of an RETF probe by reducing reagents. A) Reduction of azide on Rhodamine by DTT or TPP as reducing reagents. B) Oxidation of DTT. C) Oxidation of TPP.

135.04, 140.56, 142.37, 151.47, 152.08, 152.95, 169.13. QSTAR (Applied Biosystems/MDS SCIEX) (ESI): [MH+] $C_{25}H_{21}N_4O_5$: calculated 457.1512, found: 457.1509

*3.2.2 Rhodamine110-azide (**3**)*

Azide-Rhodamine110-t-Boc (**2**) (30.8 mg, 67.5 μmol) was dissolved in 4.0 M HCl solution in dioxane (3 ml). The resulting solution was stirred at ambient temperature for 3 h. Solvent was removed under reduced pressure, and the residue was purified by TLC plate (9:1 $CHCl_3$:MeOH). Azide-Rhodamine110 (**3**) was isolated as a pale pink crystalline solid (23.8 mg, 66.8 μmol, 99%). ^{1}H NMR (400 MHz, $CDCl_3$) δ 3.92 (2H, s), 6.36 (1H, dd, J = 2.4 Hz, 8.5 Hz), 6.52 (1H, d, J = 2.2 Hz), 6.55 (1H, d, J = 8.5 Hz), 6.67 (1H, dd, J = 2.2 Hz, 8.5 Hz), 6.74 (1H, d, J = 8.5 Hz), 6.92 (1H, d, J = 2.2 Hz), 7.16 (1H, d, J = 7.6 Hz), 7.61 (1H, dt, J = 1.0 Hz, 7.3 Hz), 7.66 (1H, dt, J = 1.2 Hz, 7.5 Hz), 8.01 (1H, d, J = 7.6 Hz). ^{13}C NMR (100 MHz, $CDCl_3$) δ 82.82, 101.15, 106.95, 108.15, 111.67, 114.39, 115.82, 123.63, 124.80, 126.54, 128.93, 129.38, 129.48, 134.73, 142.03, 148.62, 151.97, 152.11, 152.73, 169.06. QSTAR (Applied Biosystems/MDS SCIEX) (ESI): [MH+] $C_{20}H_{13}N_4O_3$: calculated 357.0988, found: 357.0988

*3.2.3 Bromoacetylamide-rhodamine110-azide (**4**)*

Azide-Rhodamine110 (**3**) (17.9 mg, 50.2 μmol) was dissolved in $CHCl_3$ (4 ml). Anhydrous potassium bicarbonate (138.2 mg, 1.0 mmol) was added. The reaction mixture was cooled to 0 °C followed by addition of bromoacetyl bromide (43.7 μl, 0.50 mmol). The resulting solution was stirred at ambient temperature for 12 h and the reaction was quenched with saturated aqueous Na_2CO_3. The aqueous layer was extracted with $CHCl_3$ (×2) and the combined organic layers were dried over Na_2SO_4, concentrated, and subjected to flash column chromatography (silica gel, 3:1 hexane:EtOAc) to give bromoacetylamide-Rhodamine110-azide (**4**) (22.6 mg, 47.4 mmol, 94%) as a pale yellow crystalline solid. ^{1}H NMR (400 MHz, CDCl3) δ 4.03 (2H, s), 6.71 (1H, dd, J = 2.2Hz, 8.6 Hz), 6.75 (1H, d, J = 8.5 Hz), 6.79 (1H, d, J = 8.6 Hz), 6.95 (1H, d, J = 2.2 Hz), 7.05 (1H, dd, J = 2.2 Hz, 8.8 Hz), 7.13 (1H, brd, J = 7.6 Hz), 7.64 (1H, dt, J = 1.0 Hz, 7.6 Hz),

7.68 (1H, dt, J = 1.2 Hz, 7.6 Hz), 7.74 (1H, d, J = 1.9 Hz), 8.04 (1H, brd, J = 6.8 Hz), 8.33 (1H, brs). ^{13}C NMR (100 MHz, $CDCl_3$) δ 29.21, 81.89, 107.11, 107.82, 114.86, 115.15, 115.43, 123.57, 125.03, 125.87, 128.38, 129.26, 129.82, 135.12, 138.86, 142.46, 151.09, 151.77, 152.68, 163.60, 169.11. QSTAR (Applied Biosystems/MDS SCIEX) (ESI): [MH+] $C_{22}H_{14}BrN_4O_4$: calculated 477.0198, found: 477.0196.

*3.2.4 t-Boc –rhodamine 110-triphenylphosphine-aza-ylide (**5a**)*

t-Boc-rhodamine 110 azide (**2**) (13.4 mg, 29.4 μmol) was dissolved in anhydrous THF (1.1 ml). Triphenylphosphine (9.1 mg, 34.7 μmol) was added. After 2 h reaction, solvent was removed under reduced pressure, and the residue was purified by PLC plate (1:1 Hexane:AcOEt). t-Boc–rhodamine 110-triphenylphosphine-aza-ylide (20.3 mg, 29.4 mmol, quantative) was obtained as red crystalline solid. ^1H NMR (400 MHz, CDCl3) δ1.50 (9H, dd, J = 3.8 Hz, 5.3 Hz), 6.34 (1H, m), 6.47 (1H, m), 6.56 (1H, m), 6.64 (1H, m), 6.73 (1H, m), 6.81 (1H, m), 7.13 (1H, m), 7.47 (6H, m), 7.54 (4H, m), 7.60 (1H, m), 7.66 (3H, m), 7.73 (3H, m), 7.97 (1H, m). QSTAR (Applied Biosystems/MDS SCIEX) (ESI): [MH+]: 691.2362, found: 691.2374

*3.2.5 Reaction of compound **2** with DTT*

t-Boc-rhodamine 110 azide (**2**) (0.37 mg, 0.8 μmol) was dissolved in methanol (2.0 ml). Dithiothreitol (30.6 mg, μmmol) was added. The reaction was monitored by fluorescence and UV spectra. The maximum wavelength of fluorescent emission was observed in 525 nm. Mass spectrometry analysis showed that the product was rhodamine amine (**1**). ([MH+] $C_{25}H_{23}N_2O_5$: 431.161, Maldi-Tof Ms found: 431.167).

*3.2.6 Reaction of compound **2** with TPP*

t-Boc-rhodamine 110 azide (**2**) (11.1 mg, 24.3 μmol) was dissolved in anhydrous THF (2.43 ml). Triphenylphosphine (7.0 mg, 30.5 μmol) was added. The reaction was monitored by fluorescence and UV spectra (Fluorescence measurements were conducted by diluting 1.5 μl reaction mixture with 1500 μl methanol. Absorption measurements were conducted by diluting 4.0 μl reaction mixture with 196 μl methanol.). As showed in

Figure 3.5.A, the maximum wavelength of fluorescent emission was observed in 550 nm 10 min later. After 1 h reaction, the fluorescent emission at 550 nm was saturated and no additional fluorescent emission was observed. Mass spectrometry analysis showed that the product was aza-ylide (**5a**). ([MH+] $C_{43}H_{36}N_2O_5P$: 691.236, Maldi-Tof Ms found: 691.304)

3.2.7 Synthesis of unmodified oligonucleotides

All oligonucleotides were synthesized on a 0.2 μmol scale on a DNA synthesizer (H-8-SE; Gene World) using standard phosphoroamidite coupling chemistry. Deprotection and cleavage from the CPG support was carried out by incubation in concentrated ammonia for 4 h at 55 °C. Following deprotection, the oligonucleotides were purified by reverse-phase column chromatography (MicroPure II column; Biosearch Technologies), and quantitated by UV absorbance using the nearest neighbor approximation to calculate molar absorptivities.

3.2.8 3′rhodamine-azide-conjugated oligonucleotide (probe 1)

The bromoacetyl group of the rhodamine-azide (**4**) was reacted with the phosphorothioate group on the ODNs. For 3′ phosphorothioate sequences, the 3′-phosphate CPG was sulfurized by the sulfurizing reagent (Glen Research) after the first nucleotide was added. 75 nmol of the 3′-phosphorothioate oligonucleotide in 50 μl of 400 mM triethylammonium bicarbonate buffer were shaken for 5 h at room temperature with 750 nmol of rhodamine-azide (**4**) in 200 μl of dimethylformamide. The reacted products were collected by ethanol precipitation. Next, the products were purified by reverse-phase HPLC (0–80% acetonitrile/50 mM triethylammonium acetate gradient). The probe structure was confirmed by ESI–TOF mass spectrometry. 5′-GCCGGCGG-Rh_azide-3′: calculated mass, $C_{104}H_{126}N_{33}O_{51}P_9$ 2942.5; found 2942.5.

3.2.9 5′dithiothreitol (DTT)-linked oligonucleotide (probe 2)

Dithiol phosphoroamidite (DTPA; Glen Research) was used to prepare 5′ DTT-modified oligonucleotide. Deprotection and cleavage from the CPG support was

carried out by the standard method. Following deprotection, the oligonucleotide was purified by reverse-phase column chromatography and quantitated by UV absorbance. To cleave the disulfide bond, 10 nmol of purified oligonucleotide was treated with 250 μl of 100 mM TCEP in phosphate buffer (pH 6.0). The reacted products were collected by ethanol precipitation, and then preserved in 100 μM DTT solution. The probe structure was confirmed by MALDI–TOF mass spectrometry. 5′-DTT-TGTGGGCA-3′: calculated mass, $C_{83}H_{108}N_{32}O_{51}P_8S_2$ 2980.4; found 2979.7.

3.2.10 5′Triphenylphosphine (TPP)-linked oligonucleotide (probe 3)

Carboxy-triphenylphosphine (TPP) NHS ester was reacted with 5′ amino-modified oligonucleotide. 5′ amino-modifier C6 (Glen Research) was used to prepare 5′ amino-modified oligonucleotide. 50 nmol of the 5′ amino-modified oligonucleotide in 135 μl of 93 mM sodium tetraborate (pH 8.5) were shaken for 5 h at room temperature with 2 μmol of TPP NHS ester in 115 μl of dimethylformamide. The reacted products were collected by ethanol precipitation. Next, the collected products were purified by reverse-phase HPLC (0–50% acetonitrile/50 mM triethylammonium acetate gradient). The probe structure was confirmed by ESI–TOF mass spectrometry. 5′-TPP-TGTGGGCA-3′: calculated mass, $C_{104}H_{126}N_{33}O_{51}P_9$ 2931.6; found 2932.6. A peak corresponding to the oxidized product (+O) was also seen and presumed to arise from oxidation during purification.

3.2.11 DNA-templated reaction

Reactions on the DNA template were performed in 1.2 ml of tris-borate buffer (70 mM, pH 8.0) containing 10 mM $MgCl_2$ with target DNA (500 nM), probe 1 (500 nM), and probe 2 (1 μM) or probe 3 (500 nM) at 25 °C. In the case of probe 2, DTT (100 μM) was added to the reaction mixture. The increase of fluorescence intensity produced by reduction of rhodamine-azide on probe 1 was continuously monitored at time intervals. Reactions were observed by fluorescence spectrometry (FP-6500; JASCO). Fluorescence spectra were measured under the following conditions: excitation, 490 nm. For the time course of the azide reduction, the fluorescence intensity was measured for 0.5 s at 1 min

intervals: excitation, 490 nm; emission, 550 nm (TPP) or 530 nm (DTT).

3.3. Results

3.3.1. The Principle of Fluorescence Emission of the RETF Probe

The RETF probe consists of two separated DNA strands, one probe having a reducible fluorogenic compound, while the other probe has reducing reagents. The chemistry of the RETF probe involves reaction between the azide group of nonfluorescent rhodamine derivatives and reducing reagents on an oligonucleotide template (Figure 3.1.A). This reaction proceeds only in the presence of complementary oligonucleotide templates. After reduction of the azide group (I), the rhodamine derivative with the aza-ylide group (III) or the amino group (IV) emits fluorescence. Dithiothreitol (DTT) or triphenylphosphine (TPP) can be used as reducing reagents for this chemistry. DTT directly reduces the azide group (I) to an amino group (IV) with the formation of a disulfide bond (Figure 3.1.B). The Staudinger reaction using TPP as a reducing reagent produces an aza-ylide (III), which hydrolyzes to give a primary amine (IV) and the corresponding phosphorus compound (Figure 3.1.C). This reaction works orthogonally in biological conditions, or even in cells.

3.3.2. Synthesis of Rhodamine Azide

The synthesis of rhodamine azide derivatives (**4**) is shown in Scheme 3.1. The previously reported mono-Boc-rhodamine 110 (**1**) [26] was transformed to the diazo derivative by treatment with $NaNO_2$, and the diazo group was replaced with an azide group by the addition of NaN_3 to the reaction mixture. Treatment with trifluoroacetic acid to remove the Boc group of compound **2** did not give the desired product **3** because of damage to the azide group. The Boc group was successfully deprotected by treatment with 4 M HCl/dioxane solution, followed by introduction of the bromoacetyl group by treatment with bromoacetyl bromide and sodium bicarbonate to give the desired compound **4**. Compound **4** was introduced into the DNA probe.

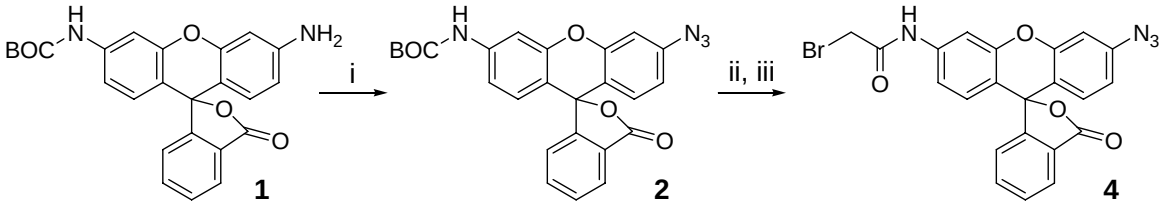

Scheme 3.1. i) isopentyl nitrite, TFA, CH_3CN/CH_2Cl_2, 0 °C, 2 h then NaN_3, CH_3CN/CH_2Cl_2, rt, 1 h, 70%; ii) 4.0 M HCl in dioxane, rt, 3 h, compound 3: 99%; iii) bromoacetyl bromide, $NaHCO_3$, $CHCl_3$, rt, 12 h, 94%.

3.3.3. Reaction of Rhodamine Azide (2) with Reducing Reagents

Rhodamine azide **2** showed no absorbance at wavelengths longer than 310 nm in methanol, but the corresponding rhodamine amine **1** showed a maximum absorption at 490 nm. When a high concentration of DTT or TPP was added to a solution of azide **2**, a peak having a maximum at 495 nm or 518 nm increased, respectively, resulting from reduction of the azide group (Figure 3.2.A). The fluorescence properties of rhodamine derivatives were also examined. No significant fluorescence with excitation at 490 nm was observed for azide **4**. On the other hand, rhodamine amine **1** showed strong fluorescence emission at around 520 nm. After the addition of DTT or TPP to the solution of azide **4**, a strong emission appeared around 520 nm or 550 nm, respectively, where the emission was enhanced almost 2100-fold (Figure 3.2.B). We isolated these products and analyzed the structures by NMR spectroscopy and mass spectrometry. The product resulting from the DTT treatment was amine **1**. In contrast, TPP treatment gave aza-ylide **5a** (Scheme 3.1). It seems that not **5a** but **5b** with longer π-conjugation in the equilibrium structures emits fluorescence at 550 nm. Thus, we conclude that both reducing reagents can transform rhodamine azide into a fluorescent form by intermolecular reaction at the small compound level.

3.3.4. Design of the RETF Probe

To test the utility of the RETF system for fluorescence-based oligonucleotide detection, we designed three new DNA probes (Figure 3.3). Probe 1 was modified at the 3′ terminal with rhodamine azide **4**, where the bromoacetyl group of **4** was reacted with the phosphorothioate group at the 3′ end of the DNA probe. Probe 2 was modified at the 5′ terminal with DTT using commercially available phosphoramidite reagents. Probe 3 was modified at the 5′ terminal with 2′-carboxytriphenylphosphine (TPP), which was conjugated with the 5′ amino linker of the DNA probe through amide bond formation. Two DNA templates originating from the human Ras gene sequence, which is known as an oncogene, were designed containing Ras-C with a full match sequence and Ras-A with a one-base mismatch, respectively (Figure 3.3). Ras-C (RNA) was also designed, corresponding to the Ras-C DNA strand.

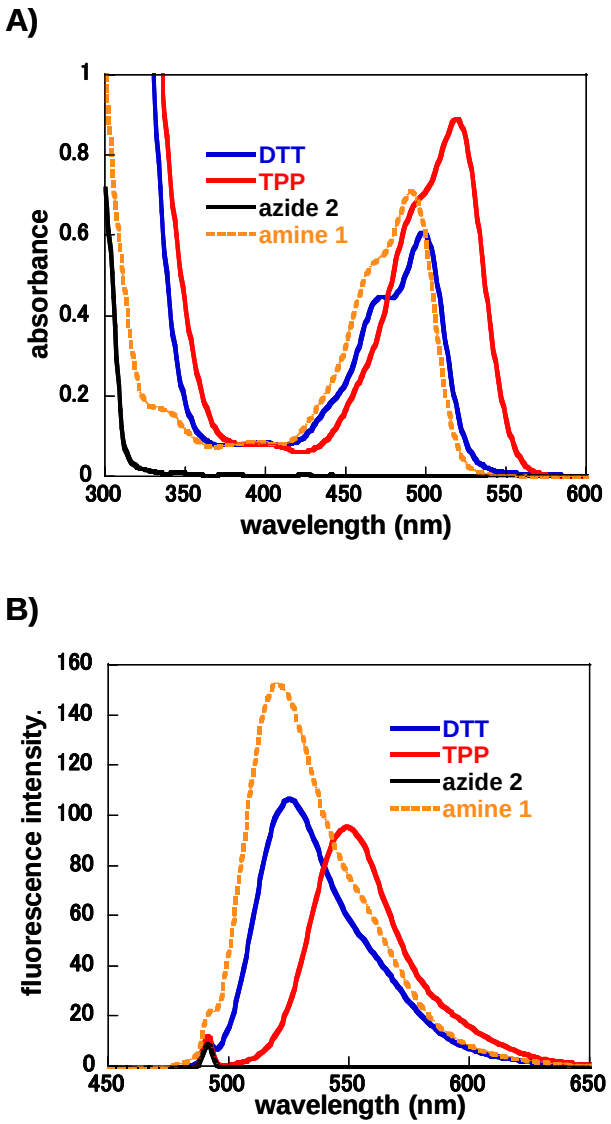

Fig. 3.2 A) Absorption spectra of 200 μM azide 2 after treatment with DTT (blue solid line) or TPP (red solid line), azide 2 (black solid line) without any treatment or amine 1 (orange broken line) in methanol; B) Fluorescent emission spectra with excitation at 490 nm of 10 μM azide 2 by treatment with DTT (blue solid line) or TPP (red solid line), azide 2 (black solid line) without any treatment or amine 1 (orange broken line) in methanol.

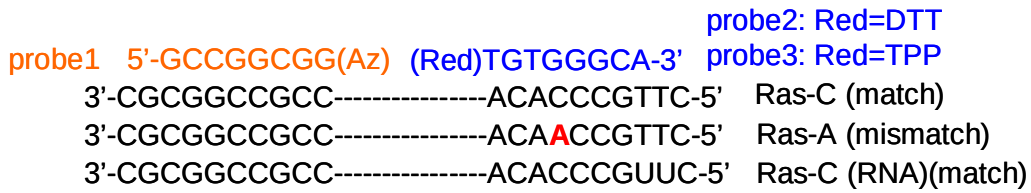

Fig. 3.3 Probe 1 is an 8-mer ODN modified with rhodamine azide **4** (Az) at the 3′ terminal. Probes 2 and 3 are 8-mer ODNs modified with DTT or TPP as reducing reagents (Red) at the 5′ terminal. The DNA targets are 20-mer ODNs with a full matched sequence (Ras-C) and a one-base mismatched sequence (Ras-A). Ras-C (RNA) is the full matched RNA target.

3.3.5. Reaction of the RETF Probe

An important issue for the detector probe is that it shows neither background fluorescence nor a false signal under biological conditions, in order to achieve a high S/B ratio. The probe should be very stable in any biological conditions. To determine the stability of the RETF probe, we treated the probe under various extreme conditions and checked the resulting signal. As a consequence, it was found that probe 1 with rhodamine azide was fully stable under acidic or basic conditions at pH 5–10 and under light irradiation at 490 nm, and at a high temperature of 90 °C for at least 10 min, as indicated by the lack of increase in fluorescence (Figures 3.4 and 3.5). However, when a high concentration of tris(2-carboxyethyl)phosphine (TCEP) was added to a solution of probe 1, a strong fluorescence signal appeared as the result of reduction of rhodamine azide on probe 1. Thus, we conclude that probe 1 with rhodamine azide was fully stable under various biological conditions to show no undesired fluorescence signal and was responsive to only the specific reducing reagents.

Next, we tested whether the RETF probe can detect target DNA or RNA sequences to produce a fluorescence signal (Figure 3.5). When 500 nM probe 1 and 1 μM probe 2 were incubated in pH 8.0 tris-borate buffer, the fluorescence signal at 530 nm increased in the presence of a target Ras-C over 60 min by reduction of the azide group to the amino group of probe 1, and no significant increase in fluorescence was observed in the absence of Ras-C (Figure 3.5.A). When 500 nM probe 1 and 500 nM probe 3 were incubated in buffer, the increase in fluorescence at 550 nm was monitored. Probe 3 reacted with probe 1 in the presence of target Ras-C much faster than did probe 2, and the signal at 550 nm reached the saturation phase within 20 min (Figure 3.5.A). The signal did not increase in the absence of Ras-C over 30 min, even under continuous light irradiation at 490 nm.

The ability to achieve single base discrimination is important for diagnostic applications. The reaction of probe 1 with probe 3 in the presence of one-base-mismatched target Ras-A was carried out and showed good single base mismatch discrimination, dropping in initial rate by 18.8-fold, compared with fully matched Ras-C (Figure 3.5.B).

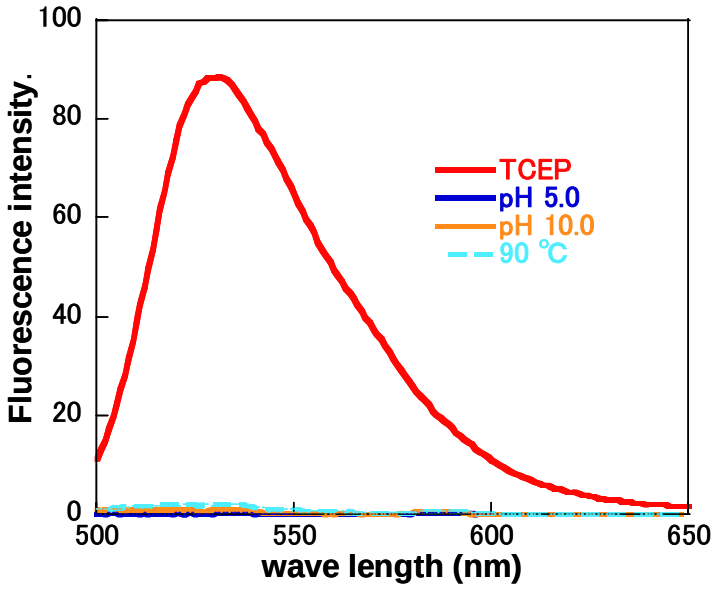

Fig. 3.4 Stability of probe 1 under various conditions. The stability of the rhodamine-azide probe (probe 1) was tested at pH 5.0, 10.0, and high temperature (90 °C) conditions. Probe 1 was incubated at pH 5.0 (blue solid line) or 10.0 (orange solid line) tris-borate buffer for 30 min at room temperature or in pH 8.0 tris-borate buffer for 10 min at 90 °C (light blue broken line). No significant fluorescence with excitation of 490 nm was observed in these conditions by comparison with the spectra after the treatment of TCEP (red solid line).

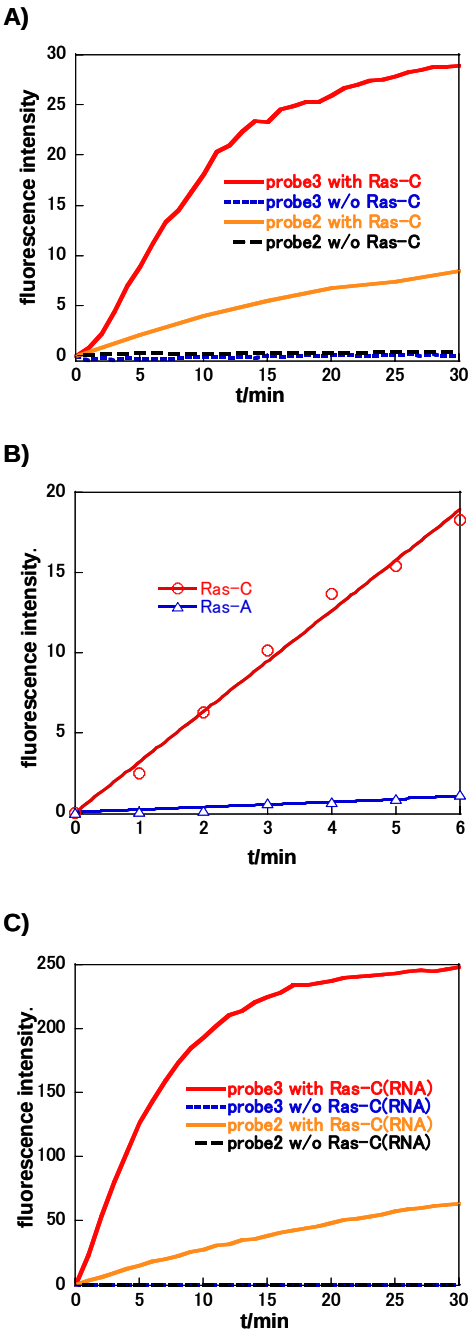

Fig. 3.5 A) Time course of the fluorescence intensity in the reaction of probe 1 with probe 2 or probe 3. Fluorescence emission at 530 nm (probe 2) or 550 nm (probe 3), respectively, was monitored by excitation at 490 nm. The reactions were carried out under the following conditions in pH 8.0 tris-borate buffer containing 10 mM $MgCl_2$, 1 μM probe 2, 100 μM DTT, and 500 nM probe 1 with (orange solid line) or without (black broken line) Ras-C, or 500 nM probe 3 and 500 nM probe 1 with (red solid line) or without (blue broken line) Ras-C. B) The time course of the fluorescence intensity in the reaction of probe 1 with probe 3 in the presence of Ras-C (match; circle) or Ras-A (mismatch; triangle). The reaction conditions were the same as above. C) Time course of the fluorescence intensity in the reaction of probe 1 with probe 2 or probe 3 with RNA target. The reaction were carried out with 500 nM probe 1 with (orange solid line) or without (black broken line) Ras-C (RNA), or 500 nM probe 3 and 500 nM probe 1 with (red solid line) or without (blue broken line).

RNA is an important target for detection, especially for imaging cellular RNA. However, because RNA–DNA duplexes form a different helical structure from DNA–DNA duplexes, there is no guarantee that such a chemical reaction on the template would proceed in the same way when detecting RNA as happened with DNA. Thus, we prepared an RNA target, Ras-C (RNA), and compared the reaction rates with the corresponding DNA target, Ras-C. When Ras-C (RNA) was targeted, almost identical time-course spectra as for Ras-C (DNA) were obtained from both probe 2 and probe 3 (Figure 3.5.C). The fluorescence signal at 550 nm from the reaction of probe 1 and probe 2 with Ras-C (RNA) reached the saturation phase in 20 min, similar to the Ras-C, DNA target. Thus, the RETF probe seems to be capable of detecting both DNA and RNA targets.

Figure 3.6.A shows the time-dependent fluorescence intensities at 530 nm and 550 nm in the reaction of probe 1 and probe 3 in the presence of the Ras-C template over 600 min. The signal at 550 nm quickly increased in the initial stage and slightly dropped after 30 min, but the signal at 530 nm continuously increased over the 600 min. The maximum wavelength in the fluorescence spectra shifted from 550 nm to 530 nm (Figure 3.6.B). HPLC (Figure 3.7) and MALDI–TOF mass analysis (Figure 3.8) showed that 67% of probe 1 had reacted with probe 3 after 10 min to give the corresponding ligated product with an aza-ylide bond (III) (peak 2: 52%) and reduced probe 1 with an amino group (IV) (peak 3: 15%) (Figures 3.1 and 3.7.A). After 24 h, the aza-ylide peak completely disappeared and the product with an amino group was obtained in 86% yield (peak 1, Figure 3.7.B). In contrast, reaction with probe 2 (DTT) showed only reduced product in 36% yield after 2 h (Figure 3.7.C). Thus, we conclude that in the reaction of probe 1 and probe 3, the increase in fluorescence at 530 nm indicates the formation of reduced probe 1 with the amino group of rhodamine (IV) from the hydrolysis of the aza-ylide product (III) [27]. In contrast, probe 2 directly reduces the azide group of probe 1 to the corresponding amine (IV).

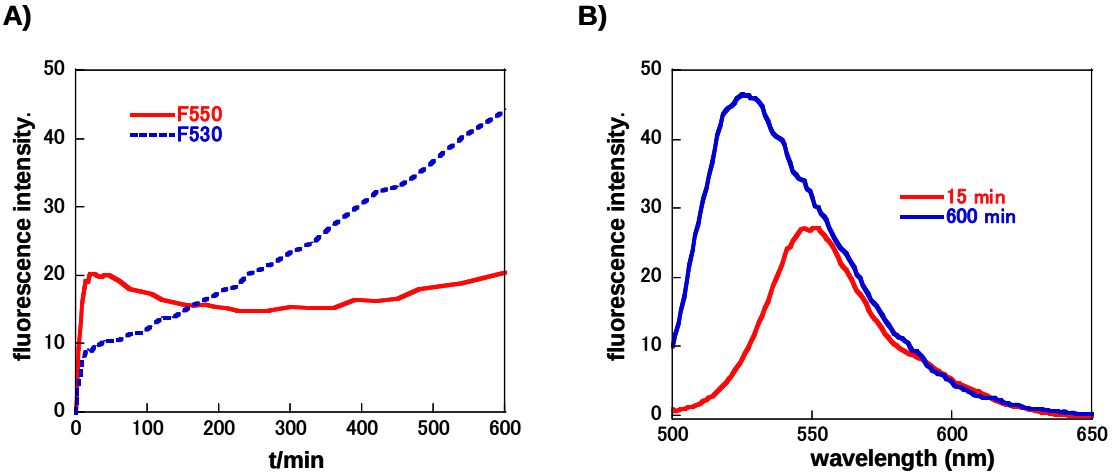

Fig. 3.6 A) Time course of the fluorescence intensity in the reaction between 500 nM probe 1 and 500 nM probe 3 in the presence of 500 nM Ras-C. Emissions at 550 nm (red solid line) and 530 nm (blue broken line) were monitored simultaneously. B) Fluorescence spectra were measured after 15 min (red solid line) and 600 min (blue solid line) incubation with probes 1 and 3 in the presence of Ras-C. The maximum wavelength in the fluorescence spectra shifted from 550 nm to 530 nm.

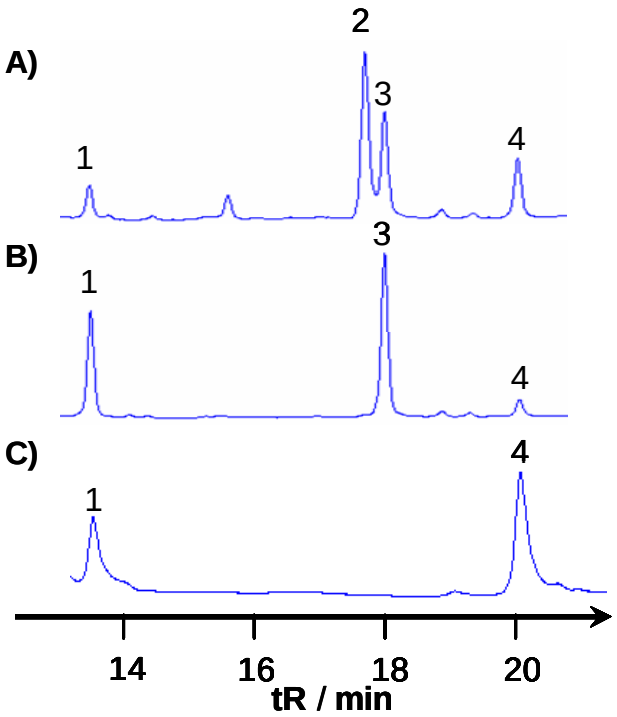

Fig. 3.7 HPLC analysis of the reaction mixture. A) 10 min reaction with probe 3, B) 24 hours reaction with probe 3. C) 2 hours reaction with probe 2. Peak 1, reduced probe 1 with amino group; Peak 2, ligated product with aza-ylide bond; Peak 3, oxidized probe 3; Peak 4, probe 1 with azide group. Each peak was analyzed by mass spectrometry.

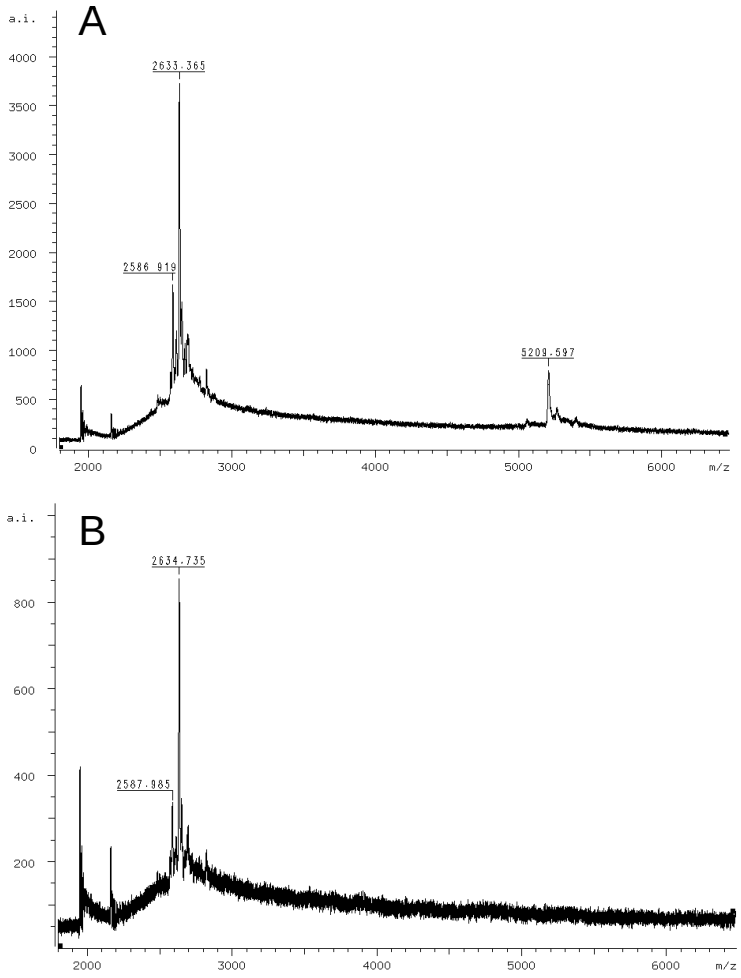

Fig. 3.8 MALDI-TOF spectra of the reaction products between probe 1 and probe 3 after 10 min (A) or 24 hour (B). The peak derived from ligated product was found only at 10min (calculated mass, $C_{183}H_{212}N_{59}O_{92}P_{15}S$ 5204.0; found 5209.6).

3.4. Discussion

Many fluorogenic probes for sensing oligonucleotides have been developed, such as MBs [6, 16] and quenched autoligation (QUAL) probes [14, 18. 28]. These probes produce a fluorescent signal based on the RET mechanism, for which a pair of quencher and fluorescence dyes is normally used. The quenching efficiency reaches a maximum of 98%, if the position of a pair of dyes is carefully optimized [24]. The corresponding S/B ratio is 50:1. In contrast, rhodamine azide of the RETF probe emits by an absorption change triggered by a chemical reaction. The S/B ratio reaches 2100:1 (Figure 3.2). This property is clearly helpful for sensing. Another issue for an MB is that protein binds to the beacon to yield a false fluorescent signal [29]. QUAL probes also have the potential to yield false fluorescent signals through automatic hydrolysis of the quencher. A novel fluorogenic system has been reported, that is nucleic acid-triggered fluorescent probe activation by the Staudinger reaction, and showed that the fluorescence signal emerged subsequent to cleavage of the ester bond, which produces the possibility of yielding background fluorescence by automatic or enzymatic hydrolysis of the ester bond [25]. The method has not been applied to the detection of cellular RNAs. On the other hand, the RETF probe accepts not only TPP in the Staudinger reaction, but also other reducing reagents, such as DTT, for reduction of the azide group to switch the fluorescence on and has no hydrolysis problems, which results in minimization of background fluorescence. In addition, as shown in Figure 3.4, the RETF probe has proved to be fully stable under various conditions such as pH 5–10, light irradiation at 490 nm, and a high temperature of 90 °C. This result implies that the RETF probe operates under wide biological conditions without producing an undesirable false fluorescence signal. An issue of our method to be solved is oxidative deactivation of the reducing reagent on the probe in solution, although that does not produce a false signal. We showed one example of single base discrimination study. The discrimination ability depends on the identity of the mutation and its nearest neighbors, as well as the length of the probe. Therefore, the probe should be carefully designed in each case to achieve single nucleotide resolution.

We carefully analyzed the reaction mechanism between rhodamine azide and reducing

reagents. The DTT probe directly reduces rhodamine azide on the probe to fluorescent rhodamine amine (Figure 3.1). On the other hand, the reaction of the TPP probe initially produces a fluorescent ligation product with an aza-ylide bond, then gives a fluorescent product with rhodamine amine through hydrolysis of the aza-ylide bond (Figure 3.1). The key finding here is that rhodamine aza-ylide derivative is fluorescent. This mechanism was supported by several experimental results. In a small compound, rhodamine azide **2** is directly reduced to amine **1** by DTT. The rhodamine aza-ylide derivative **5b** was isolated from the reaction of **2** with TPP (Scheme 3.2). Aza-ylide **5b** with open lactone form was stable in methanol and showed fluorescence emission at 550 nm, as opposed to amine **2**, which emits fluorescence at 520 nm (Figure 3.2). Interestingly, when the trialkylphosphine TCEP was employed as a reducing reagent, rhodamine azide **2** was directly reduced to amine **2** without formation of the aza-ylide product in methanol (Figure 3.4). This result suggests that TPP as a triarylphosphine can stabilize the aza-ylide intermediate due to the presence of long π-conjugation. The reaction of the rhodamine azide probe with the reducing probe on the DNA template proceeded in a similar manner as the reaction of rhodamine azide **2** in the small compound. The existence of a ligated product with an aza-ylide linkage was verified by HPLC and mass spectrometric analysis shown in Figure 3.7 and Figure 3.8. Further spectroscopic analysis clearly indicates hydrolysis of the aza-ylide bond in solution with increasing emission signal at 530 nm resulting from the formation of the amino rhodamine probe (Figure 3.6).

Fluorescence activation by reduction of the azide group of rhodamine is a new molecular mechanism as a fluorogenic compound. After reduction of the azide group, the rhodamine derivative opens the lactone ring to form a carboxylate and emits fluorescence. The reaction of the TPP probe is complete within 10–15 min with both DNA and RNA targets. The reaction speed is faster than other DNA templated chemical reactions that are able to produce fluorescence. It could be applied to detect RNA species in living cells. Future work will be aimed at making new azide fluorescent compounds for multiple color detection and sensing RNA species in living cells.

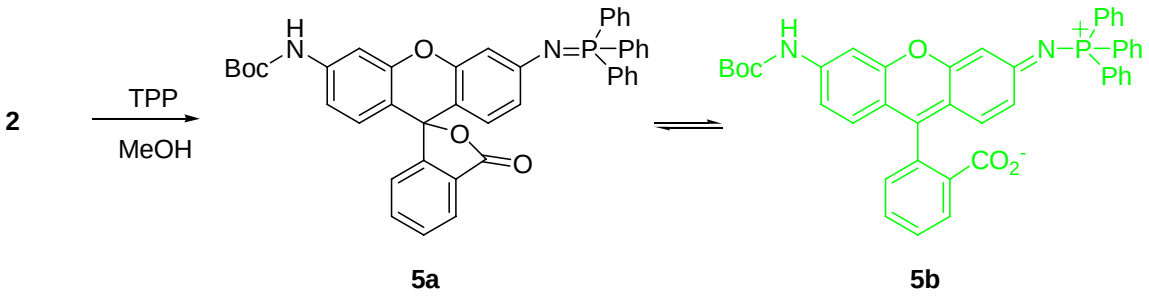

Scheme 3.2

References

1. DeLong, E. F., Wickham, G. S., and Pace, N. R. (1989) Phylogenetic stains: ribosomal RNA-based probes for the identification of single cells. *Science 243*, 1360-1363.
2. Levsky, J. M., and Singer, R. H. (2003) Fluorescence in situ hybridization: past, present and future. *J. Cell Sci. 116*, 2833-2838.
3. Amann, R., Fuchs, B. M., and Behrens, S. (2001) The identification of microorganisms by fluorescence in situ hybridisation. *Curr. Opin. Biotechnol. 12*, 231-236.
4. Moter, A., and Gobel, U. B. (2000) Fluorescence in situ hybridization (FISH) for direct visualization of microorganisms. *J. Microbiol. Methods 41*, 85-112.
5. Levsky, J. M., Shenoy, S. M., Pezo, R. C., and Singer, R. H. (2002) Single-cell gene expression profiling. *Science 297*, 836-840.
6. Tyagi, S., and Kramer, F. R. (1996) Molecular beacons: probes that fluoresce upon hybridization. *Nature Biotechnol. 14*, 303-308.
7. Sando, S., and Kool, E. T. (2002) Quencher as leaving group: efficient detection of DNA-joining reactions. *J. Am. Chem. Soc. 124*, 2096-2097.
8. Okamoto, A., Tanaka, K., Fukuta, T., and Saito, I. (2003) Design of base-discriminating fluorescent nucleoside and its application to t/c SNP typing. *J. Am. Chem. Soc. 125*, 9296-9297.
9. Babendure, J. R., Adams, S. R., and Tsien, R. Y. (2003) Aptamers switch on fluorescence of triphenylmethane dyes. *J. Am. Chem. Soc. 125*, 14716-14717.
10. Kolpashchikov, D. M. (2006) A binary DNA probe for highly specific nucleic Acid recognition. *J. Am. Chem. Soc. 128*, 10625-10628.
11. Ha, T., Enderle, T., Ogletree, D. F., Chemla, D. S., Selvin, P. R., and Weiss, S. (1996) Probing the interaction between two single molecules: Fluorescence resonance energy transfer between a single donor and a single acceptor. *Proc. Nat. Acad. Sci. USA 93*, 6264-6268.
12. Piatek, A. S., Tyagi, S., Pol, A. C., Telenti, A., Miller, L. P., Kramer, F. R., and Alland, D. (1998) Molecular beacon sequence analysis for detecting drug resistance in Mycobacterium tuberculosis. *Nature Biotechnol. 16*, 359-363.
13. Sando, S., and Kool, E. T. (2002) Imaging of RNA in bacteria with self-ligating quenched probes. *J. Am. Chem. Soc. 124*, 9686-9687.
14. Abe, H., and Kool, E. T. (2006) Flow cytometric detection of specific RNAs in native human cells with quenched autoligating FRET probes. *Proc. Nat. Acad. Sci. USA 103*, 263-268.
15. Sokol, D. L., Zhang, X., Lu, P., and Gewirtz, A. M. (1998) Real time detection of DNA.RNA hybridization in living cells. *Proc. Nat. Acad. Sci. USA 95*, 11538-11543.
16. Bratu, D. P., Cha, B.-j., Mhlanga, M. M., Kramer, F. R., and Tyagi, S. (2003) Visualizing the distribution and transport of mRNAs in living cells. *Proc. Nat. Acad. Sci. USA 100*, 13308-13313.
17. Tsuji, A., Koshimoto, H., Sato, Y., Hirano, M., Sei-Iida, Y., Kondo, S., and Ishibashi, K. (2000) Direct observation of specific messenger RNA in a single living cell under a fluorescence microscope. *Biophys. J. 78*, 3260-3274.
18. Sando, S., Abe, H., and Kool, E. T. (2004) Quenched auto-ligating DNAs: multicolor identification of nucleic acids at single nucleotide resolution. *J. Am. Chem. Soc. 126*, 1081-1087.
19. Maeda, H., Fukuyasu, Y., Yoshida, S., Fukuda, M., Saeki, K., Matsuno, H., Yamauchi, Y., Yoshida, K., Hirata, K., and Miyamoto, K. (2004) Fluorescent probes for hydrogen peroxide based on a non-oxidative mechanism. *Angew. Chem. Int. Ed. Engl. 43*, 2389-2391.
20. Miller, E. W., Tulyathan, O., Isacoff, E. Y., and Chang, C. J. (2007) Molecular imaging of hydrogen peroxide produced for cell signaling. *Nat. Chem. Biol. 3*, 263-267.
21. Kojima, H., Nakatsubo, N., Kikuchi, K., Kawahara, S., Kirino, Y., Nagoshi, H., Hirata, Y., and Nagano, T. (1998) Detection and imaging of nitric oxide with novel fluorescent indicators: Diaminofluoresceins. *Anal. Chem. 70*, 2446-2453.
22. Dale, T. J., and Rebek, J., Jr. (2006) Fluorescent Sensors for Organophosphorus Nerve Agent Mimics. *J. Am. Chem. Soc. 128*, 4500-4501.
23. Lemieux, G. A., de Graffenried, C. L., and Bertozzi, C. R. (2003) A fluorogenic dye activated by the Staudinger ligation. *J. Am. Chem. Soc. 125*, 4708-4709.
24. Marras, S. A., Kramer, F. R., and Tyagi, S. (2002) Efficiencies of fluorescence resonance energy transfer and contact-mediated quenching in oligonucleotide probes. *Nucleic Acids Res. 30*, e122.
25. Cai, J., Li, X., Yue, X., and Taylor, J. S. (2004) Nucleic acid-triggered fluorescent probe activation by the Staudinger reaction. *J. Am. Chem. Soc. 126*, 16324-16325.

26. Lavis, L. D., Chao, T. Y., and Raines, R. T. (2006) Fluorogenic label for biomolecular imaging. *ACS Chem. Biol*. *1*, 252-260.
27. Sakurai, K., Snyder, T. M., and Liu, D. R. (2005) DNA-templated functional group transformations enable sequence-programmed synthesis using small-molecule reagents. *J. Am. Chem. Soc. 127*, 1660-1661.
28. Silverman, A. P., and Kool, E. T. (2006) Detecting RNA and DNA with templated chemical reactions. *Chem. Rev. 106*, 3775-3789.
29. Molenaar, C., Marras, S. A., Slats, J. C., Truffert, J. C., Lemaitre, M., Raap, A. K., Dirks, R. W., Tanke, H. J., Dirks, R. W., Molenaar, C., and Tanke, H. J. (2001) Linear 2' O-Methyl RNA probes for the visualization of RNA in living cells. *Nucleic Acids Res. 29*, E89.

Chapter 4

Reduction-triggered red fluorescent probes for dual-color detection of oligonucleotide sequences

Chapter 4

Reduction-triggered red fluorescent probes for dual-color detection of oligonucleotide sequences

4

4.1. Introduction

Single nucleotide polymorphisms (SNPs) in human genes, which cause various genetic disorders are important targets for diagnosis [1]. Fluorescence-based reactions based on nucleic acid templates are used for detection of nucleic acids with single nucleotide specificity [2-7]. This strategy exploits the target strand as a template between two functionalized DNAs or PNAs. For example, native chemical ligation [8, 9], catalytic hydrolysis [10-13], the Staudinger reaction [14-16], transfer of reporter group [17], DNAzyme [18, 19], an S_N2 quencher displacement reaction [20-25], and organomercury-activated reaction [26] have been applied to fluorescent nucleic acid reactions. In addition to DNA, these methods could allow for detection of RNAs in cells [15, 18, 20, 23, 25]. Designing stable fluorescent probes specific for the target under physiological conditions continues to be a challenge.

Recently, we designed a new fluorogenic molecule, rhodamine azide, that is activated by a specific reducing reagent on the oligonucleotide target and is very stable under biological conditions (Scheme 4.1.A) [15]. The reaction of rhodamine azide triggered by reduction of the azide group opens the lactone ring to activate the fluorescence. The reduction-triggered fluorescence (RETF) probe consists of two DNA strands, with one

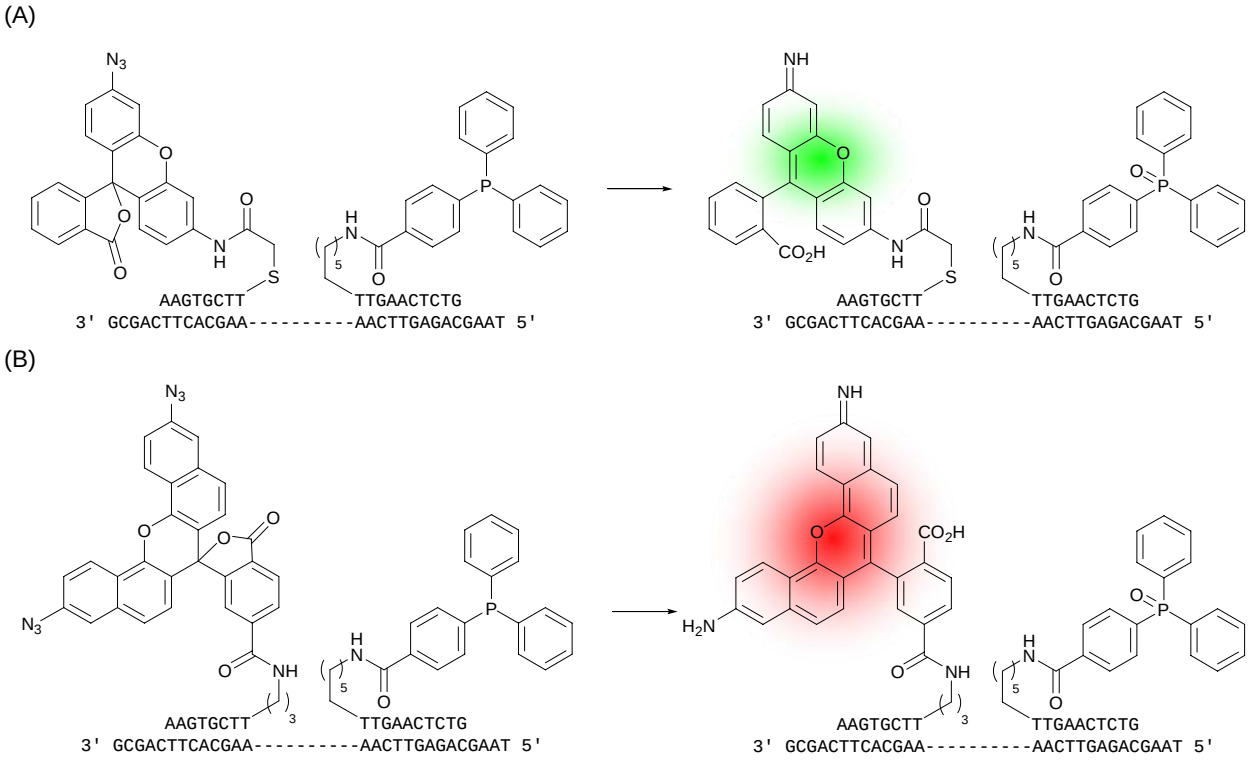

Scheme 4.1 Probe sequences and structures of (A) previous and (B) new RETF system.

probe having a rhodamine azide and the other having reducing reagents such as dithiothreitol or triphenylphosphine. The RETF probe uses a reaction between the azide group of nonfluorescent rhodamine derivatives and reducing reagents on an oligonucleotide template. This reaction proceeds only in the presence of complementary oligonucleotide templates. The RETF probe was used to sense the nucleic acids in vitro and endogenous RNA in bacterial cells. A single nucleotide difference is most easily distinguished by using two colors, generating a qualitative difference when the target is altered [27, 28]. Imaging of cellular RNA requires a fluorogenic molecule with an emission wavelength toward the red end of the spectrum [29, 30]. Here we synthesized a new red fluorogenic molecule derived from naphthorhodamine (Scheme 4.1.B). Our dual-color RETF system can distinguish single nucleotide differences in a target.

4.2. Materials and Methods

*4.2.1. Carboxylic naphthorhodamine (**1**)*

To a mixture of 6-amino-1-naphthol (95.8 mg, 0.602 mmol) and 4-carboxyphthalic anhydride (86.8 mg, 0.452 mmol) was added triflic acid (1.5 ml). The reaction mixture was stirred at 100 °C for 2 h and at 140 °C for 2 h, then was cooled to room temperature and poured into 40 ml brine (including 5 ml 5% H_2SO_4). The product was extracted into CH_2Cl_2/MeOH (4:1). The organic layer was combined and washed with brine, dried by Na_2SO_4, concentrated, and subjected to flash column chromatography (silica gel, 4:1,CH_2Cl_2:MeOH) to give a crude product (78.3 mg, 0.536 mmol, 89%) as black crystalline solid. ^{1}H NMR (δ_H)(400 MHz, CD_3OD) 6.74 (1/2H, d, J = 8.3 Hz), 6.89 (1H, d, J = 7.1 Hz), 6.91 (1H, d, J = 8.8 Hz), 7.28 (1/2H, d, J = 8.0 Hz), 7.57 (1H, d, J = 5.8 Hz), 7.59 (1H, d, J = 5.8 Hz), 7.70 (2H, m), 7.85 (2H, brd, J = 7.8 Hz), 8.32 (1/2H, dd, J = 1.4 Hz, 8.0 Hz), 8.45 (1/2H, d, J = 9.0 Hz), 8.69 (1/2H, s), 8.96 (2H, d, J = 9.0 Hz), 9.37 (1/2H, m). ^{13}C NMR (δ_C)(100 MHz, CD_3OD) 108.31, 120.02, 120.90, 121.89, 122.92, 123.22, 124.20, 124.21, 125.32, 125.68, 125.96, 126.10, 126.27, 126.42, 128.05, 128.21, 129.29, 129.78, 129.85, 129.90, 129.98, 131.26, 131.34, 131.40, 131.55, 131.96, 132.20, 132.43, 133.01, 133.86, 134.09, 134.25,

134.70, 135.07, 137.51, 138.41, 138.67, 140.78, 140.85, 144.37, 148.22, 155.61, 160.22, 160.31, 167.46, 167.77, 167.85, 167.91, 169.50. QSTAR (Applied Biosystems/MDS SCIEX) (ESI): [M+H^+]: 475.1294, found: 475.1260

*4.2.2. Carboxylic naphthorhodamine bisazide (**2**)*

Compound **1** was dissolved in water (5 ml) and 12N HCl (1 ml). Then sodium nitrite (92.5 mg, 1.34 mmol) was added. The reaction mixture was stirred for 1 h and NaN_3 (104.5 mg, 1.61 mmol) was added slowly. After stirring for 1 h at ambient temperature the product was extracted into CH_2Cl_2. The organic layer was washed with brine, dried by Na_2SO_4, concentrated, and subjected to flash column chromatography (silica gel, 7:1, CH_2Cl_2:MeOH) to give bis-azide (16.7 mg, 31.7 μmol, 10.5% for two steps) as pale yellow crystalline solid. ^{1}H NMR (δ_H) (300 MHz, DMSO) 6.97 (2H, d, J = 6.0 Hz), 7.47-7.80 (7H, m), 8.30 (2H, d, J = 9.0 Hz), 8.52 (1H, s), 8.85 (2H, d, J = 9.0 Hz). ^{13}C NMR (δ_C) (75 MHz, DMSO) 82.56, 111.34, 116.16, 120.06, 120.55, 123.62, 124.33, 124.83, 125.05, 125.88, 126.27, 134.99, 136.41, 139.67, 145.69, 156.36, 166.01, 167.89. QSTAR (Applied Biosystems/MDS SCIEX) (ESI): [M+H^+]: 527.1104, found: 527.1089

*4.2.3. Naphthorhodamine bisazide NHS ester (**3**)*

To a solution of compound **2** (67.7 mg, 0.129 mmol) in DMF (3 ml) was added N-hydroxysuccinimide (16.9 mg, 0.146 mmol) and DCC (31 mg, 0.150 mmol). The reaction mixture was stirred at ambient temperature for 3 h and filtered. The filtrate was partitioned by AcOEt and H_2O (x 2). The organic layer was washed by brine, dried by Na_2SO_4, concentrated, and subjected to flash column chromatography (silica gel, 2:1, Hexane:AcOEt) to give the NHS ester (78.3 mg, 0.125 mmol, 97%) as pale yellow crystalline solid. ^{1}H NMR (δ_H)(400 MHz, $CDCl_3$) 2.84 (2H, brs), 2.95 (2H, brs), 6.81 (1H, d, J = 8.0 Hz), 6.81 (1H, d, J = 8.8 Hz), 7.29 (1/2H, d, J = 8.3 Hz), 7.35 (2H, m), 7.45 (4H, m), 7.85 (1/2H, s), 8.25 (1/2H, d, J = 8.0 Hz), 8.40 (1H, m), 8.64 (2H, d, J = 9.0 Hz), 8.90 (1/2H, d, J = 0.7 Hz). ^{13}C NMR (δ_C)(100 MHz, $CDCl_3$)

24.89, 25.51, 25.56, 25.64, 83.29, 83.50, 110.62, 115.66, 119.53, 119.57, 121.01, 121.05, 123.19, 123.25, 123.94, 124.50, 124.80, 125.63, 126.11, 127.05, 127.28, 127.81, 131.08, 131.27, 131.85, 135.11, 136.64, 139.91, 139.97, 146.17, 146.21, 153.58, 156.41, 158.57, 160.19, 160.21, 167.27, 167.50, 168.32, 168.49. QSTAR (Applied Biosystems/MDS SCIEX) (ESI): $[M+Na^+]$: 646.1087, found: 646.1076

*4.2.4. Carboxylic naphthorhodamine monoazide (**4**)*

To a solution of **2** (10 mg, 0.02 mmol) in DMF (280 μl) was added tris(2-carboxyethyl)phosphine hydrochloride (5.44 mg, 0.02 mmol) in H_2O (100 μl) slowly. After the reaction mixture was stirred for 1 h, the product was extracted into $CHCl_3$. The organic layer was washed by brine, dried by Na_2SO_4, concentrated, and subjected to flash column chromatography (silica gel, 10:1,CH_2Cl_2:MeOH) to give the mono-azide (7.0 mg, 0.014 mmol, 74%) as pale blue crystalline solid. ^{1}H NMR (δ_H)(400 MHz, $CDCl_3$) 6.51-6.54 (1H, m), 6.69-6.73 (1H, m), 6.87 (1H, s), 7.08-7.39 (6H, m), 7.64 (1/2H, s), 8.07 (1/2H, d, J = 8.0 Hz), 8.23-8.35 (2H, m), 8.58 (1H, t, J = 16.0 Hz). ^{13}C NMR (δ_C)(100 MHz, $CDCl_3$) 108.98, 109.20, 109.25, 110.94, 112.85, 116.96, 118.04, 119.94, 120.08, 120.76, 112.64, 123.71, 124.02, 124.21, 124.49, 125.32, 125.47, 125.98, 127.25, 128.17, 132.40, 136.78, 137.71, 138.15, 141.49, 146.11, 147.96, 148.06, 148.13, 149.61, 158.14. QSTAR (Applied Biosystems/MDS SCIEX) (ESI): $[M+H^+]$: 501.1193, found: 501.1206

4.2.5. Synthesis of unmodified oligonucleotides

All oligonucleotides were synthesized on a 0.2 μmol scale on a DNA synthesizer (H-8-SE; Gene World) using standard phosphoroamidite coupling chemistry. Deprotection and cleavage from the CPG support was carried out by incubation in concentrated ammonia for 4 h at 55 °C. Following deprotection, the oligonucleotides were purified by reverse-phase column chromatography (MicroPure II column; Biosearch Technologies), and quantitated by UV absorbance using the nearest neighbor approximation to calculate molar absorptivities.

4.2.6. 3' naphthorhodamine azide-conjugated oligonucleotide (probe 5)

Compound **3** was reacted with 3′ amino-modified oligonucleotide. 3′ PT-amino-modifier C3 CPG (Glen Research) was used to prepare 3' amino-modified oligonucleotide. 50 nmol of the 3′ amino-modified oligonucleotide in 50 μl of 80 mM sodium tetraborate (pH 8.5) were shaken for 5 h at room temperature with 0.75 μmol of compound 3 in 200 μl of dimethylformamide. The reacted products were collected by ethanol precipitation. Next, the collected products were purified by reverse-phase HPLC (0–80% acetonitrile/50 mM triethylammonium acetate gradient). The probe structure was confirmed by ESI–TOF mass spectrometry. 5′-compound 3-AAG**G**GCTT-3′: calculated mass, $C_{111}H_{119}N_{39}O_{53}P_8$ 3093.57; found 3093.77.

4.2.7. 5' Triphenylphosphine (TPP)-linked oligonucleotide (probe 6)

Carboxy-triphenylphosphine (TPP) NHS ester was reacted with 5′ amino-modified oligonucleotide. 5′ amino-modifier C6 (Glen Research) was used to prepare 5′ amino-modified oligonucleotide. 50 nmol of the 5′ amino-modified oligonucleotide in 135 μl of 93 mM sodium tetraborate (pH 8.5) were shaken for 5 h at room temperature with 2 μmol of TPP NHS ester in 115 μl of dimethylformamide. The reacted products were collected by ethanol precipitation. Next, the collected products were purified by reverse-phase HPLC (0–50% acetonitrile/50 mM triethylammonium acetate gradient). The probe structure was confirmed by ESI–TOF mass spectrometry. 5′-TPP-TTGAACTCTG-3′: calculated mass, $C_{123}H_{152}N_{35}O_{64}P_{11}$ 3483.68; found 3483.70. A peak corresponding to the oxidized product (+O) was also seen and presumed to arise from oxidation during purification.

4.2.8. 3' rhodamine-azide-conjugated oligonucleotide (probe 10)

The bromoacetyl group of the rhodamine-azide was reacted with the phosphorothioate group on the ODNs. For 3′ phosphorothioate sequences, the 3′-phosphate CPG was sulfurized by the sulfrizing reagent (Glen Research) after the

first nucleotide was added. 75 nmol of the 3′-phosphorothioate oligonucleotide in 50 μl of 400 mM triethylammonium bicarbonate buffer were shaken for 5 h at room temperature with 750 nmol of rhodamine-azide in 200 μl of dimethylformamide. The reacted products were collected by ethanol precipitation. Next, the products were purified by reverse-phase HPLC (0–80% acetonitrile/50 mM triethylammonium acetate gradient). The probe structure was confirmed by ESI–TOF mass spectrometry. 5′-AAG**T**GCTT-Rh_azide-3′: calculated mass, $C_{101}H_{113}N_{33}O_{53}P_8S$ 2915.48; found 2915.69.

4.2.9. Measurement of quantum yield

A 1 mM DMF stock solution of each compound was prepared. Absorption spectra were obtained with a 190 mM tris-HCl buffer (pH 7.2) solution of each compound at the desired concentration, adjusted by appropriate dilution of the 1 mM DMF stock solution. For determination of the quantum efficiency of fluorescence ($\boldsymbol{\Phi}_{fl}$), naphthofluorescein in carbonate/bicarbonate buffer (pH 9.5) was used as a fluorescence standard (Φ = 0.14). The quantum efficiency of fluorescence was obtained with the following equation (F denotes fluorescence intensity at each wavelength and $\boldsymbol{\Sigma}$ [F] was calculated by summation of fluorescence intensity).

$$\boldsymbol{\Phi}_{fl}^{\ sample} = \boldsymbol{\Phi}_{fl}^{\ standard} \mathrm{Abs}^{\ standard} \boldsymbol{\Sigma}\,[F^{\ sample}] \,/\, \mathrm{Abs}^{\ sample} \boldsymbol{\Sigma}\,[F^{\ standard}]$$

4.2.10. Detection of DNA sequence with red colored RETF probe

Reactions on the DNA template were performed in 1.2 ml of tris-HCl buffer (20 mM, pH 7.2) containing 100 mM $MgCl_2$ and 0.01 mg/ml BSA with target *bcr/abl-1* (250 nM), probe **5** (250 nM), and probe **6** (250 nM) at 37 °C. The increase of fluorescence intensity produced by reduction of compound **3** on probe **5** was continuously monitored at time intervals. Reactions were observed by fluorescence spectrometry (FP-6500; JASCO). For the time course of the azide reduction, the fluorescence intensity was measured for 0.5 s at 1 min intervals: excitation, 595 nm; emission, 655 nm.

4.2.11. Dual color SNP typing

The probe **5** (red) and probe **10** (green) were used for the dual-color SNPs typing. Reactions on the DNA template were performed in 1.2 ml of tris-HCl buffer (20 mM, pH 7.2) containing 100 mM $MgCl_2$ and 0.01 mg/ml BSA with 250 nM of *bcr/abl-1* (5'-TAA GCA GAG TTC AAA AGC **C**CT TCA GCG-3'; complementary to probe 1) or *bcr/abl-2* (5'-TAA GCA GAG TTC AAA AGC **A**CT TCA GCG-3'; complementary to probe 2), probe **5** (250 nM), probe **6** (250 nM) and probe **10** (250 nM) at 37 °C. The increase of fluorescence intensity was continuously monitored at time intervals. For the time course of the azide reduction, the fluorescence intensity was measured for 0.5 s at 1 min intervals: ex/em 490 nm/550 nm (for probe **10**); 595 nm/655 nm (for probe **5**). For standardization, all fluorescence intensities derived from both probes were divided by the intensity in case of using each full-match target DNA at 30 min.

4.3. Results and Discussion

4.3.1. Design and synthesis of red colored naphthorhodamine azide

Previous studies showed that rhodamine fluorescence was controlled by the lactone ring, which is altered by reduction of the azide group (Scheme 4.1.A) [15]. After opening the lactone, the longer conjugated system emits fluorescence. This mechanism can help design other fluorogenic compounds [31]. We expanded the two phenyl groups of rhodamine to naphthyl groups for naphthorhodamine (Scheme 4.1.B). The expanded π system of the naphthyl group red shifts emission compared with rhodamine. In addition, the conjugated system of naphthorhodamine should have a similar fluorogenic molecular mechanism to rhodamine. We designed a new fluorogenic molecule of naphthorhodamine bis-azide and N-hydroxysuccinimide (NHS)-activated carboxyl group for conjugation with a DNA probe. The synthesis of naphthorhodamine azide derivative **3** is shown in Scheme 4.2. A solution of 6-amino-1-naphthol and 4-carboxyphthalic anhydride in trifluoromethane sulfonic

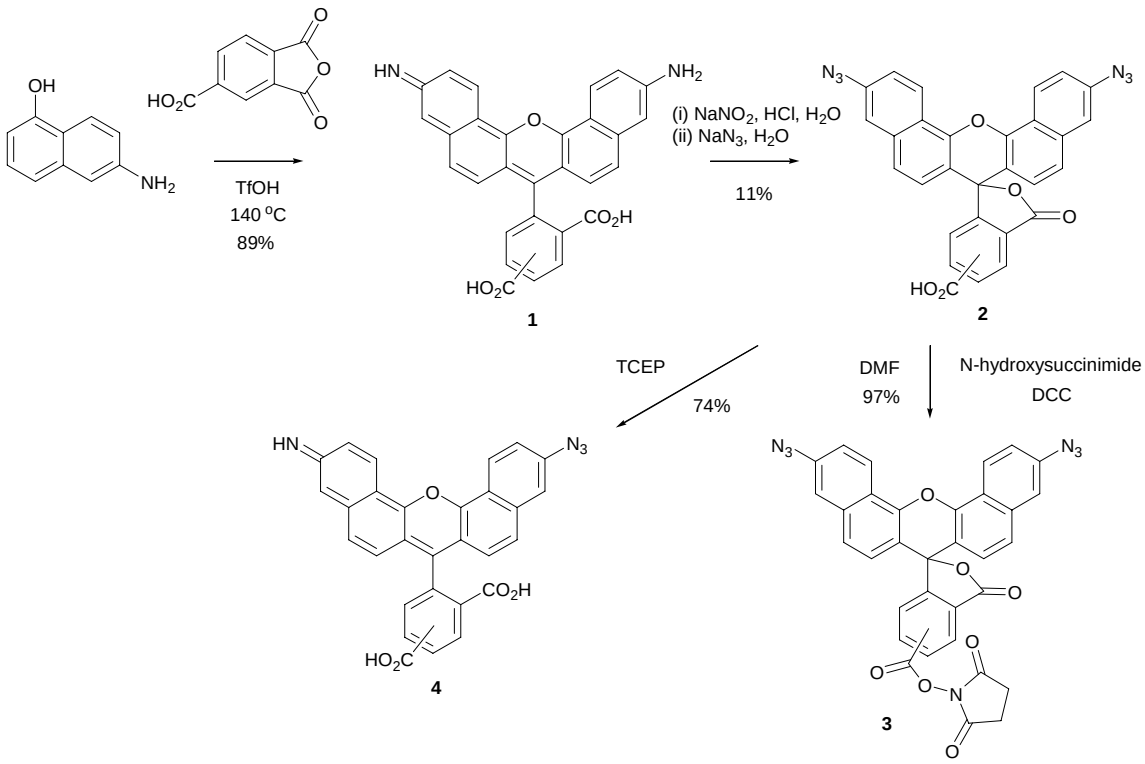

Scheme 4.2 Synthesis of fluorogenic compound **3**.

acid was heated at 140 °C for 2 hours to give a mixture of two regioisomers of carboxynaphthorhodamine **1** with a yield of 89%. Two isomers were not clearly separated by silica gel chromatography. Finally, preparative reverse-phase HPLC was used to purify the two isomers. HPLC peak area analysis showed that the isomers existed in a 2:1 ratio, and the major isomer eluted slowly (Figure 4.1.A). The major isomer was shown to be 5-carboxynaphthorhodamine by NMR analysis. HMBC spectrum indicated long-range correlations from H-4 to both carbonyl carbons of 3- and 5-carboxyl groups (Figure 4.2). We found that compound **1** consists of 5-carboxynaphthorhodamine and 6-carboxynaphthorhodamine in a 2:1 ratio. Bisamino-naphthorhodamine **1** was transformed to the diazo intermediate by treatment with $NaNO_2$, and the diazo group was replaced with an azide group by addition of NaN_3 to give carboxynaphthorhodamine-azide **2** in a 2:1 mixture of 5-carboxy or 6-carboxy isomers (Figure 4.1.B) with an 11% yield. The desired NHS ester **3** was prepared by dicyclohexylcarbodiimde-mediated coupling of N-hydroxysuccinimide with compound **2**. Compound **3** was introduced into the DNA probe.

4.3.2. Spectroscopic properties of naphthorhodamin derivatives

We tested the photochemical properties of naphthorhodamine derivatives. Naphthorhodamine azide **2** showed no absorbance at wavelengths longer than 550 nm in 20 mM Tris-HCl buffer (pH 7.2), but the corresponding naphthorhodamine **1** showed a maximum absorption at 585 nm (Figure 4.3.A). When a high concentration of tris(2-carboxyethyl)phosphine hydrochloride (TCEP) was added as a reducing reagent to a solution of azide **2**, a peak with a maximum of 600 nm increased because of reduction of the azide group. Naphthorhodamine monoazide **4** (see supporting information) also showed absorption in the long-wavelength region (maximum at 560 nm), although it was weaker than that of bisamino **1** and TCEP-treated **2**.

We also examined the fluorescence properties of naphthorhodamine derivatives (Figure 4.3.B). No significant fluorescence with excitation at 595 nm was observed for bis-azide **2**. On the other hand, naphthorhodamine **1** showed strong fluorescence

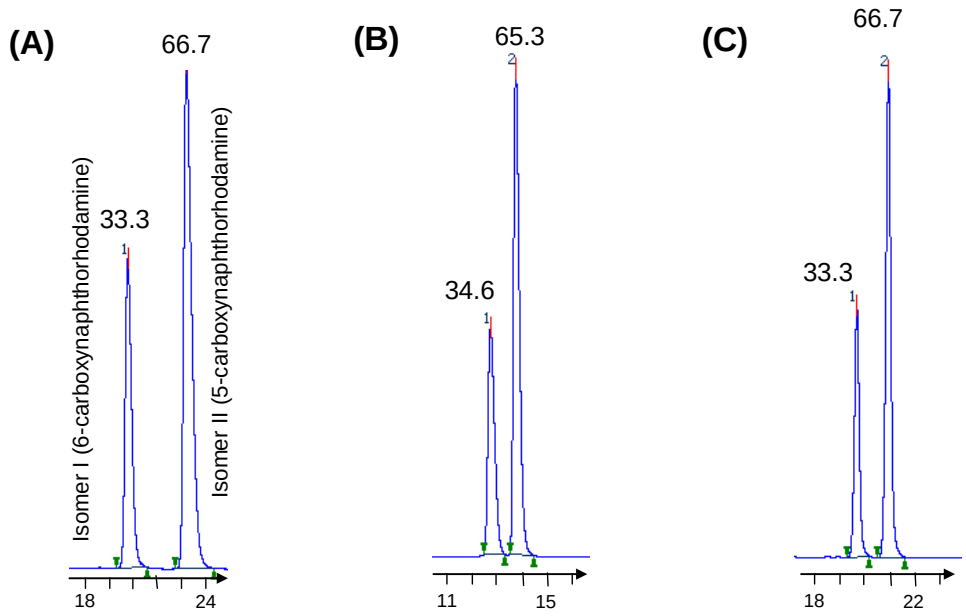

Fig. 4.1. Reverse phase HPLC analysis of the compound 1 (A), 2 (B), and 3 (C). The values indicate that percentage of the area. The HPLC conditions are as follows: 30-30 % (A), 80-80 % (B), or 80-100 % (C), 50 mM triethylammonium acetate / acetonitrile gradient using hydrosphere C18 column (250×4.6 mm; YMC Co., Ltd, Japan). HMBC experiment revealed that isomer I was 6-carboxynaphthorhodamine derivatives and isomer II was 5-carboxynaphthorhodamine derivatives.

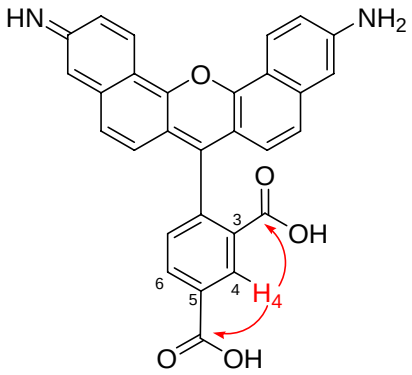

Fig. 4.2. Partial HMBC (1H → 13C) correlations in Isomer II (5-carboxynaphthorhodamine).

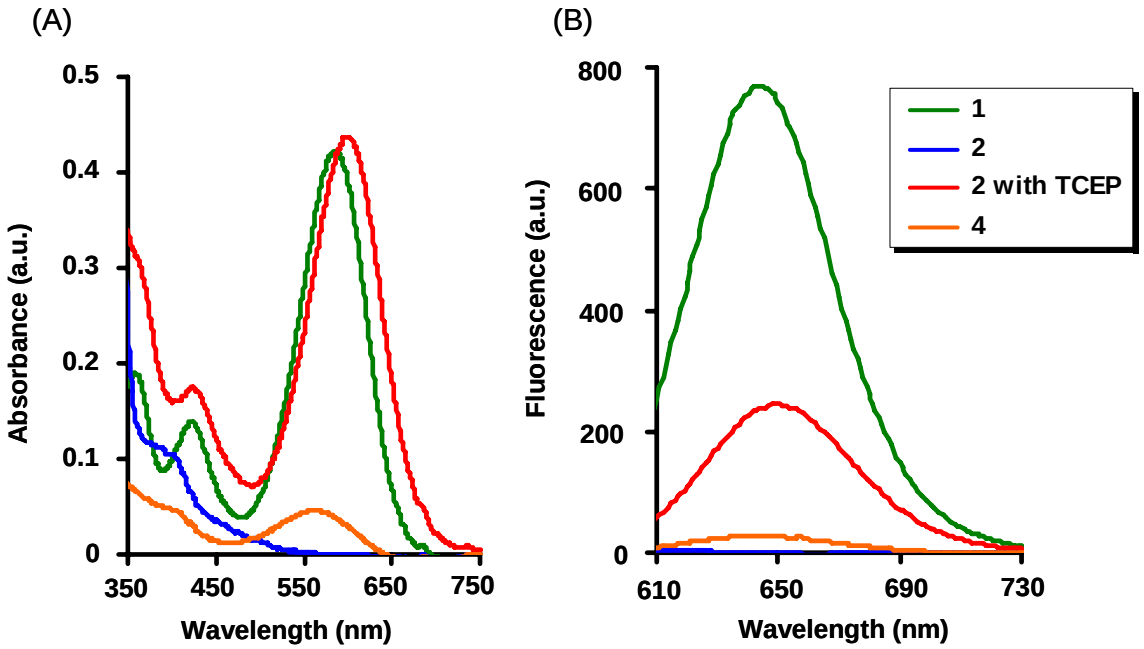

Fig. 4.3. Spectrum analysis. (A) Absorption spectra of 100 μM of **1** (green), **2** (blue), **2** treatment with 10 mM of tris(2-carboxyethyl)phosphine (TCEP) at 25 °C for 1 hour (red), and **4** (orange) in 20 mM Tris-HCl (pH 7.2) buffer at 25 °C; (B) Fluorescent emission spectra with excitation at 595 nm of 10 μM of **1** (green), **2** (blue), **2** treatment with 10 mM of TCEP at 25 °C for 1 hour (red), and **4** (orange) in 20 mM Tris-HCl (pH 7.2) buffer at 25 °C.

emission around 650 nm. After addition of TCEP to the solution of azide **2**, a strong emission appeared around 650 nm, where the emission was enhanced 550-fold. Naphthorhodamine monoazide **4** also had intense fluorescence in the red region. The fluorescent intensity of monoazide **4** was 27 times less than that of **1**. This is likely due to the different *pKa* values for the amino groups of **1** and **4**. Naphthorhodamine **1** and monoazide naphthorhodamine **4** showed high fluorescence quantum yields, 0.13 and 0.068, respectively, in contrast with the low yield of azide **2**, 0.0087 (Table 4.1). This indicates that the observed fluorescence comes from **1** or **4** when a DNA probe with naphthorodamine bis-azide was reacted with the target sequence. We also measured the quantum yields of separated two isomers of compound 1. The quantum yields of 5-carboxy isomer and 6-carboxy isomer were 0.13 and 0.12, respectively (Table 4.1), indicating that the position of carboxylic group has negligible effects on fluorescence emission. The mixture of isomers could be used for further experiments.

4.3.3. Design of RETF probe with napthorhoadmine azide

Next, we synthesized three new DNA probes (Figure 4.4) and two DNA targets. Probe **5** was modified at the 3' terminus with NHS ester-naphthorhodamine-azide **3**, in the location where the NHS ester group of **3** was reacted with the amino linker at the 3' end of the oligonucleotide. Similarly, probe **10** was modified with rhodamine azide by conjugation of phosphorothioate group at the 3' end of the oligonucleotide. Probe **6** was modified at the 5' terminus with 2-carboxytriphenylphosphine, which was conjugated with the 5' amino linker of the DNA probe through an amide bond. DNA target sequences were derived from the human *bcr/abl* gene, which is related to chronic myelogenous leukemia. We designed a wild-type *bcr/abl* sequence (*bcr/abl-1*) as well as a single-base mismatched sequence (*bcr/abl-2*). Probes **5** and **10** were fully matched with targets *bcr/abl-1* and *bcr/abl-2*, respectively. As shown in Scheme 4.3, a reduction–oxidization reaction between probe **5** and **6** on *bcr/abl-1* should produce moderately fluorescent product **7** and phosphine oxide **8** as the product of the first stage of the reaction. As there are reports of catalytic turnover for DNA-templated reactions, our probes could be involved in multiple chemical

Table 1 The quantum yields of the compounds[a]

compound	**1**	**2**	**4**	5-carboxy	6-carboxy
Φ_F[b]	0.13	0.0087	0.068	0.13	0.12

[a]All measurements were performed in Tris-HCl buffer (190 mM, pH 7.2). Compounds were excited at 595 nm.

[b]Quantum yields were determined using naphthofluorescein in carbonate/bicarbonate buffer (pH 9.5) as standard (Φ_F = 0.14).

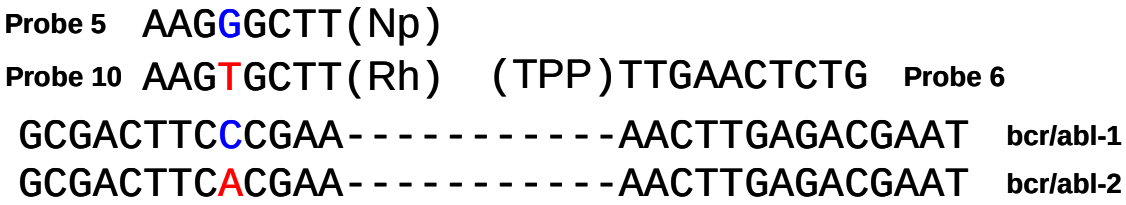

Fig. 4.4. Probe and target DNA sequences of dual color SNP detection. “Np”, “Rh”, and “TPP” indicate naphthorhodamine azide, rhodamine azide, and triphenylphosphine, respectively.

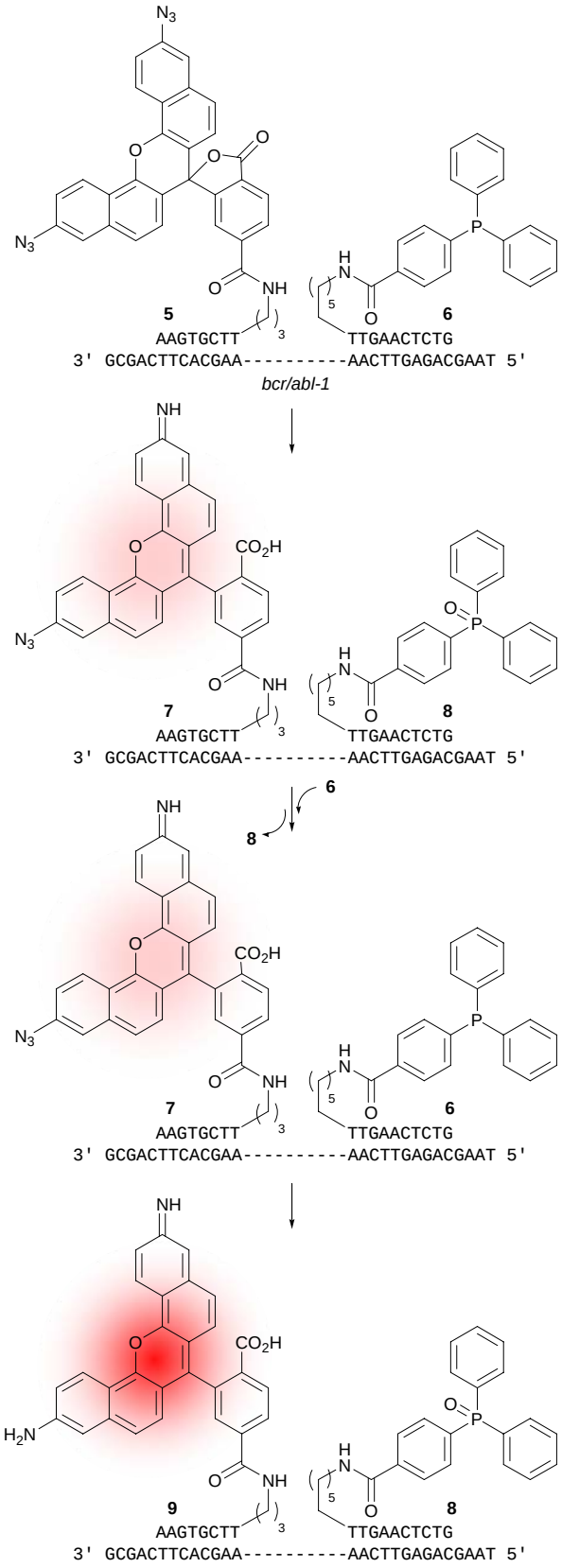

Scheme 4.3. Schematic presentation of a reduction–oxidization reaction between probe **5** and **6** on *bcr/abl-1*.

reactions on DNA templates [4, 11, 22, 32]. We assumed that bis-azide probe **5** reacted with two eq. of phosphine probe **6** and became bis-amino product **9** to yield a strong fluorescence signal. The mechanism is explained by phosphine oxide **8** from the first stage of the reaction falling off of the target, and a second phosphine probe **6** binding to the target and reacting with monoazide probe **7** (Scheme 4.3).

4.3.4. Fluorescence detection of DNA sequence

To prove whether the probes could detect target DNA sequences and emit fluorescence, we tested our naphthorhodamine probe in solution (Figure 4.5). When 250 nM of probes **5** and **6** were incubated in pH 7.2 Tris-HCl buffer, the fluorescence signal at 655 nm increased in the presence of target *bcr/abl-1* over 30 min by reduction of the azide group to the amino group of probe **5**, and no significant increase in fluorescence was observed in the absence of *bcr/abl-1* over 30 min. HPLC and MALDI–TOF mass analyses (Figure 4.6) showed that 80.8% of probe **5** reacted with probe **6** after 30 min to give the corresponding product with monoamino (probe **7**, 61.6%) and bisamino (probe **9**, 19.2%). When two eq. of probe **6** to 250 nM of probe **5** was used, fluorescence signal increased more rapidily than in the case of one eq. of probe **6**. The reaction with two eq. of probe **6** offered 3 times higher intensity in fluorescence than that with one eq. of probe **6** after 30 min. HPLC analysis showed that the reaction of probe **5** (250 nM) and probe **6** (500 nM) gave bisamino probe **9** in yield of 91% and only trace amount of monoamino probe **7** after 24 h. Therefore, in the reaction of probes **5** and **6**, the increase in fluorescence at 655 nm was caused by the mixture of reduced monoamino product **7** and bisamino product **9**, where the bis-amino product was more fluorescent than the monoamino product. In addition, we confirmed that the multiple chemical reactions occurred on the DNA target and that bis-azide naphthorhodamine was transformed to bis-amino naphthorhodamine by two eq. of phosphine (Scheme 4.3).

4.3.5. Dual color discrimination of single base difference

To examine whether the RETF probe could distinguish DNA sequences at the

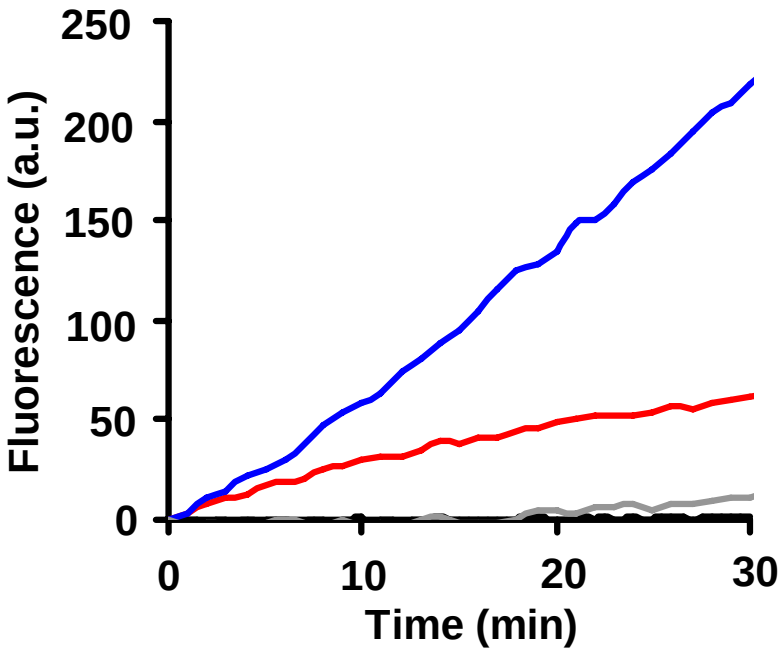

Fig. 4.5. Time course of the fluorescence intensity for the reaction between 250 nM of probe **5** and 250 nM of probe **6** in the presence (red) or absence (black) of 250 nM of *bcr/abl-1*, or between 250 nM of probe **5** and 500 nM of probe **6** in the presence (blue) or absence (gray) of 250 nM of *bcr/abl-1*.

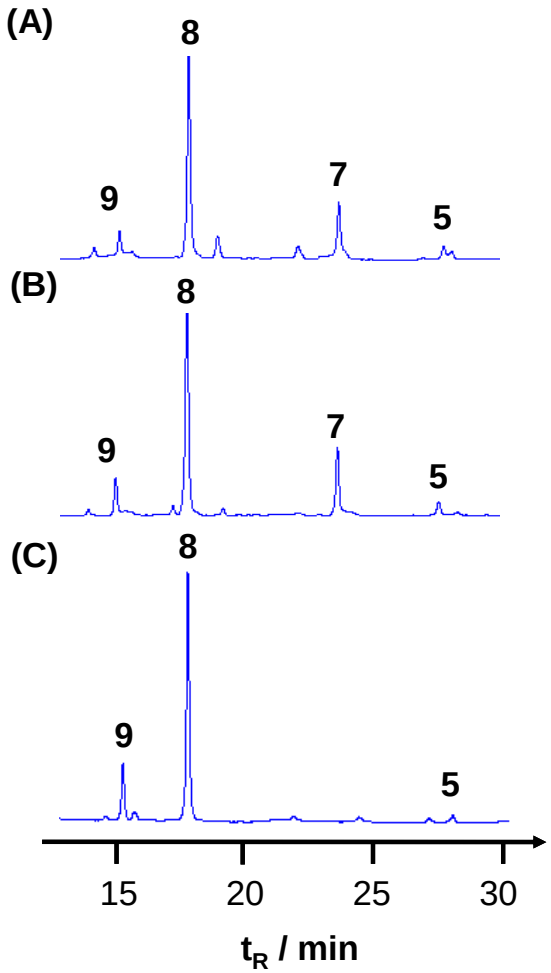

Relative peak area analysis (%)

	1eq. of TPP		2eq. of TPP
	30 min	24 hr	24 hr
Probe **5**	19.2	13.0	9.5
Probe **7**	61.6	57.8	0
Probe **9**	19.2	29.2	90.5

Fig. 4.6. HPLC analysis of the DNA-templated reaction mixture. A) 30 min reaction with 1 equivalent of probe **6**, B) 24 hours reaction with 1 equivalent of probe **6**, C) 24 hours reaction with 2 equivalent of probe **6**. Peak 1, probe **9** (reduced probe **5** with diamino group), calculated: 3042.0, observed: 3041.6; Peak 2, probe **8** (oxidized probe **6**), calculated: 3499.5, observed: 3499.7; Peak 3, probe **7** (reduced probe **5** with monoamino group), calculated: 3067.4, observed: 3067.6; Peak 4, probe **5** with bisazide group, calculated: 3093.3, observed: 3093.6. The reaction products were analyzed by reverse-phase HPLC (0-80 % acetonitrile/50 mM triethylammonium acetate gradient) using hydrosphere C18 column (250×4.6 mm; YMC Co., Ltd, Japan). Each peak was characterized by ESI-mass spectrometry.

single nucleotide level using dual colors, we designed red fluorescent probe **5** as well as green fluorescent probe **10**, previously reported as rhodamine azide probe. Fluorescence signals from the two probes were well separated in their excitation and emission wavelengths (naphthorhodamine ex/em 595/655 nm, rhodamine ex/em 490/550 nm). The target sequences *bcr/abl-1* or *-2* derived from the human *bcr/abl* gene are different at only a single base. In this dual-color probe strategy, the red fluorescent signal should appear when *bcr/abl-1* is added to the solution because only red probe **5** binds to the target and reacts with phosphine probe **6**. Green signal should appear when *bcr/abl-2* exists in solution. Reactions were carried out using one eq. of probe **6** to azide probe **5** or **10**, because two eq. of probe **6** gave undesired background fluorescence signal.

The fluorescence intensities of each color probe were monitored as a function of time in the presence of *bcr/abl-1* or *-2* (Figure 4.7). Fluorescence intensities of the red and green probes were normalized by dividing the initial intensity by the intensity after 30 min for the full-match target and multiplying by factor of 100. A strong fluorescence signal was observed, corresponding to the predicted, correctly matched color probes and targets.

For *bcr/abl-1*, the emission of red probe **5** was 8.1 times higher than the emission of green probe **10** after 30 min. In contrast, the emission of green probe **10** in the presence of *bcr/abl-2* was 30.3 times higher than the emission of red probe **5** after 30 min. To distinguish a single base difference clearly, the ratio of fluorescence intensity of R/G (red/green) must be significant. In this experiment, the C/A difference in *bcr/abl* was achieved by an R/G factor of 8.1 or a G/R factor of 30.3. A lower R/G factor for *bcr/abl-1* is likely caused by a small amount of T-C mismatching between *bcr/abl-1* and green probe **10**, and by a difference in the chemical reaction rate between red probe **5** and green probe **10**. For *bcr/abl-2*, the signal intensity from green probe **10** increased quickly in the initial stage and reached saturation within 20 min, whereas that from red probe **5** increased continuously over 30 min for *bcr/abl-1*, where 19.2% of probe **5** remained after 30 min (Figure 4.6), indicating that the chemical reaction rate of green probe **10** was faster than that of red probe **5**. Our

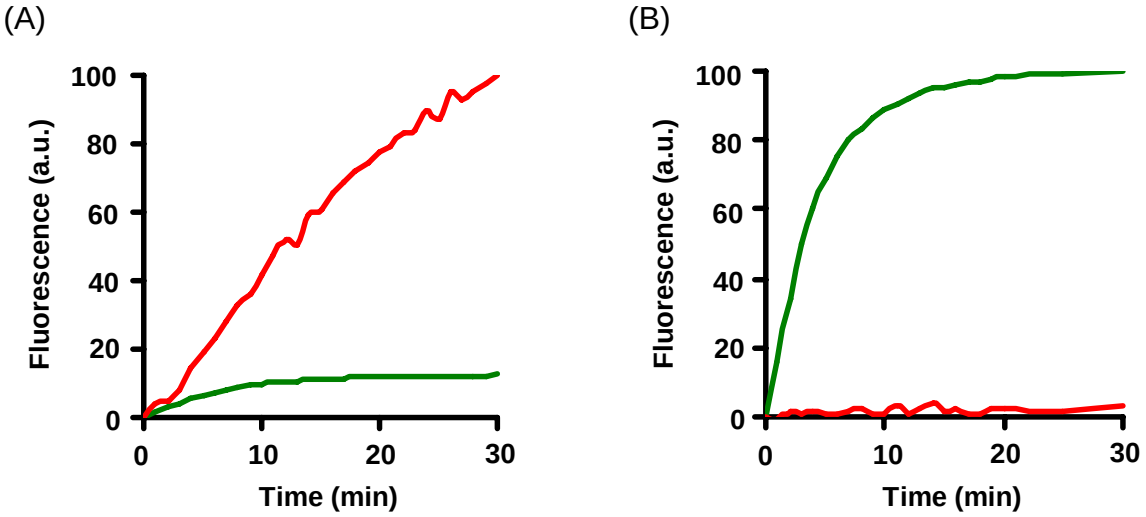

Fig. 4.7. Time course of the fluorescence intensity in the reaction with 250 nM of *bcr/abl-1* (A) or *-2* (B), probe **5** (250 nM), probe **6** (250 nM), and probe **10** (250 nM) at 37 °C. The fluorescence intensity was measured for 0.5 s at 1 min intervals: ex/em 490 nm/550 nm (for probe **10**: green line) and 595 nm/655 nm (for probe **5**: red line).

dual-color RETF system has the potential to detect SNPs rapidly with high sensitivity and selectivity.

References

1. Pinnisi, E. (1998) A closer look at SNPs suggests difficulties. *Science 281*, 1787-1789.
2. Tyagi, S., Bratu, D. P., and Kramer, F. R. (1998) Multicolor molecular beacons for allele discrimination., *Nat. Biotechnol. 16*, 49-58.
3. Silverman, A. P. and Kool, E. T. (2006) Detecting RNA and DNA with templated chemical reactions., *Chem. Rev. 106*, 3775-3789.
4. Grossmann, T. N., Strohbach, A. and Seitz, O. (2008) Achieving turnover in DNA-templated reactions. *Chembiochem 9*, 2185-2192.
5. Li, X. and Liu, D. R. (2004) DNA-templated organic synthesis: nature's strategy for controlling chemical reactivity applied to synthetic molecules. *Angew. Chem. Int. Ed. 43*, 4848-4870.
6. Tyagi, S. and Kramer, F. R. (1996) Molecular beacons: probes that fluoresce upon hybridization. *Nat. Biotechnol. 14*, 303-308.
7. Okamoto, A., Tanaka, K., Fukuta, T. and Saito, I. (2003) Design of base-discriminating fluorescent nucleoside and its application to t/c SNP typing. *J. Am. Chem. Soc. 125*, 9296-9297.
8. Dose, C., Ficht, S. and Seitz, O. (2006) Reducing product inhibition in DNA-template-controlled ligation reactions. *Angew. Chem. Int. Ed. 45*, 5369-5373.
9. Dose, C. and Seitz, O. (2008) Single nucleotide specific detection of DNA by native chemical ligation of fluorescence labeled PNA-probes. *Bioorg. Med. Chem. 16*, 65-77.
10. Ma, Z. and Taylor, J. S. (2000) Nucleic acid-triggered catalytic drug release. *Proc. Natl. Acad. Sci. U.S.A. 97*, 11159-11163.
11. Ma, Z. and Taylor, J. S. (2001) Nucleic acid triggered catalytic drug and probe release: a new concept for the design of chemotherapeutic and diagnostic agents. *Bioorg. Med. Chem. 9*, 2501-2510.
12. Ma, Z. and Taylor, J. S. (2003) PNA-based RNA-triggered drug-releasing system. *Bioconjugate Chem. 14*, 679-683.
13. Brunner, J., Mokhir, A. and Kraemer, R. (2003) DNA-templated metal catalysis. *J. Am. Chem. Soc. 125*, 12410-12411.
14. Cai, J., Li, X., Yue, X. and Taylor, J. S. (2004) Nucleic acid-triggered fluorescent probe activation by the Staudinger reaction *J. Am. Chem. Soc. 126*, 16324-16325.
15. Abe, H., Wang, J., Furukawa, K., Oki, K., Uda, M., Tsuneda, S. and Ito, Y. (2008) A reduction-triggered fluorescence probe for sensing nucleic acids. *Bioconjugate Chem. 19*, 1219-1226.
16. Pianowski, Z. L. and Winssinger, N. (2007) Fluorescence-based detection of single nucleotide permutation in DNA via catalytically templated reaction *Chem. Commun. 7*, 3820-3822.
17. Grossmann, T. N. and Seitz, O. (2006) DNA-catalyzed transfer of a reporter group *J. Am. Chem. Soc., 128*, 15596-15597.
18. Sando, S., Narita, A., Sasaki, T. and Aoyama, Y. (2005) Locked TASC probes for homogeneous sensing of nucleic acids and imaging of fixed E. coli cells. *Org. biomol. Chem. 3*, 1002-1007.
19. Sando, S., Sasaki, T., Kanatani, K. and Aoyama, Y. (2003) Amplified nucleic acid sensing using programmed self-cleaving DNAzyme. *J. Am. Chem. Soc. 125*, 15720-15721.
20. Sando, S. and Kool, E. T. (2002) Imaging of RNA in bacteria with self-ligating quenched probes *J. Am. Chem. Soc. 124*, 9686-9687.
21. Sando, S. and Kool, E. T. (2002) Quencher as leaving group: efficient detection of DNA-joining reactions *J. Am. Chem. Soc. 124*, 2096-2097.
22. Abe, H. and Kool, E. T. (2004) Destabilizing universal linkers for signal amplification in self-ligating probes for RNA *J. Am. Chem. Soc. 126*, 13980-13986.
23. Sando, S., Abe, H. and Kool, E. T. (2004) Quenched auto-ligating DNAs: multicolor identification of nucleic acids at single nucleotide resolution. *J. Am. Chem. Soc. 126*, 1081-1087.
24. Silverman, A. P. and Kool, E. T. (2005) Quenched probes for highly specific detection of cellular RNAs *Trends Biotechnol. 23*, 225-230.
25. Abe, H. and Kool, E. T. (2006) Flow cytometric detection of specific RNAs in native human cells with quenched autoligating FRET probes *Proc. Natl. Acad. Sci. U.S.A. 103*, 263-268.

26. Franzini, R. M. and Kool, E. T. (2008) Organometallic activation of a fluorogen for templated nucleic Acid detection *Org. Lett. 10*, 2935-2938.
27. Hsu, T. M., Law, S. M., Duan, S., Neri, B. P. and Kwok, P. Y. (2001) Genotyping single-nucleotide polymorphisms by the invader assay with dual-color fluorescence polarization detection *Clin. Chem. 47*, 1373-1377.
28. Liu, H., Li, S., Wang, Z., Ji, M., Nie, L. and He, N. (2007) High-throughput SNP genotyping based on solid-phase PCR on magnetic nanoparticles with dual-color hybridization *J. Biotechnol. 131*, 217-222.
29. Rao, J., Dragulescu-Andrasi, A. and Yao, H. (2007) Fluorescence imaging in vivo: recent advances. *Curr. Opin. Biotechnol. 18*, 17-25.
30. Fabian, J., Nakazumi, H. and Matsuoka, M. (1992) Near-infrared absorbing dyes. *Chem. Rev. 92*, 1197-1226.
31. Lavis, L. D., Chao, T. Y. and Raines, R. T. (2006) Fluorogenic label for biomolecular imaging. *ACS Chem. biol. 1*, 252-260.
32. Ficht, S., Mattes, A. and Seitz, O. (2004) Single-nucleotide-specific PNA-peptide ligation on synthetic and PCR DNA templates. *J. Am. Chem. Soc. 126*, 9970-9981.

Chapter 5

Intracellular RNA detection with reduction-triggered fluorescence probe in fixed bacterial cells

Chapter 5

Intracellular RNA detection with reduction-triggered fluorescence probe in fixed bacterial cells

5

5.1. Introduction

In recent years the field of microbiology has been greatly impacted by the application of fluorescent-labeled oligonucleotides, which have made it possible to identify strains of bacteria and other single-celled microorganisms in a few hours [1-3]. Standard labeled oligonucleotides, commonly 15-30 nucleotides long, can be hybridized to ribosomal RNAs in fixed bacterial cells, allowing identification by fluorescence microscopy. A large database of rRNA sequences from many microorganisms now exists [4, 5], allowing the identification of widely different organisms by in situ hybridization. However, such standard oligonucleotide probes have a number of limitations; for example, they show low selectivity and are generally unable to distinguish related sequences of RNA unless there are multiple nucleotide differences [2, 6-8]. Second, standard probes require careful handling to avoid nonspecific signals. Typically, cells are first fixed (killed, permeabilized, and cross linked with formaldehyde). Hybridization is followed by several careful washes to remove unbound probes [1-3]. This preparation takes time, increases the chances of error, and prevents application in live cells.

Here we report on the application of a new class of synthetic quenched DNA probes, RETF probe [9], that involves the reaction between the azide group of rhodamine

derivative and reducing reagent such as triphenylphosphine (described in chapter 3). Such probes display high selectivity for even single nucleotide differences, and because quenching is efficient they require no washing away of unbound probes to observe the signal. We demonstrate their use for direct detection of rRNA sequences in fixed bacterial cells.

5.2. Materials and Methods

5.2.1. Synthesis of unmodified oligonucleotides

All oligonucleotides were synthesized on a 0.2 μmol scale on a DNA synthesizer (H-8-SE; Gene World) using standard phosphoroamidite coupling chemistry. Deprotection and cleavage from the CPG support was carried out by incubation in concentrated ammonia for 4 h at 55 °C. Following deprotection, the oligonucleotides were purified by reverse-phase column chromatography (MicroPure II column; Biosearch Technologies), and quantitated by UV absorbance using the nearest neighbor approximation to calculate molar absorptivities.

5.2.2. 3′rhodamine-azide-conjugated oligonucleotide

The bromoacetyl group of the rhodamine-azide was reacted with the phosphorothioate group on the ODNs. For 3′ phosphorothioate sequences, the 3′-phosphate CPG was sulfurized by the sulfurizing reagent (Glen Research) after the first nucleotide was added. 75 nmol of the 3′-phosphorothioate oligonucleotide in 50 μl of 400 mM triethylammonium bicarbonate buffer were shaken for 5 h at room temperature with 750 nmol of rhodamine-azide in 200 μl of dimethylformamide. The reacted products were collected by ethanol precipitation. Next, the products were purified by reverse-phase HPLC (0–80% acetonitrile/50 mM triethylammonium acetate gradient).

5.2.3. 5′Triphenylphosphine (TPP)-linked oligonucleotide

Carboxy-triphenylphosphine (TPP) NHS ester was reacted with 5′ amino-modified oligonucleotide. 5′ amino-modifier C6 (Glen Research) was used to prepare 5′

amino-modified oligonucleotide. 50 nmol of the 5′ amino-modified oligonucleotide in 135 μl of 93 mM sodium tetraborate (pH 8.5) were shaken for 5 h at room temperature with 2 μmol of TPP NHS ester in 115 μl of dimethylformamide. The reacted products were collected by ethanol precipitation. Next, the collected products were purified by reverse-phase HPLC (0–50% acetonitrile/50 mM triethylammonium acetate gradient). A peak corresponding to the oxidized product (+O) was also seen and presumed to arise from oxidation during purification.

5.2.4. Fluorescence measurement

Reactions on the DNA template were performed in 1.2 ml of tris-borate buffer (70 mM, pH 8.0) containing 10 mM $MgCl_2$ with target DNA (500 nM), probe 1 (500 nM), and probe 2 (1 μM) or probe 3 (500 nM) at 25 °C. In the case of probe 2, DTT (100 μM) was added to the reaction mixture. The increase of fluorescence intensity produced by reduction of rhodamine-azide on probe 1 was continuously monitored at time intervals. Reactions were observed by fluorescence spectrometry (FP-6500; JASCO). Fluorescence spectra were measured under the following conditions: excitation, 490 nm. For the time course of the azide reduction, the fluorescence intensity was measured for 0.5 s at 1 min intervals: excitation, 490 nm; emission, 550 nm (TPP) or 530 nm (DTT).

5.2.5. Detection of RNA in fixed E. coli cells

Escherichia coli K12 (NBRC 3301) and *Paracoccus denitrificans* (IFO 16712) were grown aerobically on a rotary shaker in Luria-Bertani broth (WAKO) at 30°C for 20 h. The cells were centrifuged and were fixed with 4% paraformaldehyde-PBS solution for 2 hour before being washed with PBS and resuspended in PBS/ethanol (1:1; vol/vol). Fixed cell were stored at -20 °C. Oligonucleotide probes were targeted to nucleotides 968-997 in 23S rRNA of *E. coli* K12 since Fuchs *et al.* described the accessibility of this site was superior to other sites [10]. Both rhodamine_azide probe (5’ CTGGCGGTCTGGGTT-Rh_azide 3’) and triphenylphosphine probe (5’ TPP-GTTTCCCTCTTCACG 3’) were 15 nt in length. After attaching fixed *E. coli* on the glass slide, 9 μL of hybridization buffer (20 mM Tris-HCl pH 7.2, 0.9 M NaCl,

0.1% SDS, 440 nM rhodamine_azide probe, 440 nM triphenylphosphine probe, and 0.025% PEG6000) were applied to each well. After incubation at 37 °C for 30 min, hybridization buffer was briefly removed with distilled water without conventional washing step, air-dried and mounted in Slow Fade® Gold antifade reagent (Invitrogen). Fluorescence images were obtained through a fluorescence microscope (Carl Zeiss Axioskop 2 Plus) with mercury lamp, using digital camera (Carl Zeiss AxioCam HRm) and imaging software (Carl Zeiss AxioVision 3.0). Microscope settings were as follows: ex. 480/40 bandpass filter; ex. 510 nm with longpass filters, exposure time 2 sec.

5.3. Results and Discussion

5.3.1. Detection of RNA in fixed E. coli cells

Fluorescence in situ hybridization (FISH) is becoming broadly adopted by microbiologists because of the existence of a growing database of ribosomal RNA (rRNA) sequences. However, the standard fluorescent probes require a careful washing step in the protocol to remove nonspecific signals. Here, we tested a nonwashing protocol for detection of 23S rRNA in the *E. coli* K12 strain (NBRC3301) by use of an RETF probe. Probes were designed for targeting sequence 968–997 on 23S rRNA, which is known to be accessible by the standard FISH probe [10]. The rhodamine azide probe and the TPP probe with matched sequence are both 15 bases long (Figure 5.1.A). The TPP probe with mismatched sequence was tested as a control. Before imaging experiments, probes were tested in *in vitro* experiments to target corresponding DNA sequences (Figure 5.1.B). The matched probe pair produced a strong fluorescent signal and completed the reaction within 10 min, and no significant signal was observed from a mismatched probe pair (Figure 5.1.B).

We then proceeded to test the probes in bacterial cells. Cells were fixed with paraformaldehyde according to literature methods and were incubated with probes at 37 °C for 30 min. Cell mixtures were directly spotted on a slide glass without a washing step and observed using a microscope. Figures 5.2 shows fluorescence images and bright field transmission images of cells. A strong fluorescent signal was observed in the case of the

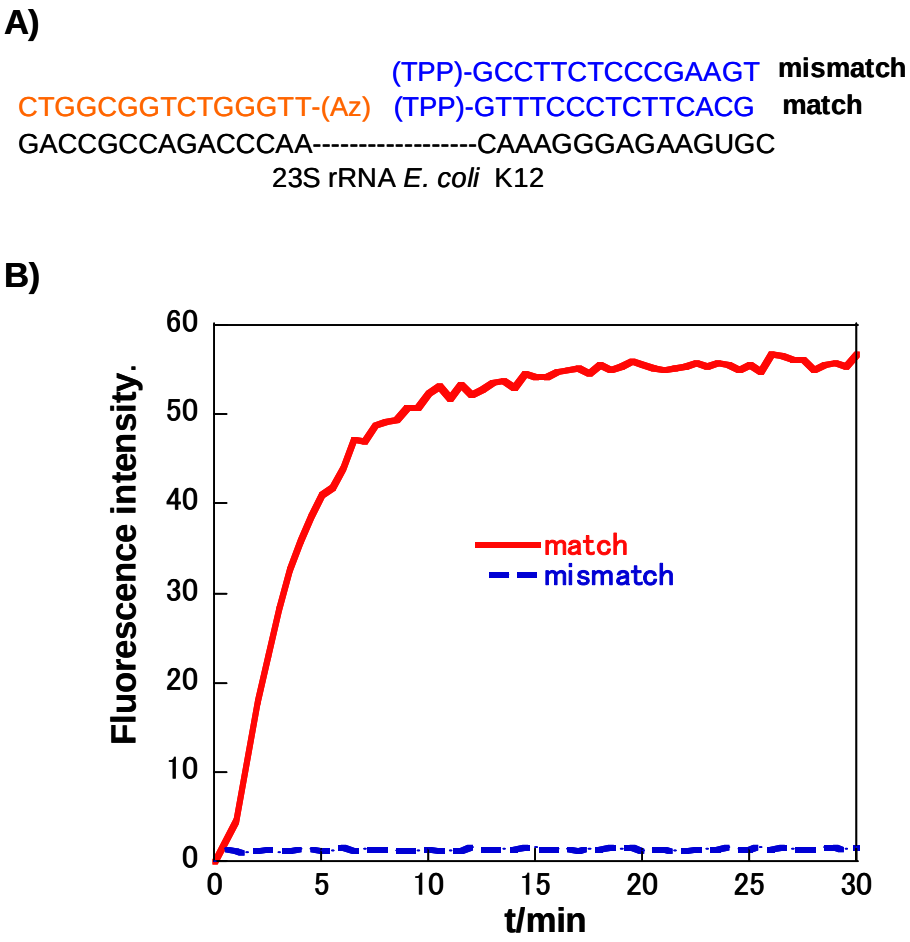

Fig. 5.1 A) Probe sequences for 23S rRNA of *E. coli* K12. Designed 15-mer probes are a rhodamine-azide probe with full matched sequence, TPP probe with full matched sequence and TPP probe with mismatched sequence. B) Time course of the fluorescence intensity in the reaction between 500 nM rhodamine-azide probe and 500 nM matched TPP probe or mismatched TPP probe in the presence of 500 nM target DNA. Reaction was monitored by excitation at 490 nm and emission at 550 nm.

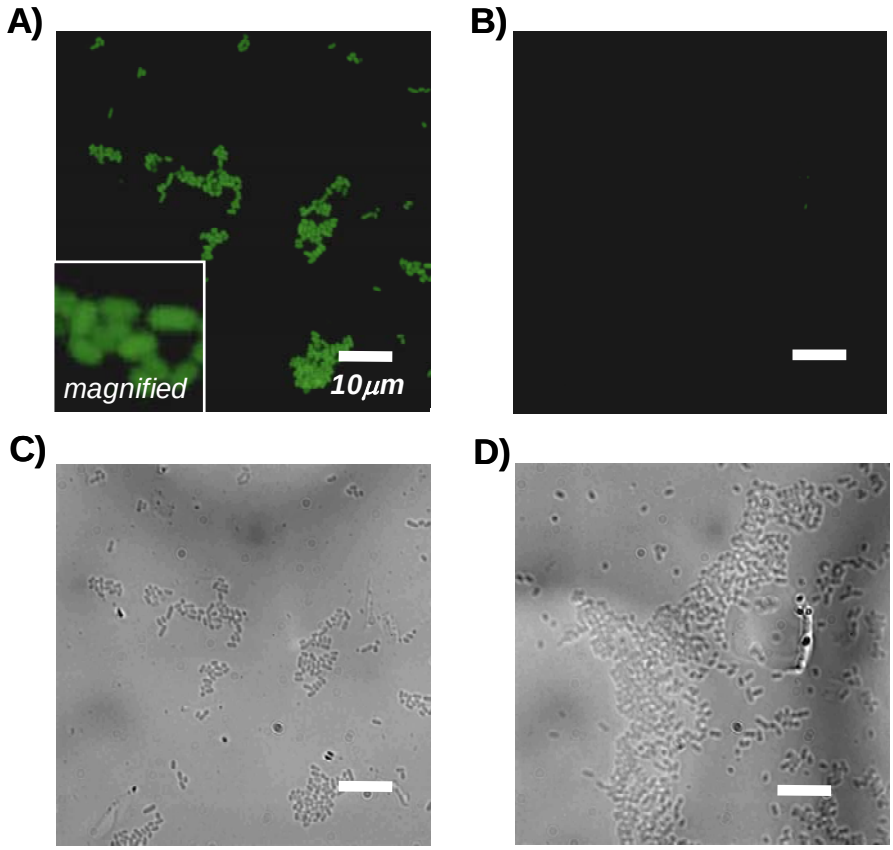

Fig. 5.2 Imaging of 23S rRNA in fixed *E. coli* K12 (NBRC3301).Pictures showed a specific signal with a matched probe pair and little or no signal with a mismatched pair. Microscope settings were as follows: excitation; 480/40 bandpass filter, emission; 510 nm with longpass filters, exposure time; 2 s. A) Rhodamine-azide probe/matched TPP probe. B) Rhodamine-azide probe/mismatched TPP probe. C) Bright field picture under the conditions of (A). D) Bright field picture under the conditions of (B).

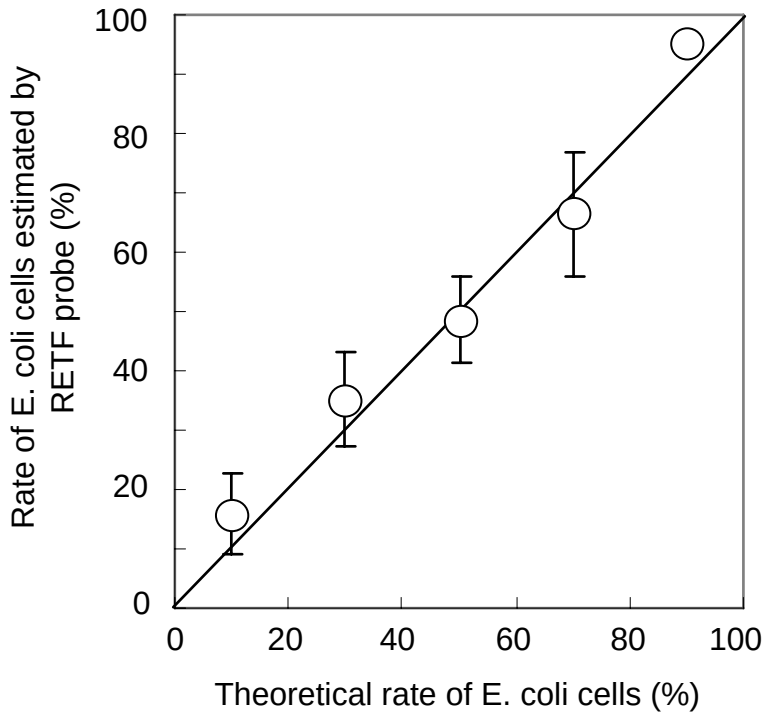

Fig. 5.3 Quantitative detection of *E. coli* cells in artificially mixed with *P. denitrificans*. Defined percentages of *E. coli* in the total cells are plotted along the x-axis, whereas the measured values of the percentages obtained by the RETF system are shown along the y-axis. The error bars represent the standard deviation (SD) of 3 replicate assays.

matched probe pair (Figure 5.2.A), but no signal was observed from the mismatched probe pair (Figure 5.2.B). The data show that the RETF probe can be used to detect specific RNA sequences in structured biological targets in cells. This suggests the possibility of their general use in identifying bacterial pathogens by their ribosomal RNAs.

5.3.2. Quantitative detection of E. coli cells in cell mixture

To gauge the usefulness of the RETF system in characterizing model microbial communities, we tried to quantitatively detect *E. coli* cells from the cell mixture of *E. coli* and *P. denitrificans*. The ratio of cell number of *E. coli* to that of *P. denitrificans* in the mixture was adjusted to 0 - 1.0 (Figure 5.3). The percentage of cell number of *E. coli* in the mixture was determined by *in situ* hybridization with *E. coli*-specific RETF probe followed by direct counting under fluorescence microscope. As shown in Figure 5.3, the plots obtained from the experiment matched theoretical values well. Again, our RETF system can detect microorganisms without labor and time-consuming washing step. From this result, RETF system can be applied to rapid detection of environmental bacteria. Moreover, RETF system has a possibility to detect living microorganisms if we can penetrate probes into living cells with a mild condition. Future studies are aimed at these points.

References

1. DeLong, E. F., Wickham, G. S., Pace, N. R. (1989) *Science 243*, 1360-1363.
2. Amann, R., Fuchs, B. M., Behrens, S. (2001) *Curr. Opin. Biotechnol. 12*, 231-236.
3. Moter, A., Gobel, U. B. (2000) *J. Microbiol. Methods 41*, 85-112.
4. Maidak, B. L., Cole, J. R., Lilburn, T. G., Parker, C. T., Saxman, P. R., Stredwick, J. M., Garrity, G. M., Li, B., Olsen, G. J., Pramanik, S., Schmidt, T. M., Tiedje, J. M. (2000) *Nucleic Acids Res. 28*, 173-174.
5. Wuyts, J., Van de Peer, Y., Winkelmans, T., De Wachter, R. (2002) *Nucleic Acids Res. 30*, 183-185.
6. Lipski, A., Friedrich, U., Altendorf, K. (2001) *Appl. Microbiol. Biotechnol. 56*, 40-57.
7. Manz, W. (1999) *Methods Enzymol. 310*, 79-91.
8. Manz, W., Amann, R., Ludwig, W., Wagner, M., Schleifer, K. H. (1992) *Syst. Appl. Microbiol. 15*, 593-600.
9. Abe, H., Wang, J., Furukawa, K., Oki, K., Uda, M., Tsuneda, S., Ito, Y. (2008) *Bioconjugate Chem.* 19, 1219-1226.
10. Fuchs, B. M., Syutsubo, K., Ludwig, W., and Amann, R. (2001) *Appl. Environ. Microbiol. 67*, 961-968.

Chapter 6

Reduction-triggered fluorescence amplifying probe for detection of RNAs in living human cells

Chapter 6

Reduction-triggered fluorescence amplifying probe for detection of RNAs in living human cells

6

6.1. Introduction

The detection and imaging of RNA species in native human cells have been gaining importance in the biological and biomedical research fields [1-7]. Several approaches for imaging mRNAs in genetically engineered cells have been reported recently [8-10]. Although such a strategy can be a useful tool for biological studies, it is not applicable for imaging native RNAs in unmodified cellular specimens. Our specific goal is the detection of RNA sequences in intact cells at single nucleotide resolution using a fluorescence signal as readout. This requires no extraction of RNA species from the cell; therefore, it should be a very rapid and simple method for disease-related RNAs as a biomedical application. Messenger RNAs are expected to be more difficult to detect than ribosomal RNAs because they exist in smaller quantities in living cells [11]. Moreover, their sequences vary widely and their structures are generally unknown; it is therefore very difficult to find an optimal target site [12-14].

No method has yet been successful enough to gain wide application for the imaging and detection of mRNA in living cells. However, a small number of molecular approaches have been reported as potentially practical methods [15-37]. Prominent among these approaches are quenched-probe strategies, including molecular beacon

(MB) probes [16-20, 28] and quenched autoligation (QUAL) probes [21-27]. The most important issue for detection in living cells is to keep a low background signal in the absence of the RNA target. These probes allow target-dependent fluorescence enhancement based on the resonance energy transfer (RET) mechanism, for which a pair of quencher and fluorescence dyes is normally used. Recent reports have shown evidence for detection by fluorescence microscopy of messenger RNAs by MB probes and QUAL probes in intact human cells [19, 21-23, 35-40]. Moreover, QUAL probes have been used for flow cytometric detection of RNA species in native human cells [23]. However, these approaches still need improvement in signal/background (S/B) ratio to become established methods.

Oligonucleotide-templated reactions (OTRs) have received attention as a potential approach for RNA detection in living cells [21, 23]. This strategy exploits the target strand as a template between two functionalized DNAs or PNAs. For example, native chemical ligation [41, 43], catalytic hydrolysis [44-46], the Staudinger reaction [47-50], transfer of a reporter group [51], DNAzyme [52], an S_N2 quencher displacement ligation reaction (QUAL probe) [25], and organomercury-activated reactions [53] have been applied to fluorescence nucleic acid reactions. However, few methods have been applied to RNA detection in living human cells [23]. We considered two important issues to develop a highly sensitive RNA detection probe based on OTR. These are a new fluorogenic system to offer a higher S/B ratio and turnover of OTR to offer amplification of RNA signal.

The catalytic turnover reaction can provide signal amplification and enable sensitive oligonucleotide detection in living cells. Various chemistries for the catalytic turnover have been reported [41, 46, 47, 49-51, 54]. A few laboratories have reported that self-ligation reactions provide amplified products. However, theoretically, ligation reactions suffer from an increased affinity of the product for the oligonucleotide template [41, 54]. This causes product inhibition and prevents higher catalytic activity of the template. Therefore, to reduce product inhibition, a few other laboratories have recently investigated unligated systems by using pairs of modified probes to generate an amplified signal. These approaches are catalytic ester hydrolysis [46], the Staudinger reaction [47,

49, 50], DNAzyme [52], and transfer of a reporter group [51]. Even though they showed significant turnover number up to 400 times in a test tube, application to living human cells has not been demonstrated. This implies that these methods still need to be improved in background fluorescence or sensitivity.

Recently, various fluorogenic compounds have been developed for the detection of small biological substances [55-59]. Fluorescence modulation of these compounds is caused by photoinduced electron transfer or absorption change triggered by chemical reaction accompanied with transformation of chemical structure. The S/B ratio for these types of molecules could exceed that of the RET mechanism [60]. Combined with the catalytic turnover mechanism, this type of fluorogenic system could become a very powerful method for RNA detection in living cells. However, there are only a few reports that describe chemical reaction-triggered fluorogenic molecules for oligonucleotide sensing with amplification of signal in test tubes [47, 49, 50].

Recently, we reported a reduction-triggered fluorescence (RETF) probe having a rhodamine azide as the fluorogenic molecule that showed a response with a high S/B ratio [48]. However, this probe did not offer a catalytic turnover because of an unexpected ligated intermediate on OTR. Here, we report another fluorogenic molecule using the azidomethyl protecting group [61, 62] for the fluorescein compound, although Kool and co-workers very recently reported an azidomethyl-protected coumarin dye for OTR that has not been applied to RNA detection in living cells [50]. The new reduction-triggered fluorescent amplification (RETFA) probe enables catalytic turnover under isothermal conditions without significant product inhibition (Figure 1). The turnover mechanism in the steady state was analyzed by fluorescence spectroscopy, and association and dissociation rate constants for the probe on a template were calculated by BIAcore technology. Finally, by using this RETFA probe design, we show that endogenous mRNA, as well as 28S ribosomal RNA in living human HL60 cells, could be imaged by fluorescence microcopy and detected by a flow cytometry.

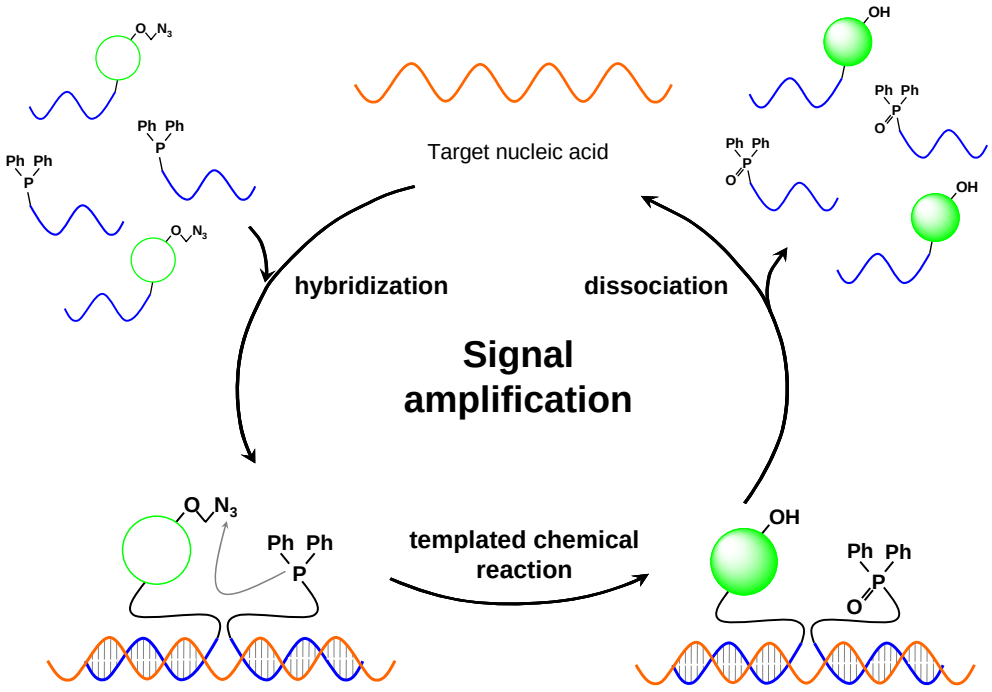

Figure 1. Illustration of the turnover of the azide reduction, which can generate multiple signals per target.

6.2. Materials and Methods

6.2.1. Monoalkyl fluorescein (1)

To a solution of fluorescein (3.00 g, 9.03 mmol) and sodium iodide (271 mg, 1.81 mmol) in DMF (50 ml) chilled via an external ice bath was added a THF (30 mL) solution of potassium *t*-butoxide (3.04 g, 27.1 mmol). After the solution was clear, methyl bromoacetate (944 μL, 9.94 mmol) was added slowly. The reaction was allowed to warm gradually to room temperature. After 2.5 h, the reaction mixture was diluted with EtOAc and washed with H_2O and brine. The combined organic extracts were pooled and dried over Na_2SO_4. The Na_2SO_4 was removed by filtration and volatiles removed *in vacuo*. The residue was purified by flash column chromatography (silica, gradient elution 30:1 $CHCl_3$/MeOH to 20:1 $CHCl_3$/MeOH with 0.5% triethylamine) to afford a clear syrup on concentration (820 mg, 23%) (**1**). ^{1}H NMR (400MHz, CD_3OD) δ7.91 (1H, d, J = 7.32Hz), 7.62 (2H, dt, J = 16.40, 15.10Hz), 7.10 (1H, d, J = 7.56Hz), 6.79 (1H, d, J = 2.20Hz), 6.67-6.55 (4H, m), 6.44 (1H, dd, J = 2.20, 2.44Hz), 4.70 (2H, s), 3.69 (3H, s). ^{13}C NMR (100MHz, CD_3OD) δ 180.6, 172.5, 169.9, 163.5, 159.4, 155.1, 138.8, 137.6, 129.6, 129.1, 124.9, 116.3, 116.0, 114.5, 104.7, 102.3, 66.1, 52.7. QSTAR (Applied Biosystems/MDS SCIEX) (ESI): *m/z* 404.0896 [MH+] $C_{23}H_{16}O_7$: 405.0974, found: 405.0987

6.2.2. Monoalkyl thiomethyl fluorescein (2)

Monoalkyl fluorescein (**1**) (720 mg, 1.78 mmol) was dissolved in dry CH_3CN (36 ml) under Ar (g). Silver oxide (620 mg, 2.67 mmol) and chloromethylmethylsulfide (223 μl, 2.67 mmol) was added followed by addition of one drop of pyridine. After stirring for 15 hour at room temperature, the remaining solid residue was removed by filtration. The filtrate was concentrated and subjected to flash column chromatography. Elution with a slow gradient of hexane/AcOEt from 6:1 to 2:1 (v/v) with 0.5% triethylamine gave monoalkyl thiomethyl fluorescein (**2**) as pale yellow crystalline solid (206 mg, 25%). ^{1}H NMR (400MHz, $CHCl_3$) δ8.01 (1H, d, J = 7.08Hz), 7.64 (2H, dt, J = 16.10, 15.10Hz), 7.15 (1H, d, J = 7.56Hz), 6.83 (1H, d, J = 2.44Hz), 6.83-6.62 (5H, m),

5.15 (2H, s), 4.66 (2H, s), 3.80 (3H, s), 2.24 (3H, s). ^{13}C NMR (100MHz, CDCl3) δ 168.94, 168.43, 159.04, 152.64, 151.86, 134.80, 129.08, 128.87, 126.41, 124.75, 123.78, 112.66, 102.82, 101.65, 82.57, 72.34, 65.12, 52.27, 14.59. QSTAR (Applied Biosystems/MDS SCIEX) (ESI): *m/z* 464.0930 [MH+] $C_{25}H_{20}O_7S$: 465.1008, found: 465.1004

6.2.3. Monoalkyl azidomethyl fluorescein (3)

Monoalkyl thiomethyl fluorescein (**2**) (164 mg, 350 μmol) was dissolved in dichloromethane (7 ml). A dichloromethane (1 ml) solution of N-chlorosuccinimide (51.8 mg, 390 μmol) and trimethylsilyl chloride (42.0 mg, 390 μmol) was added. The resulting solution was stirred at ambient for 1 h and the reaction was quenched with saturated Na_2CO_3 aqueous. The aqueous layer was extracted with $CHCl_3$ (×2) and the combined organic layers was concentrated in vacuum to give the crude which was subjected to the next reaction. Sodium azide (34.4 mg, 530 mmol) was dissolved in H_2O (3.5 ml) and added to a solution of the crude in DMF (7 ml) in room temperature. After stirring for 1 hour, the reaction was quenched with saturated Na_2CO_3 aqueous. The aqueous layer was extracted with AcOEt (×2) and the combined organic layers was concentrated in vacuum and subjected to flash column chromatography. Elution with a slow gradient of hexane/AcOEt from 5:1 to 3:2 (v/v) with 0.5% triethylamine gave monoalkyl azidomethyl fluorescein (**3**) as pale yellow crystalline solid (71.3 mg, 44%). ^{1}H NMR (400MHz, $CHCl_3$) δ8.02 (1H, d, J = 7.80Hz), 7.65 (2H, dt, J = 15.2, 14.9Hz), 7.16 (1H, d, J = 7.32Hz), 6.90 (1H, d, J = 2.20Hz), 6.76-6.63 (5H, m), 5.18 (2H, s), 4.66 (2H, s), 3.82 (3H, s). ^{13}C NMR (100MHz, CDCl3) δ 169.02, 168.54, 157.87, 152.64, 152.76, 152.08, 134.95, 129.70, 129.27, 126.46, 124.95, 123.80, 111.79, 103.26, 101.80, 82.46, 79.43, 65.27, 52.42. QSTAR (Applied Biosystems/MDS SCIEX) (ESI): [MH^+] $C_{24}H_{17}N_3O_7$: 460.1145, found: 460.1134

6.2.4. Azidomethyl carboxyfluorescein (4)

Monoalkyl azidomethyl fluorescein (**3**) (27.8 mg, 60 μmol) was dissolved in methanol (605 μl). An aqueous solution of 1M NaOH (66.6 μl, 66.6 μmol) was added. The

resulting solution was stirred at ambient for 1 h and the reaction was quenched with 0.1M HCl. The aqueous layer was extracted with AcOEt (×2) and the combined organic layers was concentrated in vacuum and subjected to flash column chromatography. Elution with a slow gradient of $CHCl_3$/MeOH from 30:1 to 20:1 (v/v) with 0.5% triethylamine gave azidomethyl carboxyfluorescein (**4**) as pale yellow crystalline solid (28.2 mg, 100%). ^{1}H NMR (400MHz, $CHCl_3$) δ 8.01 (1H, d, J = 7.32Hz), 7.64 (2H, dt, J = 14.9, 15.2 Hz), 7.16 (1H, d, J = 7.56Hz), 6.88 (1H, d, J = 2.20Hz), 6.82 (1H, d, J = 2.20Hz), 6.73-6.63 (4H, m), 5.18 (2H, s), 4.51 (2H, s). ^{13}C NMR (100MHz, CDCl3) δ 173.69, 169.17, 157.76, 152.79, 152.30, 134.83, 129.23, 128.61, 126.62, 124.82, 123.91, 112.30, 103.22, 101.74, 82.50, 79.41, 67.57. QSTAR (Applied Biosystems/MDS SCIEX) (ESI): *m/z* 445.0910 [MH+] $C_{23}H_{15}O_7N_3$: 446.0988, found: 468.0808

6.2.5. Azidomethyl fluorescein NHS ester

Azidomethyl carboxyfluorescein (**4**) (4.60 mg, 10.3 μmol) and N-hydroxysuccinimide (1.30 mg, 11.4 μmol) was dissolved in DMF (205 μl). DCC (2.35 mg, 11.4 μmol) was added. After stirring for 2 days at room temperature, the remaining solid residue was removed by filtration. The filtrate was subjected to the coupling with 3'-amino DNA without purification.

6.2.6. Synthesis of unmodified oligonucleotides

All oligonucleotides were synthesized on a 0.2 μmol scale on a DNA synthesizer (H-8-SE; Gene World) using standard phosphoroamidite coupling chemistry. Deprotection and cleavage from the CPG support was carried out by incubation in concentrated ammonia for 4 h at 55 °C. Following deprotection, the oligonucleotides were purified by reverse-phase column chromatography (MicroPure II column; Biosearch Technologies), and quantitated by UV absorbance using the nearest neighbor approximation to calculate molar absorptivities.

6.2.7. 3' mono-azidomethyl fluorescein-conjugated oligonucleotide

The crude product of azidomethyl fluorescein NHS ester was reacted with 3′ amino-modified oligonucleotide. 3′ PT-amino-modifier C3 CPG (Glen Research) was used to prepare 3′ amino-modified oligonucleotide. 50 nmol of the 3′ amino-modified oligonucleotide in 50 μl of 80 mM sodium tetraborate (pH 8.5) were shaken for 5 h at room temperature with 0.75 μmol of the compound in 200 μl of dimethylformamide. The reacted products were collected by ethanol precipitation. Next, the collected products were purified by reverse-phase HPLC (0–80% acetonitrile/50 mM triethylammonium acetate gradient). The probe structure was confirmed by ESI–TOF mass spectrometry.

6.2.8. 5' Triphenylphosphine (TPP)-linked oligonucleotide

Carboxy-triphenylphosphine (TPP) NHS ester was reacted with 5′ amino-modified oligonucleotide. 5′ amino-modifier C6 (Glen Research) was used to prepare 5′ amino-modified oligonucleotide. 50 nmol of the 5′ amino-modified oligonucleotide in 135 μl of 93 mM sodium tetraborate (pH 8.5) were shaken for 5 h at room temperature with 2 μmol of TPP NHS ester in 115 μl of dimethylformamide. The reacted products were collected by ethanol precipitation. Next, the collected products were purified by reverse-phase HPLC (0–50% acetonitrile/50 mM triethylammonium acetate gradient). The probe structure was confirmed by ESI–TOF mass spectrometry.

6.2.9. 3' bis-azidomethyl fluorescein-conjugated oligonucleotide

The bromoacetyl group of the bis-azidomethyl fluorescein was reacted with the phosphorothioate group on the oligonucleotides. For 3′ phosphorothioate sequences, the 3′-phosphate CPG was sulfurized by the sulfrizing reagent (Glen Research) after the first nucleotide was added. 75 nmol of the 3′-phosphorothioate oligonucleotide in 50 μl of 400 mM triethylammonium bicarbonate buffer were shaken for 5 h at room temperature with 750 nmol of compound 9 in 200 μl of dimethylformamide. The reacted products were collected by ethanol precipitation. Next, the products were purified by reverse-phase HPLC (0–80% acetonitrile/50 mM triethylammonium acetate gradient). The probe structure was confirmed by ESI–TOF mass spectrometry.

6.2.10. Measurement of quantum yield

A 1 mM DMF stock solution of each compound was prepared. Absorption spectra were obtained with a 20 mM tris-HCl buffer (pH 7.2) solution of each compound at the desired concentration, adjusted by appropriate dilution of the 1 mM DMF stock solution. For determination of the quantum efficiency of fluorescence (Φ_{fl}), fluorescein in 0.1 M NaOH was used as a fluorescence standard (Φ = 0.85). The quantum efficiency of fluorescence was obtained with the following equation (F denotes fluorescence intensity at each wavelength and Σ [F] was calculated by summation of fluorescence intensity).

$$\Phi_{fl}^{\ sample} = \Phi_{fl}^{\ standard} \mathrm{Abs}^{\ standard} \Sigma [F^{\ sample}] / \mathrm{Abs}^{\ sample} \Sigma [F^{\ standard}]$$

6.2.11. DNA-templated reaction

Reactions on the DNA template were performed in 1.2 ml of tris-HCl buffer (20 mM, pH 7.2) containing 100 mM $MgCl_2$ and 0.01 mg/ml BSA with *bcr/abl*-1 or -2, probe 1 (50 nM), and probe 2 (50 nM) at 37 °C. The increase of fluorescence intensity produced by reduction of probe 1 was continuously monitored at time intervals. Reactions were observed by fluorescence spectrometry (FP-6500; JASCO). For the time course of the azide reduction, the fluorescence intensity was measured for 0.5 s at 1 min intervals: excitation, 490 nm; emission, 520 nm.

6.2.12. Cell culture and Streptolysin O (SLO) permeabilization

HL60 cells (RIKEN BRC cell bank) were grown in DMEM without phenol red and containing 10% FCS, 50 units/ml penicillin, and 50 mg/ml streptomycin. They were passaged in 75-cm^2 culture flasks (Falcon). Cells were maintained at 37°C in an atmosphere of 5% CO_2 at 1 × 10^5 cells/ml and within 0~20 passages after purchasing from the supplier.

SLO was purchased from BioAcademia (Japan). SLO was activated according to the procedure reported by Abe *et al.* [23]. Briefly, SLO (10,000 units/ml) was incubated in Mg^{2+}/Ca^{2+}-free PBS buffer solution containing 10 mM DTT and 0.05% BSA at 37°C for 2 h. Small aliquots of activated SLO were stored at –20°C. To introduce probes into cells,

HL60 cells were washed with Mg^{2+}/Ca^{2+}-free PBS twice and then incubated with 300 ml of Mg^{2+}/Ca^{2+}-free PBS buffer solution containing SLO (50 units/ml), BSA (0.01 mg/ml), and calf thymus DNA (1 mg/ml). After 15 min, 3'-bis-azidomethyl fluorescein-conjugated probe (200 nM) and TPP-conjugated probe (200 nM) were added. After 30 min, cells were resealed by the addition of 1 ml of DMEM containing $CaCl_2$ (0.2 g/l) and incubated for 1 h at 4°C.

6.2.13. Flow cytometry

The live cell suspension was directly analyzed without any washing step with a Cytomics FC500 instrument (Beckman Coulter). Fluorescent signals were observed under the following conditions: excitation by argon laser, 488 nm; emission, 515-535 nm. Forward angle light scatter (FSC), side angle light scatter (SSC), and fluorescence data were recorded, and for each measurement, above 1,000 events were stored. Data were analyzed with the CXP analysis software (Beckman Coulter). Fluorescent intensity was determined as the mean of fluorescent value of single cells lying in a gate that were defined in a FSC vs. SSC dot plot.

6.2.14. Microscopy and data processing

Intracellular distributions of 28S rRNA and β-actin mRNA were observed using an inverted microscope (IX-81, Olympus). Specimens were illuminated with the 488-nm line of an Ar^+ laser (Omnichrome) through a 60x oil-immersion objective (PlanApo, Olympus). Fluorescence images were acquired at 500-550 nm through the same objective using an image intensifier (C8600-05; Hamamatsu) and an EB-CCD camera (C7190-20; Hamamatsu) and recorded on a digital videotape. Bright field images of cells in the same field of view were recorded successively to the fluorescence images. Image processing was carried out using MetaMorph software (Molecular Devices). Experiments were performed at 27 ºC.

6.2.15. Surface plasmon resonance analysis

Kinetic parameters were assessed using BIAcore equipment with a Series S SensorChip SA (GE Healthcare bioscience). The central part of this equipment is the sensor-chip consisting of a gold surface covered with a layer of dextran, which in our case contained streptavidin chemically coupled to the dextran. The biotinylated DNA strands (target DNA: *bcr/abl-1*) were immobilized to the streptavidin chip. The association as well as dissociation kinetics of two probes, probe 1 and probe 2, were studied. All kinetics experiments were performed in 20 mM Tris-HCl buffer (pH 7.2) containing 100 mM $MgCl_2$ at 37 ˚C. To immobilize the biotinylated DNA strand to the streptavidin on the chip surface, 5'-biotin-labeled DNA was dissolved in Tris-HCl buffer at a concentration of 600 nM. The solution (15 μL) was injected with a flow rate of 5 μl/min, and the immobilization was followed in the corresponding sensorgram as a function of time. Probes were dissolved in running buffer at appropriate concentrations (15.6-150 nM). A volume of 75 μl (30 μl/min) was injected to measure the association kinetics, and immediately thereafter the dissociation was followed by purging running buffer through the system. After approximately 150 s buffer wash, the immobilized DNA surface was regenerated with 30 μl of 10 mM HCl (30 μl/ min). The association and dissociation rate constants for each probe were calculated with BIAcore T100 evaluation software (GE Healthcare bioscience).

6.3. Results

6.3.1. Design and molecular mechanism of the RETFA probe

Our chief goal was to develop a new RNA detection probe having a chemical reaction-based fluorogenic compound that was capable of signal amplification under isothermal conditions. As one achievement, we recently reported a RETF system that uses a fluorogenic compound, rhodamine azide derivative, that is activated only by reducing reagents and enhanced 2100 times in fluorescence intensity (Figure 2A) [48]. Reaction of the RETF probe on an oligonucleotide target proceeded without any enzymes or reagents, and offered high signal and very low background fluorescence under

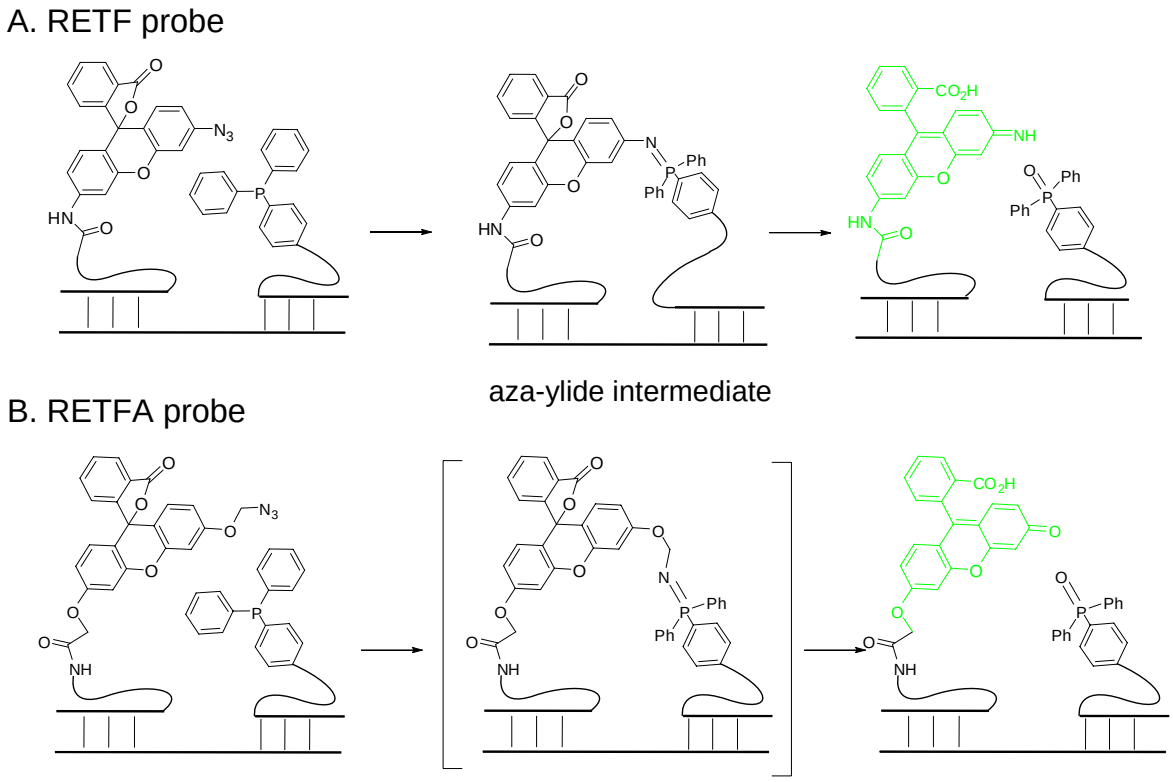

Figure 2. Fluorescence emission of an RETF probe (A) and RETFA probe (B) by triphenylphosphine as reducing reagents.

biological conditions. We successfully applied the probe to the detection of oligonucleotides in solution and endogenous RNA in bacterial cells. However, the reaction between the rhodamine azide probe and the TPP probe in the RETF system initially produces a ligated intermediate between the two halves of the probe connected with a stable aza-ylide bond, and then gradually gives half of the fluorescent rhodamine product through hydrolysis of the aza-ylide bond over 24 h (Figure 2A). Formation of a ligated product with an aza-ylide bond between the two probes prevents catalytic turnover because the long product binds the template with higher affinity than the reactant probe did before reaction. To achieve higher sensitivity for detecting less abundant RNA species such as intracellular mRNA, the RETF system still shows room for improvement to achieve efficient turnover.

To obtain a high turnover in the reaction mechanism of the RETF probe, the aza-ylide bond of the ligated intermediate must be quickly hydrolyzed to reduce product inhibition. We assumed that the aza-ylide bond in the RETF system is stabilized by long π-conjugation between rhodamine and triphenylphosphine [63]. Therefore, it was suggested that to destabilize the aza-ylide bond, π-conjugation of the intermediate should be minimized. Here, we designed a fluorogenic molecule based on azidomethyl-protected fluorescein that was switched on by reduction (Figure 2B). In the first step of the reaction, the unstable aza-ylide bond is formed and quickly hydrolyzed. Consequently, the azide group is transformed to an amino group and TPP is transformed to the corresponding phosphorus compound. The resulting amino-hemiacetal group is quickly hydrolyzed to give an unmasked phenol group and the probe emits a fluorescence signal. A reduction-triggered fluorescence amplification (RETFA) system with azidomethyl-protected fluorescein is expected to offer efficient turnover because of the short life of the ligated intermediate (Figure 2B).

6.3.2. Synthesis of azidomethyl fluorescein

We designed two fluorogenic compounds, monoazidomethyl fluorescein (MAF) and bisazidomethyl fluorescein (BAF). MAF offers a quantitative fluorescence signal to give a single product after deprotection of the azidomethyl group. On the other hand, BAF

offers a more potent fluorescent signal after deprotection of the two azidomethyl groups. The synthesis of MAF (**4**) is shown in Scheme 1. Mono-*O*-carboxymethyl fluorescein **1** was synthesized by treatment with one equivalent of methyl bromoacetate in the presence of potassium *tert*-butoxide and sodium iodide from commercially available fluorescein in 23% yield [64]. The treatment of compound **1** with chloromethyl methyl sulfide and Ag_2O in pyridine gave methyl thioacetal **2** in 25% yield [62]. Activation of the O,S-acetal with *N*-chlorosuccinimide (NCS) in the presence of *tert*-butyldimethylsilyl chloride (TMS-Cl) provides the chloromethyl intermediate. The intermediate was unstable during purification by flash chromatography and was used for the next reaction without further purification. The transformation of the intermediate to the azide **3** was carried out by treatment with sodium azide in 44% yield in two steps. Hydrolysis of methyl ester **3** with NaOH provided the desired azidomethyl carboxyfluorescein (**4**). The NHS ester was prepared by dicyclohexylcarbodiimide-mediated coupling of *N*-hydroxysuccinimide with compound **4**. This activated ester cannot be purified by flash chromatography because of hydrolysis; therefore, the crude product of the NHS ester was directly used for coupling with the DNA probe. Synthesis of BMS is shown in Scheme 2. 5-iodofluorescein was protected with chloromethyl methyl sulfide to give bismethyl thioacetal **6** in 25% yield. Compound **6** was transformed to bisazidomethyl fluorescein **7** by treatment with NCS and NaN_3. Finally, the desired BMS **9** was obtained by Sonogashira coupling between **7** and 2-bromoacetyl propargylamide**.**

6.3.3. Spectrum analysis of azidomethyl fluorescein

We tested the photochemical properties of azidomethyl fluorescein (Figure 3). MAF **3** showed no absorbance at wavelengths longer than 350 nm in 20 mM Tris–HCl (pH 7.2), whereas the corresponding monoalkyl fluorescein **1** showed absorption band at 455 and 490 nm. When a high concentration of dithiothreitol (DTT) was added to a solution of MAF **3**, a peak having a maximum at 455 nm appeared, resulting from reduction followed by hydrolysis of the azidomethyl group (Figure 3A). The fluorescence properties of azidomethyl fluorescein (MAF) were also examined. No significant fluorescence with excitation at 490 nm was observed for MAF **3**. On the other hand,

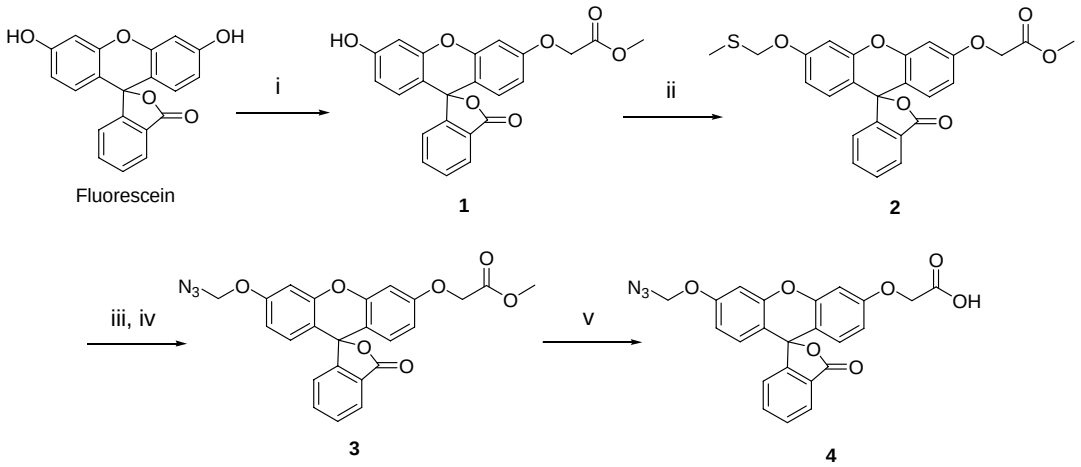

Scheme 1. (i) Methyl bromoacetate, sodium iodide, NaI, DMF, rt, 2.5 h, 23%; (ii) Chloromethylmethylsulfide, Ag_2O, pyridine, CH_3CN, rt, 15 h, 25%; (iii) NCS, TMSCl, CH_2Cl_2, rt, 1 h; (iv) NaN_3, DMF, rt, 1 h, 44% over 2 steps from 2; (v) NaOH, MeOH, rt, 1 h, 100%. NCS = N-chlorosuccinimide, TMSCl = trimethylsilyl chloride.

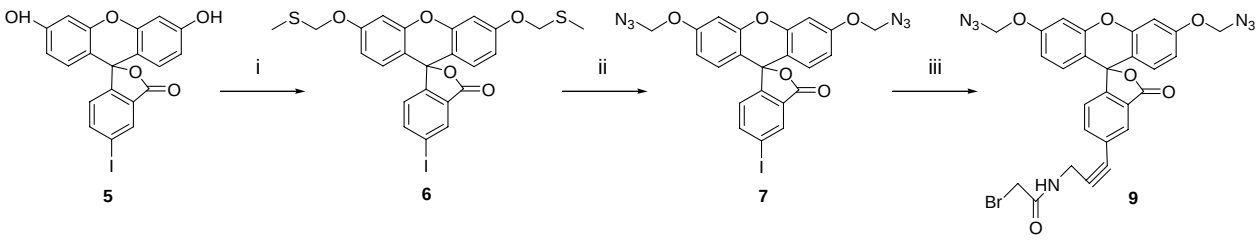

Scheme 2. (i) Chloromethylmethylsulfide, Ag_2O, pyridine, CH_3CN, 40 °C, 24 h, 25%; (ii) NCS, TMSCl, CH_2Cl_2, rt, 8 h; (iii) NaN_3, DMF, rt, 30 h, 21 % over 2 steps from 2; (iv) 5, Tetrakis (triphenylphosphine) palladium, CuI, TEA, THF, rt, 3 h, 37%. NCS = N-chlorosuccinimide, TMSCl=Trimethylsilyl chloride, TEA=Triethylamine, THF=Tetrahydrofuran.

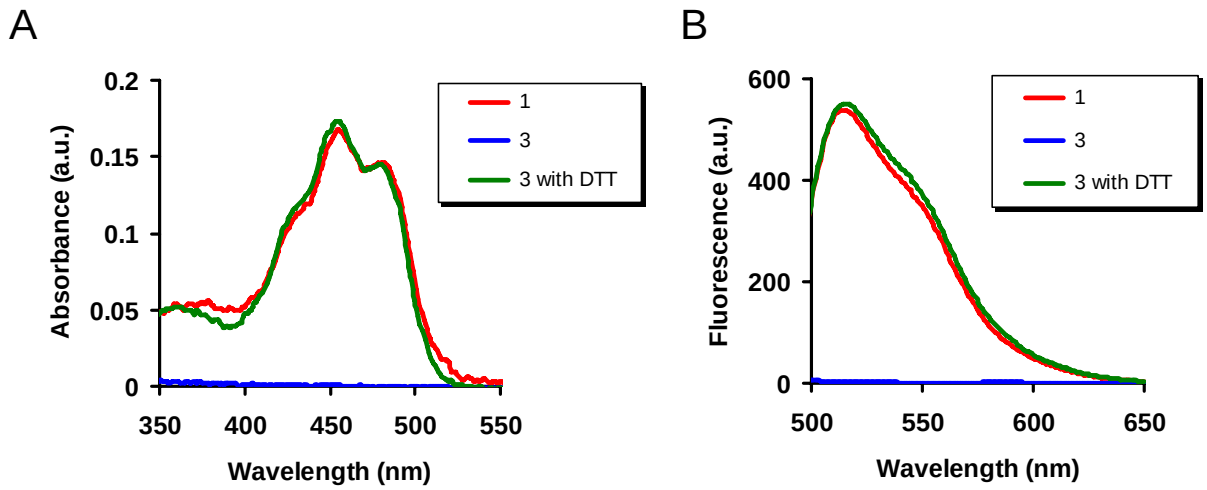

Figure 3. Spectrum analysis. (A) Absorption spectra of 100 μM of **1** (red), **3** (blue) or **3** treatment with 100 mM DTT (green) in 20 mM Tris-HCl (pH 7.2) in 50% DMF/H_2O at 25 °C; (B) Fluorescent emission spectra with excitation at 490 nm of 500 nM of **1** (red), **3** (blue) or **3** treatment with 100 mM DTT (green) in 20 mM Tris-HCl (pH 7.2) in 5% DMF/ H_2O at 25 °C.

monoalkyl fluorescein **1** showed strong fluorescence emission at around 520 nm. After the addition of DTT to the solution of MAF **3**, a strong emission appeared around 515 nm; the emission was enhanced almost 300-fold (Figure 3B). Monoalkyl fluorescein **1** showed high fluorescence quantum yields (0.20) in contrast with the low yield of MAF **3** (< 0.01) (Table 1). We also measured the quantum yields of BMF **7** and its deprotected form **5**. The quantum yields of **5** were 0.68, which is higher than monoalkyl fluorescein **1**, whereas BMF **7** also shows a low quantum yield (< 0.01) (Table 1).

6.3.4. Reaction of the RETFA probe in vitro

We designed two DNA probes to test the utility of the RETFA system for fluorescence-based oligonucleotide detection (Figure 4). The probes and target sequences are shown in Figure 4A. Probe 1 was modified at the 3′ terminal with MAF, where the crude NHS-ester product derived from **4** was reacted with the amino group at the 3′ end of the DNA probe. Probe **2** was modified at the 5′ terminal with 2′-carboxytriphenylphosphine (TPP), which was conjugated with the 5′ amino linker of the DNA probe through amide bond formation. Two DNA templates originating from the human *bcr/abl* junction site sequence, which is related to chronic myelogenous leukemia, were designed containing *bcr/abl-1* with a full match sequence and also *bcr/abl-2* with a one-base mismatch to evaluate the ability for single-base discrimination that is important for diagnostic applications [65].

To prove whether the probes could function by emitting fluorescence, we tested the RETFA probe *in vitro*. The RETFA probe pairs consisted of an 8-mer MAF probe (probe 1) and a 10-mer TPP probe (probe 2). The T_m of two adjacent probes and target DNA was 46.7 °C (data not shown). When 50 nM probe 1 and probe 2 were incubated in Tris–HCl buffer (pH 7.2) at 37 °C, the increase in fluorescence at 520 nm was monitored. In the presence of target *bcr/abl-1*, the signal at 520 nm reached saturation within 3 min by deprotection of the azidomethyl group of probe 1 (Figure 4B). The signal did not increase in the absence of target *bcr/abl-1* for 3 min. HPLC and MALDI–TOF mass analyses showed that 97.7% of probe 1 that reacted with probe 2 on the template after 5 min was converted to the deprotected product (data not shown). Next, the reaction of

Table 1. The quantum yields of the compounds[a]

compound	**1**	**3**	**5**	**7**
Φ_F[b]	0.202	< 0.001	0.683	0.002

[a]All measurements were performed in Tris–HCl buffer (20 mM, pH 7.2). Compounds were excited at 490 nm.

[b]Quantum yields were determined using fluorescein in 0.1 M NaOH as a standard (Φ_F = 0.85).

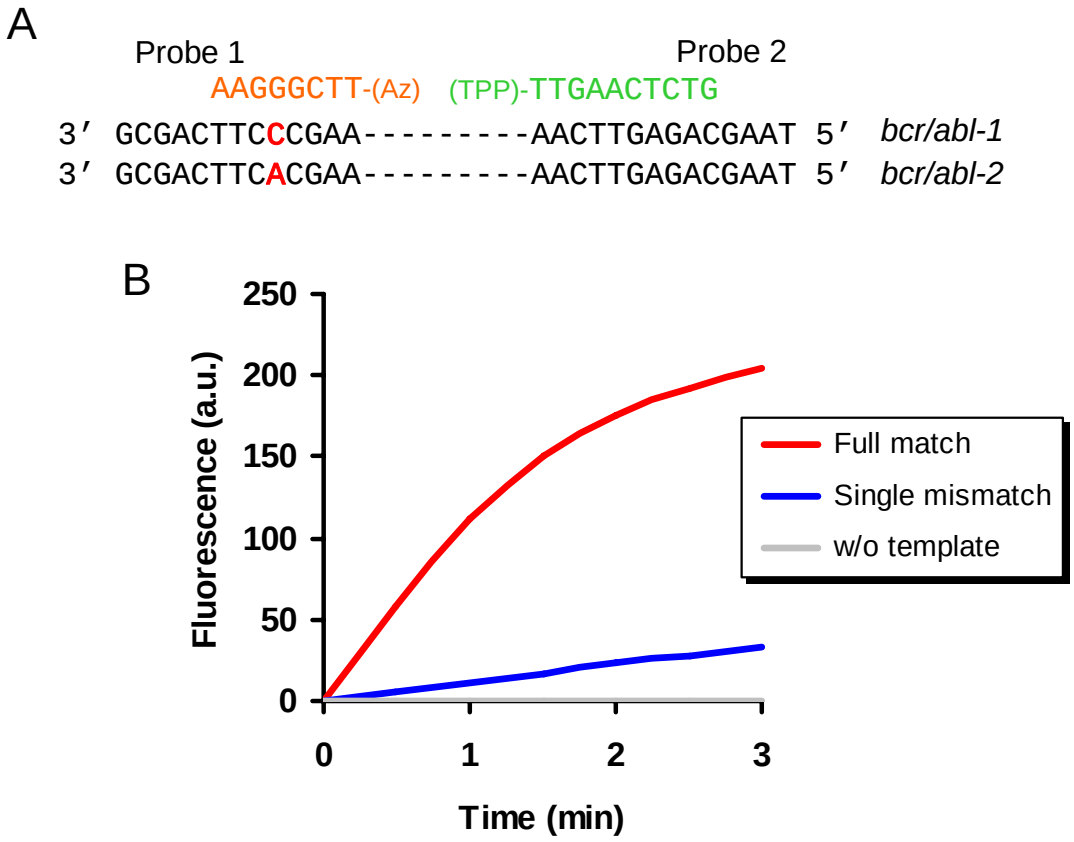

Figure 4. (A) Probe sequences for *bcr/abl* gene. Designed 8 or 10 mer probes are azidomethyl fluorescein probe or TPP probe, respectively. The DNA targets are 27-mer ODNs with a full matched sequence *bcr/abl-1* and a single mismatched sequence *bcr/abl-2*. (B) Time course of the fluorescence intensity in the reaction between 50 nM of probe 1 and 2 with 50 nM of matched *bcr/abl-1* or mismatched DNA *bcr/abl-2* in pH 7.2 Tris-HCl buffer containing 100 mM $MgCl_2$ and 10 μg/ml BSA. Reaction was monitored by excitation at 490 nm and emission at 520 nm.

probe 1 and probe 2 in the presence of one-base-mismatched target *bcr/abl*-2 was tested and showed good single-base mismatch discrimination, dropping in initial rate by 9.5-fold, compared with fully matched *bcr/abl-1* (Figure 4B).

6.3.5. Turnover measurements

The RETFA system was expected to cause multiple reactions with turnover using target oligonucleotide as a catalytic template. Thus, we tested the ability for fluorescent signal amplification. Catalytic turnover, and the associated signal amplification, is useful when target concentrations are low [49, 51, 54]. Under these conditions, one would typically use a large excess of probe relative to the number of targets. To measure turnover with the current probes, we compared the number of equivalents of fluorescent signal with moles of target. This required the development of a method for carefully quantitating the signal, and confirming that the signal arises from true template-dependent intermolecular reactions rather than from background sources such as intermolecular reaction independent of the template strand or photolysis of the azidomethyl group by the excitation light.

To evaluate this, we performed DNA-templated reactions at various target concentrations and continuously monitored the fluorescent signals as a function of time (Figure 5A). We first prepared a standard dilution curve to make a calibration plot of fluorescent intensity as a function of the amount of the deprotected (= fluorescent) probe 1. This plot showed good linearity and allowed us to take a given signal and, from the plot, extract the number of moles of fluorescent product in solution. Turnover (TO) number was obtained by dividing the number of moles of fluorescent product by that of template DNA (Figure 5B). The turnover of reaction products from the target DNA is expected to increase as the concentration of target decreases. To test this, we varied target concentrations over the range from 50 nM to 50 pM. The probe concentrations were held constant at a considerable excess (50 nM). To ensure that the signal was not the result of template-independent reactions or hydrolysis, we subtracted background signals from identical reactions lacking templates.

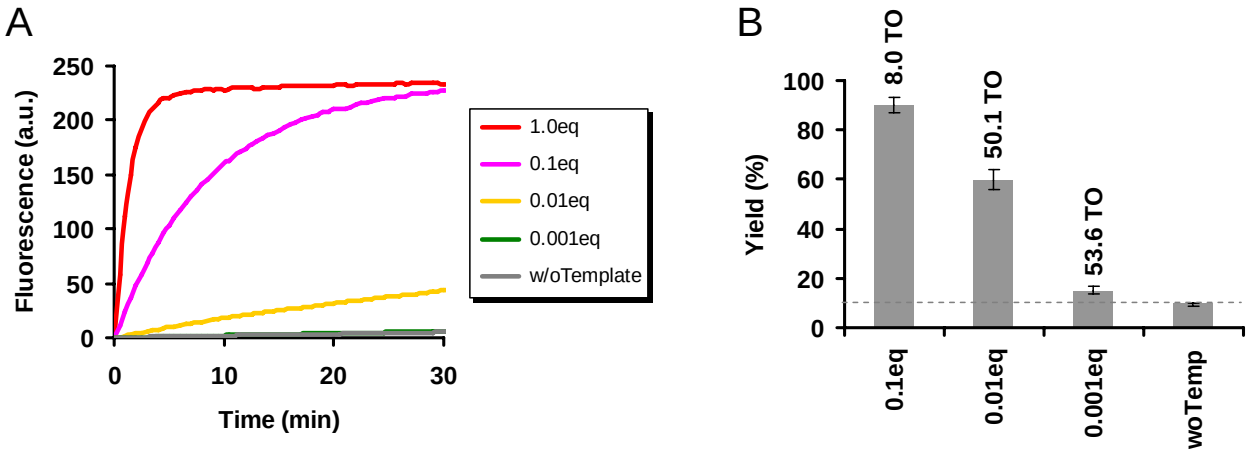

Figure 5. Turnover experiment. (A) Time course of fluorescence intensity in the reaction between 50 nM matched azidomethyl fluorescein and 50 nM matched TPP probe at shown target DNA concentrations in pH 7.2 Tris-HCl buffer containing 100 mM $MgCl_2$ and 10 μg/ml BSA. (B) Reaction yields after 4 hr and turnover numbers (TO).

The time course of the fluorescent signal at 520 nm showed a rapid signal increase in the presence of 1 equiv of matched DNA *bcr/abl-1* (Figure 5A, red line) within 5 min. Catalytic amounts of *bcr/abl-1* (0.1 equiv, 5 nM) also proved efficient in conferring a rapid signal increase, reaching a plateau within 30 min, which is the same level of fluorescence signal to the stoichiometric amount of *bcr/abl-1* (Figure 5A, pink line), and provided 90% yield of reaction product after 4 h calculated from the fluorescence standard curve (Figure 5B). In the absence of DNA, 50 nM probes 1 and 2 yielded 9.7% background reaction after 4 h (Figure 5A, gray line). When the background signal is subtracted, the RETFA probe achieved 8.0 TO in the case of 0.1 equiv *bcr/abl-1*. With a load of 0.01 equiv (500 pM) *bcr/abl-1*, the reaction showed slower fluorescence increase than in the case of 0.1 equiv *bcr/abl-1* (Figure 5A, yellow line) and furnished 69% of the fluorescent product with 50 TO after 4 h. The highest TO number of 54 was achieved with 0.001 equiv *bcr/abl-1* (50 pM; Figure 5A, green line). The speed of the DNA-catalyzed reaction is reduced at very low DNA/probe ratios to an extent that reaction yields are dominated by the off-template background reaction. However, the 15% reaction product obtained with 0.001 equiv *bcr/abl-1* (50 pM) demonstrates that the DNA-templated reaction (5.4%) proceeds more efficiently than the background reaction (9.7%), even with such a very low concentration of target.

6.3.6. Kinetic analysis of the DNA-templated reaction

The mechanism of a DNA-catalyzed reaction gives important information for optimizing the RETFA probe and designing new probes. However, a study of the mechanism has not been carefully carried out. In particular, the rate-limiting step of the DNA-catalyzed reaction is still unclear. Thus, we evaluated the association and dissociation rate constants for the DNA hybridization between *bcr/abl-1* and the RETFA probe, and the rate constants of the azide reduction on DNA templates to obtain information on the rate-limiting step.

The kinetics of association (k_a) and dissociation (k_d) of probe 1 or probe 2 to the immobilized *bcr/abl-1* were successfully monitored using BIAcore technology [66]. Figure 6 shows BIAcore trajectories of *bcr/abl-1*/probe 1 or *bcr/abl-1*/probe 2

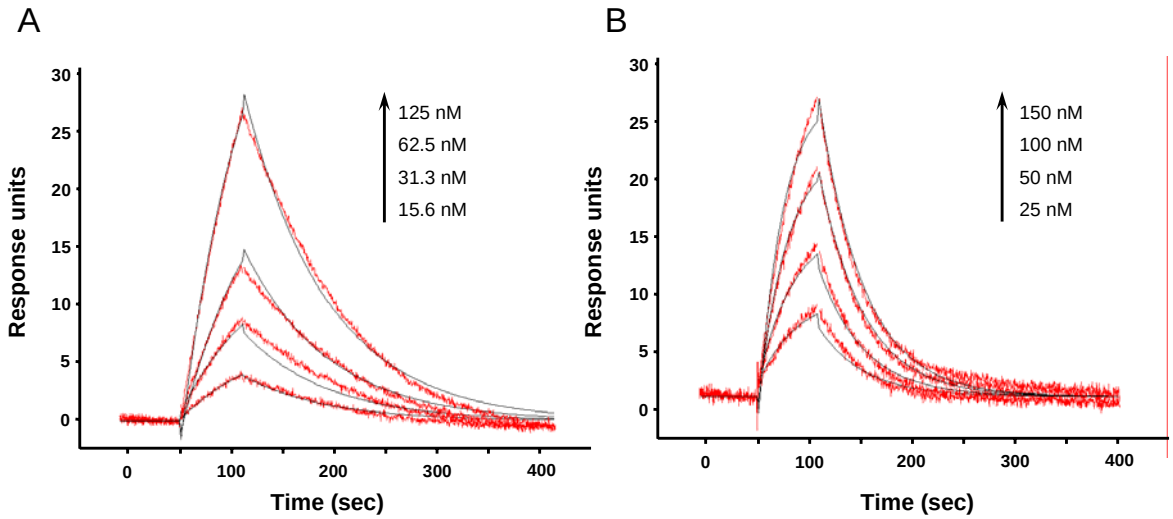

Figure 6. DNA hybridization sensorgrams (fully complementary duplex) analyzed by biacore with varying concentrations of the azidomethyl fluorescein probe (A) or TPP probe (B). The values inside the graphs indicate the probe concentrations.

hybridization runs at different concentrations of each probe in solution. The k_a and k_d for each probe were calculated with BIAcore T100 evaluation software and were summarized in Table 2. The k_a for probes 1 and 2 are 3.1×10^4 M^{-1} s^{-1} (k_{a1}) and 1.3×10^4 M^{-1} s^{-1} (k_{a2}), respectively. The concentration of the DNA-templated reaction (C_0) was 50 nM. Therefore, the k_a' ($k_a \times C_0$) for probes 1 and 2 are calculated as 1.5×10^{-3} s^{-1} (k_{a1}') and 6.3×10^{-3} s^{-1} (k_{a2}'), respectively. On the other hand, the k_d for probes 1 and 2 showed about 10 times higher values, 2.2×10^{-2} s^{-1} (k_{d1}) and 1.2×10^{-2} s^{-1} (k_{d2}), than k_a'.

Next, to determine the rate constant of azide reduction on DNA templates, the plots of ln[**probe 1**]$_t$/[**probe 1**]$_0$ versus time were analyzed by linear regression as simple first-order kinetics by Microsoft Excel (Figure 7). [**probe 1**]$_0$, [**probe 1**]$_t$, and [**reduced probe 1**]$_t$ correspond to initial concentration of probe 1, time dependent concentration of probe 1, and concentration of reduced product. [**probe 1**]$_t$ was calculated according to [**probe 1**]$_t$ = [**probe 1**]$_0$ − [**reduced probe 1**]$_t$, and [**reduced probe 1**]$_t$ was calculated from a standard curve. The apparent first-order rate constant, k_{app}, was obtained from the slope of this plot as 5.9×10^{-3} s^{-1}. The value of k_{app} is very close to the association rate constants k_{a1}' and k_{a2}', which is the slower step in the hybridization kinetics. This similarity suggests that the actual reaction rate of an azide reduction on DNA templates (k_{act}) is close to or even faster than the hybridization kinetics. Therefore, we assumed that the association of the probe to the DNA template might be the rate-limiting step for the DNA-catalyzed reaction for RETFA probe.

6.3.7. Flow cytometric analysis of RNAs in HL60 cells

So far, there has only been one example of quenched probes in living human cells. Flow cytometry (FC) offers the possibility of rapid analysis of a large number of cells and quantitative evaluation of an average over all RNA signals. Thus, we evaluated the feasibility of FC analysis of RNAs by the RETFA probe in HL60 cells. In the *in cell* experiment, we used the bisazidomethyl-quenched fluorescein probe because the quantum yield for the deprotected form of **9**, 0.683, is higher than that of monoazide **3**, 0.202. As described above, our probes have a potential for catalytic turnover. Therefore, both azidomethyl groups on **9** should be deprotected. The targets we chose were 28S

Table 2. Kinetic parameters for the hybridization of each probe and DNA-templated reaction

	k_a ($\times 10^4$ M^{-1} s^{-1})	k_a' ($\times 10^{-3}$ s^{-1})	k_d ($\times 10^{-2}$ s^{-1})	k_{app} ($\times 10^{-3}$ s^{-1})
Hybridization (Probe 1) [a]	3.06	1.53	1.25	–
Hybridization (Probe 2) [a]	1.26	6.29	2.24	–
DNA-templated reaction [b]	–	–	–	5.91

[a] Analyzed by BIAcore instrument.

[b] Analyzed by linear regression as simple first-order kinetics by Microsoft Excel.

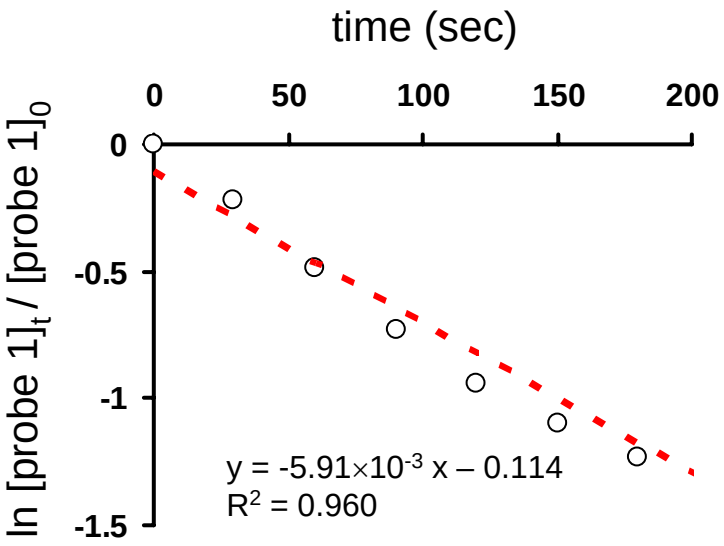

Figure 7. Plots of ln[probe 1]$_t$/[probe 1]$_0$ versus time for 50 nM azidomethyl fluorescein and TPP probe with 50 nM target in 20 mM Tris-HCl (pH 7.2) containing 100 mM $MgCl_2$ and 10 μg/ml BSA.

rRNA, which is abundant in cells, and β-actin mRNA, which has relatively low copies in cells (~2500 molecules per cell) [36]. To decide if the RETFA probe offers the desired fluorescent signal from the target and evaluate any undesired background fluorescence signal from nontemplated reaction or decomposition of the probe, we carried out a series of control experiments by testing the following conditions: the scramble probes, only the profluorescent azide probe, and no probe (the cellular autofluorescence). The sequence of the scramble probe was designed so as not to hybridize next to each other on the target RNA. Prior to the FC analysis, we determined whether the probes could generate a target-dependent fluorescence signal *in vitro* using a short DNA target. No significant background fluorescence was observed in the absence of short 28S rRNA target. In the case of targeting β-actin mRNA, we used three sets of probes for multiple target sites to increase sensitivity. The three sets of probes for β-actin mRNA (33.3 nM each) and DNA targets (33.3 nM each) were mixed to adjust the total concentrations to 100 nM. Reaction of the scramble probe was tested under a same condition. The reaction with the β-actin probe shows a strong fluorescence signal with the target and generated a slight background signal without the target, which was comparable with the background level in the case of the scramble probes.

The FC data are summarized in Figure 8. To introduce the probes into cells, the cells were permeabilized with streptolysin O (SLO) according to the previously reported method. The cells were incubated with SLO in the presence of the RETFA probe for 30 min, resealed with cell culture medium containing $CaCl_2$, and incubated for 1 h at 37 °C and analyzed by FC. The histogram data indicate cell populations with varied fluorescence intensity, which correspond to 28S rRNA, three sets of β-actin mRNA, scramble probes, only azide probe, and no probe (Figure 8A). The median values of fluorescence intensity after subtraction of autofluorescence from cells (no probe) are plotted in Figure 8B. The values on the bars indicate signal to background (S/B) ratio, which is defined as the relative ratios of fluorescence intensity to background signal from the scramble probe. Both 28S rRNA and the three sets of β-actin mRNA probes offered significantly higher fluorescence signals than did the controls, although each set of β-actin mRNA probes did not produce a significant signal. The background value from

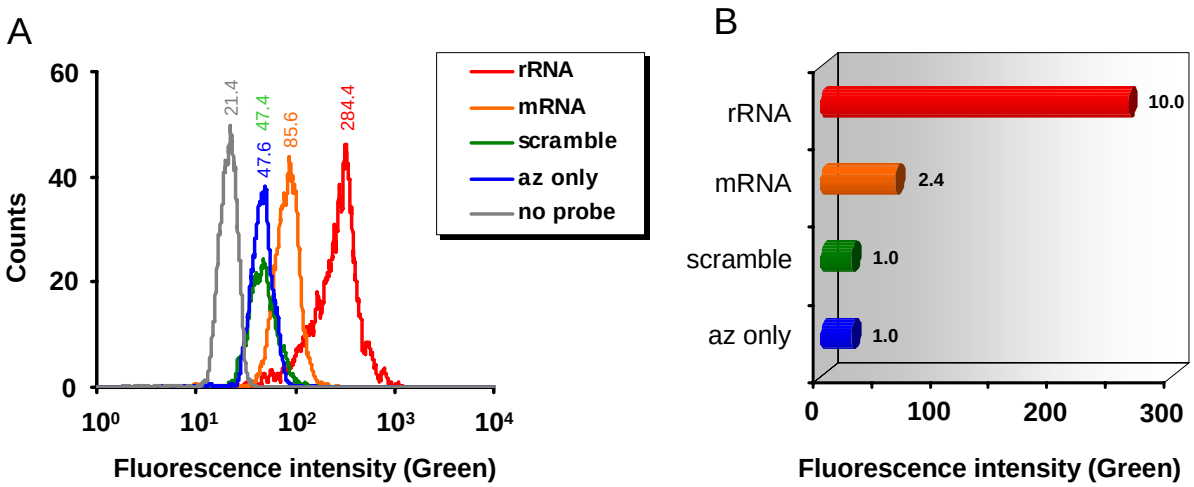

Figure 8. Detection of intracellular RNAs in HL60 cells by flow cytometry. (A) Flow cytometry histogram showing cell-count frequency versus fluorescence intensity for each probe. These histograms correspond to cells that were treated by no probe (negative control, grey); by azidomethyl fluorescein probe only (negative control, blue); by scramble probe (negative control, green); by β-actin mRNA targeted probes (orange); by 28S rRNA targeted probes (red). The values on the each histogram indicate the mean fluorescent signals. (B) Means of fluorescence intensity and signal to background calculated from the histograms. The bars were corrected by cell autofluorescence background (no probe). The values next to the bars indicate the ratios between each probe and scramble probe as a signal to background.

the scramble probes was comparable with that from the azide probe alone, indicating that undesirable intermolecular reactions between the TPP probe and the azidomethyl probe did not occur in living cells. The S/B ratios were 10.0 and 2.4 for 28S rRNA and β-actin mRNA, respectively. This result clearly showed that cellular endogenous 28S rRNA and β-actin mRNA can be detected by our RETFA probes and is consistent with the notion that 28S rRNA is more abundant than β-actin mRNA in the cells.

6.3.8. Fluorescence microscopic analysis of RNAs in HL60 cells

To demonstrate that our approach can give a clear and detailed picture of intracellular localization in living cells, we carried out fluorescence microscopic analysis of RNA species. Imaging technique may reveal important information on mRNA processing, transport, and protein production. Fluorescence images of 28S rRNA and β-actin mRNA in HL60 cells are shown in Figure 9. First, imaging 28S rRNA was performed using bisazidomethyl fluorescein and TPP probes as for the FC experiment. After the probes were introduced into cells using the SLO method, the cell suspension was directly spotted on glass slides without any washing step and was imaged by a fluorescence microscope. Specific fluorescent signals were observed by excitation at 488 nm and collecting 520 nm fluorescein emissions using a band-pass filter. Panels C and D in Figure 9 display the fluorescent signal of the scramble probes, showing that little or no signal was observed. On the other hand, a strong signal was observed in the nucleolus using target-specific probes (Panels A and B), which is in fair agreement with previous results by FISH in fixed specimens [67].

Next, to confirm that our system can detect low-expression RNA in cells, β-actin mRNA probes were delivered into HL60 cells using SLO. Again, the majority of the fluorescent signals was observed around the nucleus only from target-specific probes (Panels E and F), whereas the scramble probes gave small signals (Panels G and H). We conclude that signals from specific RNAs can be observed using the designed RETFA probe in human cells.

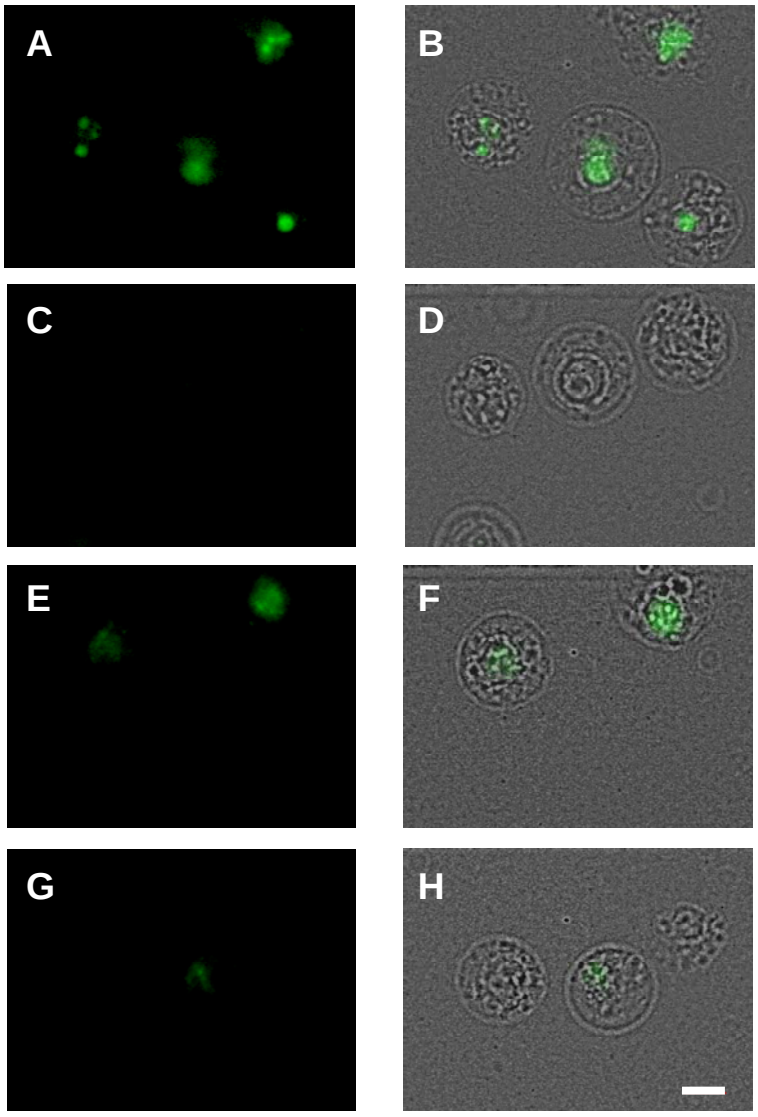

Figure 9. Detection of intracellular human 28S rRNA and β–actin mRNA by fluorescence microscopy. (A-D) 28S rRNA probe (A and B) and scramble control (C and D). A and C show fluorescent signal only. B and D show its overlay with bright field image. (E-H) beta-actin mRNA probe (E and F) and scramble control (G and H). E and G show fluorescent signal only. F and H show its overlay with bright field image.

6.4. Discussion

The Staudinger reduction of organic azides by TPP holds promise for OTR, because of its exceptional degree of bioorthogonality. Several ideas have been applied to link the Staudinger reaction to the fluorescence turn-on event for OTR. These strategies can be categorized into two types. One strategy involves the reaction step where the azide probe unmasks a 2-(diphenylphosphino)benzoate derivative of fluorescein. Alternatively, a TPP-probe activates the azide-masked fluorophores, which are 7-azidocoumarin and azide-substituted rhodamines (RETF probe). In addition, azidomethyl-protected coumarin has very recently been reported as a new fluorogenic molecule. These probes demonstrate excellent signal amplification with fluorescence readout except for the RETF probe. However, possible drawbacks limit the scope of *in cell* applications because of increased undesired background fluorescence. This may be due to hydrolysis of the phenolic ester or light decomposition of azide group when azide-protected coumarin is irradiated with excitation light in the ultraviolet region. In general, oxidation of TPP in living cells was also involved. Consequently, these previous approaches have not been applied to imaging or detection of RNA in living cells.

In this paper, we have demonstrated that the RETFA probe with azidomethyl-protected fluorescein can detect endogenous RNAs in living cells. Azidomethyl-protected fluorescein is quickly uncaged by reduction of the azide group and emits fluorescence at 520 nm with excitation at 490 nm, which is a suitable wavelength for *in cell* detection. In addition, the RETFA probe completed stoichiometric reaction within 3 min and can amplify fluorescence signals based on a catalytic OTR when the target is at a very low concentration compared with the probes. The TO number reached up to 50 when 100 times excess of probe was used. This amplification property is one of the great improvements compared with our previous RETF probe.

Quantitative detection of 28S rRNA and β-actin mRNA was successfully carried out on the FC instrument. A single probe was sufficient for detection of 28S rRNA. On the other hand, simultaneous introduction of three sets of probes offered significant signal for detection of β-actin, although each individual probe offered no significant signal.

Cellar mRNA is known to form complex secondary or tertiary structures. It is very hard to design an optimum probe with accessibility to target sites. This result indicates that introducing multiple sets of probes might be one solution to achieve accessibility by opening up the complex mRNA structure.

Finally, development of an efficient catalytic reaction on the oligonucleotide template is still challenging. We carried out a mechanistic study of the catalytic reaction on the RETFA probe to obtain clues for designing efficient turnover probes. Kinetic analysis by BIAcore technology showed that the association step of the probe (k_a') is 10 times slower than the dissociation step (k_d') on probe hybridization. The apparent rate constant of the fluorogenic chemical reaction (k_{app}) has a similar value to k_a'. Presumably, association might be the rate-limiting step for the amplification reaction from these results, although this experiment did not reflect an exact phenomenon in solution. We assume that new probe designs should enhance association speed to achieve more efficient turnover.

References

1. Shav-Tal, Y., Darzacq, X., and Singer, R. H. (2006) Gene expression within a dynamic nuclear landscape. *EMBO J. 25,* 3469-3479.
2. Dirks, R. W., and Tanke, H. J. (2006) Advances in fluorescent tracking of nucleic acids in living cells. *Biotechniques 40,* 489-496.
3. Behrens, S., Fuchs, B. M., Mueller, F., and Amann, R. (2003) Is the in situ accessibility of the 16S rRNA of Escherichia coli for Cy3-labeled oligonucleotide probes predicted by a three-dimensional structure model of the 30S ribosomal subunit? *Appl. Environ. Microbiol. 69,* 4935-4941.
4. Dirks, R. W., Molenaar, C., and Tanke, H. J. (2001) Methods for visualizing RNA processing and transport pathways in living cells. *Histochem. Cell Biol. 115,* 3-11.
5. Czaplinski, K., and Singer, R. H. (2006) Pathways for mRNA localization in the cytoplasm. *Trends Biochem. Sci.* 31, 687-693.
6. Shav-Tal, Y., Darzacq, X., Shenoy, S. M., Fusco, D., Janicki, S. M., Spector, D. L., and Singer, R. H. (2004) Dynamics of single mRNPs in nuclei of living cells. *Science 304,* 1797-1800.
7. Levsky, J. M., and Singer, R. H. (2003) Fluorescence in situ hybridization: past, present and future. *J. Cell Sci. 116,* 2833-2838.
8. Isaacs, F. J., Dwyer, D. J., Ding, C. M., Pervouchine, D. D., Cantor, C. R., and Collins, J. J. (2004) Engineered riboregulators enable post-transcriptional control of gene expression. *Nat. Biotechnol. 22,* 841-847.
9. Hasegawa, S., Jackson, W. C., Tsien, R. Y., and Rao, J. (2003) Imaging Tetrahymena ribozyme splicing activity in single live mammalian cells. *Proc. Nat. Acad. Sci. U.S.A. 100,* 14892-14896.
10. Rodriguez, A. J., Condeelis, J., Singer, R. H., and Dictenberg, J. B. (2007) Imaging mRNA movement from transcription sites to translation sites. *Semin. Cell Dev. Biol. 18,* 202-208.
11. Lewin, B. (1997) Gene VI ed., Oxford university press, Inc., New York.
12. Giles, R. V., and Tidd, D. M. (1992) Increased specificity for antisense oligodeoxynucleotide targeting of RNA cleavage by RNaseH using chimeric methylphosphonodiester phosphodiester structures. *Nucleic Acids Res. 20,* 763-770.

13. Tu, G. C., Cao, Q. N., Zhou, F., and Israel, Y. (1998) Tetranucleotide GGGA motif in primary RNA transcripts - Novel target site for antisense design. *J. Biol. Chem. 273,* 25125-25131.
14. Sohail, M., and Southern, E. M. (2000) Selecting optimal antisense reagents. *Adv. Drug Deliv. Rev. 44,* 23-34.
15. Tyagi, S., Bratu, D. P., and Kramer, F. R. (1998) Multicolor molecular beacons for allele discrimination. *Nat. Biotechnol. 16,* 49-58.
16. Tyagi, S., and Kramer, F. R. (1996) Molecular beacons: probes that fluoresce upon hybridization. *Nat. Biotechnol. 14,* 303-308.
17. Piatek, A. S., Tyagi, S., Pol, A. C., Telenti, A., Miller, L. P., Kramer, F. R., and Alland, D. (1998) Molecular beacon sequence analysis for detecting drug resistance in Mycobacterium tuberculosis. *Nat. Biotechnol. 16,* 359-363.
18. Tyagi, S., Marras, S. A., and Kramer, F. R. (2000) Wavelength-shifting molecular beacons. *Nat. Biotechnol. 18,* 1191-1196.
19. Bratu, D. P., Cha, B. J., Mhlanga, M. M., Kramer, F. R., and Tyagi, S. (2003) Visualizing the distribution and transport of mRNAs in living cells. *Proc. Nat. Acad. Sci. U.S.A. 100,* 13308-13313.
20. Vargas, D. Y., Raj, A., Marras, S. A. E., Kramer, F. R., and Tyagi, S. (2005) Mechanism of mRNA transport in the nucleus. *Proc. Nat. Acad. Sci. U.S.A. 102,* 17008-17013.
21. Sando, S., and Kool, E. T. (2002) Imaging of RNA in bacteria with self-ligating quenched probes. *J. Am. Chem. Soc. 124,* 9686-9687.
22. Silverman, A. P., and Kool, E. T. (2006) Detecting RNA and DNA with templated chemical reactions. *Chem. Rev. 106,* 3775-3789.
23. Abe, H., and Kool, E. T. (2006) Flow cytometric detection of specific RNAs in native human cells with quenched autoligating FRET probes. *Proc. Nat. Acad. Sci. U.S.A. 103,* 263-268.
24. Silverman, A. P., and Kool, E. T. (2007) Oligonucleotide probes for RNA-targeted fluorescence in situ hybridization. *Adv. Clin. Chem. 43,* 79-115.
25. Sando, S., and Kool, E. T. (2002) Quencher as leaving group: efficient detection of DNA-joining reactions. *J. Am. Chem. Soc. 124,* 2096-2097.
26. Abe, H., and Kool, E. T. (2004) Destabilizing universal linkers for signal amplification in self-ligating probes for RNA. *J. Am. Chem. Soc. 126,* 13980-13986.
27. Sando, S., Abe, H., and Kool, E. T. (2004) Quenched auto-ligating DNAs: multicolor identification of nucleic acids at single nucleotide resolution. *J. Am. Chem. Soc. 126,* 1081-1087.
28. Fang, X. H., Li, J. J., and Tan, W. H. (2000) Using molecular beacons to probe molecular interactions between lactate dehydrogenase and single-stranded DNA. *Anal. Chem. 72,* 3280-3285.
29. Tsuji, A., Koshimoto, H., Sato, Y., Hirano, M., Sei-Iida, Y., Kondo, S., and Ishibashi, K. (2000) Direct observation of specific messenger RNA in a single living cell under a fluorescence microscope. *Biophys. J. 78,* 3260-3274.
30. Molenaar, C., Marras, S. A., Slats, J. C. M., Truffert, J. C., Lemaitre, M., Raap, A. K., Dirks, R. W., and Tanke, H. J. (2001) Linear 2' O-methyl RNA probes for the visualization of RNA in living cells. *Nucleic Acids Res. 29,* e89.
31. Perlette, J., and Tan, W. (2001) Real-time monitoring of intracellular mRNA hybridization inside single living cells. *Anal. Chem. 73,* 5544-5550.
32. Bratu, D. P., Cha, B. J., Mhlanga, M. M., Kramer, F. R., and Tyagi, S. (2003) Visualizing the distribution and transport of mRNAs in living cells. *Proc. Nat. Acad. Sci. U.S.A. 100,* 13308-13313.
33. Santangelo, P. J., Nix, B., Tsourkas, A., and Bao, G. (2004) Dual FRET molecular beacons for mRNA detection in living cells. *Nucleic Acids Res. 32,* e57.
34. Nitin, N., Santangelo, P. J., Kim, G., Nie, S., and Bao, G. (2004) Peptide-linked molecular beacons for efficient delivery and rapid mRNA detection in living cells. *Nucleic Acids Res. 32,* e58.
35. Matsuo, T. (1998) In situ visualization of messenger RNA for basic fibroblast growth factor in living cells. *Biochim. Biophy. Acta (General Subjects) 1379,* 178-184.
36. Tyagi, S., and Alsmadi, O. (2004) Imaging native beta-actin mRNA in motile fibroblasts. *Biophy. J. 87,* 4153-4162.
37. Sokol, D. L., Zhang, X., Lu, P., and Gewirtz, A. M. (1998) Real time detection of DNA.RNA

hybridization in living cells. *Proc. Nat. Acad. Sci. U.S.A. 95,* 11538-11543.
38. Wang, W., Cui, Z. Q., Han, H., Zhang, Z. P., Wei, H. P., Zhou, Y. F., Chen, Z., and Zhang, X. E. (2008) Imaging and characterizing influenza A virus mRNA transport in living cells. *Nucleic Acids Res. 36,* 4913-4928.
39. Chen, A. K., Behlke, M. A., and Tsourkas, A. (2007) Avoiding false-positive signals with nuclease-vulnerable molecular beacons in single living cells. *Nucleic Acids Res. 35,* e105.
40. Kubota, T., Ikeda, S., and Okamoto, A. (2009) Doubly thiazole orange-labeled DNA for live cell RNA imaging. *Bull. Chem. Soc. Jpn. 82,* 110-117.
41. Dose, C., Ficht, S., and Seitz, O. (2006) Reducing product inhibition in DNA-template-controlled ligation reactions. *Angew. Chem., Int. Ed. 45,* 5369-5373.
42. Dose, C., and Seitz, O. (2008) Single nucleotide specific detection of DNA by native chemical ligation of fluorescence labeled PNA-probes. *Bioorg. Med. Chem. 16,* 65-77.
43. Dose, C., and Seitz, O. (2005) Convergent synthesis of peptide nucleic acids by native chemical Ligation. *Org. Lett. 7,* 4365-4368.
44. Ma, Z., and Taylor, J. S. (2003) PNA-based RNA-triggered drug-releasing system. *Bioconjugate Chem. 14,* 679-683.
45. Ma, Z., and Taylor, J. S. (2001) Nucleic acid triggered catalytic drug and probe release: a new concept for the design of chemotherapeutic and diagnostic agents. *Bioorg. Med. Chem. 9,* 2501-2510.
46. Ma, Z., and Taylor, J. S. (2000) Nucleic acid-triggered catalytic drug release. *Proc. Nat. Acad. Sci. U.S.A. 97,* 11159-11163.
47. Cai, J., Li, X., Yue, X., and Taylor, J. S. (2004) Nucleic acid-triggered fluorescent probe activation by the Staudinger reaction. *J. Am. Chem. Soc. 126,* 16324-16325.
48. Abe, H., Wang, J., Furukawa, K., Oki, K., Uda, M., Tsuneda, S., and Ito, Y. (2008) A reduction-triggered fluorescence probe for sensing nucleic acids. *Bioconjugate Chem. 19,* 1219-1226.
49. Pianowski, Z. L., and Winssinger, N. (2007) Fluorescence-based detection of single nucleotide permutation in DNA via catalytically templated reaction. *Chem. Commun.37,* 3820-3822.
50. Franzini, R. M., and Kool, E. T. (2008) 7-azidomethoxy-coumarins as profluorophores for templated nucleic acid detection. *Chembiochem 9,* 2981-2988.
51. Grossmann, T. N., and Seitz, O. (2006) DNA-catalyzed transfer of a reporter group. *J. Am. Chem. Soc. 128,* 15596-15597.
52. Sando, S., Sasaki, T., Kanatani, K., and Aoyama, Y. (2003) Amplified nucleic acid sensing using programmed self-cleaving DNAzyme. *J. Am. Chem. Soc. 125,* 15720-15721.
53. Franzini, R. M., and Kool, E. T. (2008) Organometallic activation of a fluorogen for templated nucleic acid detection. *Org. Lett. 10,* 2935-2938.
54. Abe, H., and Kool, E. T. (2005) Universal linkers for signal amplification in auto-ligating probes. *Nucl. Acids Symp. Ser. 49,* 37-38.
55. Lemieux, G. A., de Graffenried, C. L., and Bertozzi, C. R. (2003) A fluorogenic dye activated by the Staudinger ligation. *J. Am. Chem. Soc. 125,* 4708-4709.
56. Kojima, H., Nakatsubo, N., Kikuchi, K., Kawahara, S., Kirino, Y., Nagoshi, H., Hirata, Y., and Nagano, T. (1998) Detection and imaging of nitric oxide with novel fluorescent indicators: Diaminofluoresceins. *Anal. Chem. 70,* 2446-2453.
57. Maeda, H., Fukuyasu, Y., Yoshida, S., Fukuda, M., Saeki, K., Matsuno, H., Yamauchi, Y., Yoshida, K., Hirata, K., and Miyamoto, K. (2004) Fluorescent probes for hydrogen peroxide based on a non-oxidative mechanism. *Angew. Chem. Int. Ed. 43,* 2389-2391.
58. Miller, E. W., Tulyathan, O., Isacoff, E. Y., and Chang, C. J. (2007) Molecular imaging of hydrogen peroxide produced for cell signaling. *Nat. Chem. Biol. 3,* 263-267.
59. Dale, T. J., and Rebek, J., Jr. (2006) Fluorescent sensors for organophosphorus nerve agent mimics. *J. Am. Chem. Soc. 128,* 4500-4501.
60. Marras, S. A., Kramer, F. R., and Tyagi, S. (2002) Efficiencies of fluorescence resonance energy transfer and contact-mediated quenching in oligonucleotide probes. *Nucleic Acids Res. 30,* e122.
61. Loubinoux, B., Tabbache, S., Gerardin, P., and Miazimbakana, J. (1988) Protection of phenols via the azidomethylene group - application in the synthesis of unstable phenolic compounds. *Tetrahedron 44,* 6055-6064.

62. Young, T., and Kiessling, L. L. (2002) A strategy for the synthesis of sulfated peptides. *Angew. Chem. Int. Ed. 41,* 3449-3451.
63. Sakurai, K., Snyder, T. M., and Liu, D. R. (2005) DNA-templated functional group transformations enable sequence-programmed synthesis using small-molecule reagents. *J. Am. Chem. Soc. 127,* 1660-1661.
64. Payne, R. J., Toscano, M. D., Bulloch, E. M., Abell, A. D., and Abell, C. (2005) Design and synthesis of aromatic inhibitors of anthranilate synthase. *Org. Biomol. Chem. 3,* 2271-2281.
65. Pinnisi, E. (1998) A closer look at SNPs suggests difficulties. *Science 281,* 1787-1789.
66. Jensen, K. K., Orum, H., Nielsen, P. E., and Norden, B. (1997) Kinetics for hybridization of peptide nucleic acids (PNA) with DNA and RNA studied with the BIAcore technique. *Biochemistry 36,* 5072-5077.
67. Paillasson, S., Van De Corput, M., Dirks, R. W., Tanke, H. J., Robert-Nicoud, M., and Ronot, X. (1997) In situ hybridization in living cells: detection of RNA molecules. *Exp. Cell Res. 231,* 226-233.

Chapter 7

General conclusions and perspectives

Chapter 7

General conclusions and perspectives

7

7.1. General conclusions

Fluorescent-labeled oligonucleotides are becoming important tools for detecting oligonucleotide sequences. A possible application is the detection of RNA species in cells by *in situ* hybridization. However, standard fluorescent probes require careful handling to avoid nonspecific signals. Fluorogenic probes with fluorescence on/off mechanism have been developed to avoid this problem. Some of these probes have been applied to the detection of RNA in cells. Examples are molecular beacon (MB) or target-assisted chemical ligation. Target-dependent fluorescence enhancement of these methods is based on the resonance energy transfer (RET) mechanism, for which a pair of quencher and fluorescence dyes is normally used. However, higher sensitivity for the detection method is still required to monitor gene expression in cells. Recently, fluorescence generation methods triggered by a chemical reaction accompanied by transformation of the chemical structure of the fluorogenic compound have been developed. Fluorescence modulation is caused by photoinduced electron transfer or absorption change. The signal/background (S/B) ratio of this type of molecule could exceed that of the RET mechanism. However, there are few reports that describe chemical reaction-triggered fluorogenic molecules for oligonucleotide sensing, although this method offers high sensitivity. In this thesis, I report a reduction-triggered fluorescence probe that shows a high S/B ratio for sensing oligonucleotides. A new fluorescence molecule, rhodamine azide naphthorhodamine azide, and fluorescein methylazide, that I designed and synthesized are activated only by a

specific reducing reagent on the oligonucleotide target and is very stable under biological conditions, showing little background fluorescence. The probe was applied to the sensing of nucleic acids *in vitro* and of endogenous RNAs in bacterial and native human cells.

In chapter 2, I described the problem of highly sensitive FISH, which amply fluorescent signals using antibody or enzyme, for the detection of bacterial cells. The development of highly sensitive methods is essential since there are many low-copy-number RNAs in cells. Several techniques have been developed for this purpose, such as catalyzed reporter deposition (CARD)-FISH. However, these signal amplification methods require the diffusion of large-molecular-weight molecules such as enzymes, antibodies, or (strept)avidin into fixed whole cells. Therefore, the cell walls must be permeabilized for probe access to the target molecule, while minimizing the loss of the target molecule and cell morphology. I tried to define the optimal digestion conditions for several bacterial strains belonging to different phylogenetic divisions by permeabilization at different concentrations of lysozyme and/or achromopeptidase solution for conventional FISH, DIG–FISH, and CARD–FISH. Consequently, most bacterial strains were successfully detected using CARD-FISH with 10 mg/ml lysozyme pretreatment. Additionally, achromopeptidase pretreatment was a highly effective means of permeabilizing the bacterial strains that were unable to be detected with lysozyme pretreatment, while it was considered impossible to visualize all bacterial strains by a universal permeabilizing procedure. My results will contribute to the optimization of permeabilizing conditions, which is one of the most important factors for the successful application of highly sensitive FISH. However, highly sensitive FISH cannot apply to living cells because permeabilization steps cause the cell damage and death.

In chapter 3, to solve the problems described above, I described the fluorescent detection method for nucleic acids sensing triggered by the reaction on the target nucleic acids, which can amplify the fluorescent signal without antibody or enzyme and can detect nucleic acids in native cells. Some methods have been applied to the detection of RNA in cells. Examples are molecular beacon (MB) or target-assisted chemical ligation. Target-dependent fluorescence enhancement of these methods is based on the resonance energy transfer (RET) mechanism, for which a pair of quencher and fluorescence dyes is

normally used. However, higher sensitivity for the detection method is still required to monitor gene expression in cells. I have developed a reduction-triggered fluorescence probe with a new fluorogenic compound derivatized from rhodamine 110 for sensing oligonucleotides. The chemistry to activate the compound involves the reaction between the azide group of rhodamine derivatives and reducing reagents, with the fluorescence signal appearing after reduction of the azide group. The signal/background ratio of this fluorogenic compound reached 2100-fold enhancement in fluorescence intensity. Dithio-1,4-threitol or triphenylphosphine as reducing reagents were successfully utilized for this chemistry to be introduced into the DNA probe. The genetic detection requires that two strands of DNA bind onto target oligonucleotides, one probe carrying a reducible fluorogenic compound while the other carries the reducing reagents. The reaction proceeds automatically without any enzymes or reagents under biological conditions to produce a fluorescence signal within 10–20 min in the presence of target DNA or RNA. In addition, the probe was very stable under biological conditions, even such extreme conditions as pH 5 solution, pH 10 solution, or high temperature (90 °C) with no undesirable background signal. The probes were successfully applied to the detection of oligonucleotides at single nucleotide level in solution.

In chapter 4, I described the newly synthesized red fluorescent molecule, naphthorhodamine bis azide. Previous studies in chapter 3 showed that rhodamine fluorescence was controlled by the lactone ring, which is altered by reduction of the azide group. After opening the lactone, the longer conjugated system emits fluorescence. I thought that this mechanism can help design other fluorogenic compounds. I expanded the two phenyl groups of rhodamine to naphthyl groups for naphthorhodamine. The expanded π system of the naphthyl group red shifts emission compared with rhodamine. In addition, the conjugated system of naphthorhodamine should have a similar fluorogenic molecular mechanism to rhodamine. I examined the fluorescence properties of naphthorhodamine derivatives. No significant fluorescence with excitation at 595 nm was observed for naphthorhodamine bis azide. After addition of TCEP to the solution of bis azide, a strong emission appeared around 650 nm, where the emission was enhanced 550-fold. This red fluorescent system could also be used for nucleic acids sensing. From these results, I

succeeded to synthesis the dual color fluorescent compounds. It could be possible to image a couple of RNA molecules in cells using these systems simultaneously.

In chapter 5, I described that the system with rhodamine azide could be applied to intracellular RNA detection. I proceeded to test the probes in bacterial cells. Cells were fixed with paraformaldehyde according to literature methods and were incubated with probes at 37 °C for 30 min. The sequences of probes were determined in perspective of accessibility according to previous literature. Cell mixtures were directly spotted on a slide glass without a washing step and observed using a microscope. A strong fluorescent signal was observed in the case of the matched probe pair, but no signal was observed from the mismatched probe pair. The data show that my system can be used to detect specific RNA sequences in structured biological targets in cells. This suggests the possibility of their general use in identifying bacterial pathogens by their ribosomal RNAs.

In chapter 6, I described that the advanced reduction-triggered fluorescence system with fluorescein methyleneazide was developed and was applied for the intracellular RNAs detection in native human cells. In the previous chapter, I successfully applied the probe to detection of oligonucleotides in solution and endogenous RNA in bacterial cells. However, the reaction between the rhodamine azide probe and the TPP probe initially produces a stable fluorescent ligation product with an aza-ylide bond due to the presence of long π-conjugation, and then gives a fluorescent product with rhodamine amine through hydrolysis of the aza-ylide bond. The formation of aza-ylide-mediated ligation product between probes exhibit catalytic turnover because the product usually binds the template with higher affinity than the reactant did before reaction. The amplification of reaction product signals is needed when the target to be detected is present at low concentration such as intracellular mRNAs. To reduce a product inhibition in RETF system, I newly designed this new system, reduction-triggered fluorescence amplification (RETFA) system, and synthesized fluorescein derivative with methyleneazide protection group. The unmasking of the desired phenols is achieved by reduction of azide group followed by rapid deprotection of methyleneazide group in mildly acid condition. Staudinger reaction using TPP as a reducing reagent produces the corresponding

phosphorus compound. The reaction between methyleneazide group and TPP does not seem to yield a stable ligation product with an aza-ylide bond; therefore, higher catalytic turnover can be expected to RETFA system. Actually, about 50 turnover of the reaction was observed at 37 °C for 4 hours *in vitro*. This means that the fluorescent signal could amplify 50 fold, suggesting that my system is considerably useful for detecting low copy number RNAs in cell. In order to evaluate whether RETF probe could successfully detect gene expression in single living cells, flow cytometry and fluorescent microscopy analysis were performed. The targets we chose were 28S rRNA, which are abundant in cell, and β-actin mRNA, which are relatively low in cell (~2500 molecules per cell). Both 28S rRNA and β-actin mRNA probes offered significantly higher intensity than did the controls. The background value from scramble probes was comparable with that from only azide probe, indicating that undesirable reaction between phosphine and methyleneazide group did not occurred. This result clearly showed that cellular endogenous 28S rRNA and β-actin mRNA can be detected by our probes and is consistent with the notion that 28S rRNA is more abundant than β-actin mRNA in the cells.

7.2. Future perspectives

My strategy described in this thesis enable us to detect RNA molecules in “native” cells, whereas the previous methods for detection of intracellular RNAs needed cell fixation inducing cell death. The combination of our strategy and fluorescent activation cell sorting (FACS) system allow us to recultivation of the sorted cells based on the genetic information. Actually, I described the intracellular RNA detection with FACS in chapter 6, it is highly possible that novel cell separation method could be brought to realization. There are many target cells to be concentrated and isolated such as useful microorganisms in environment and undifferentiated cells in our bodies.

The culturing technique for bacteria and the molecular biology such as PCR and metagenome have powerfully developed microbiology, but they are not complete technology. Conventional culturing technique can isolate only 1% of bacteria in the

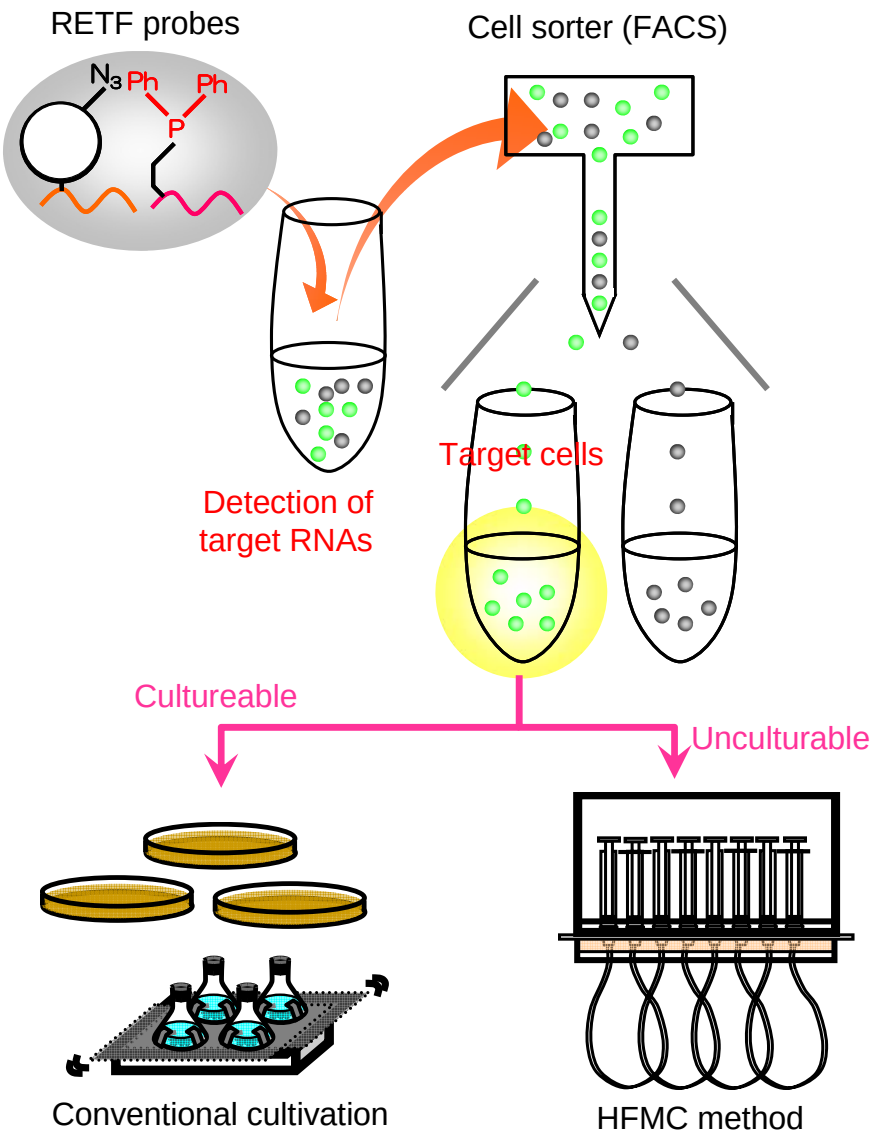

Figure 7.1 Schematic presentation of microorganism separation method based on genetic information using RETF system and cell sorter.

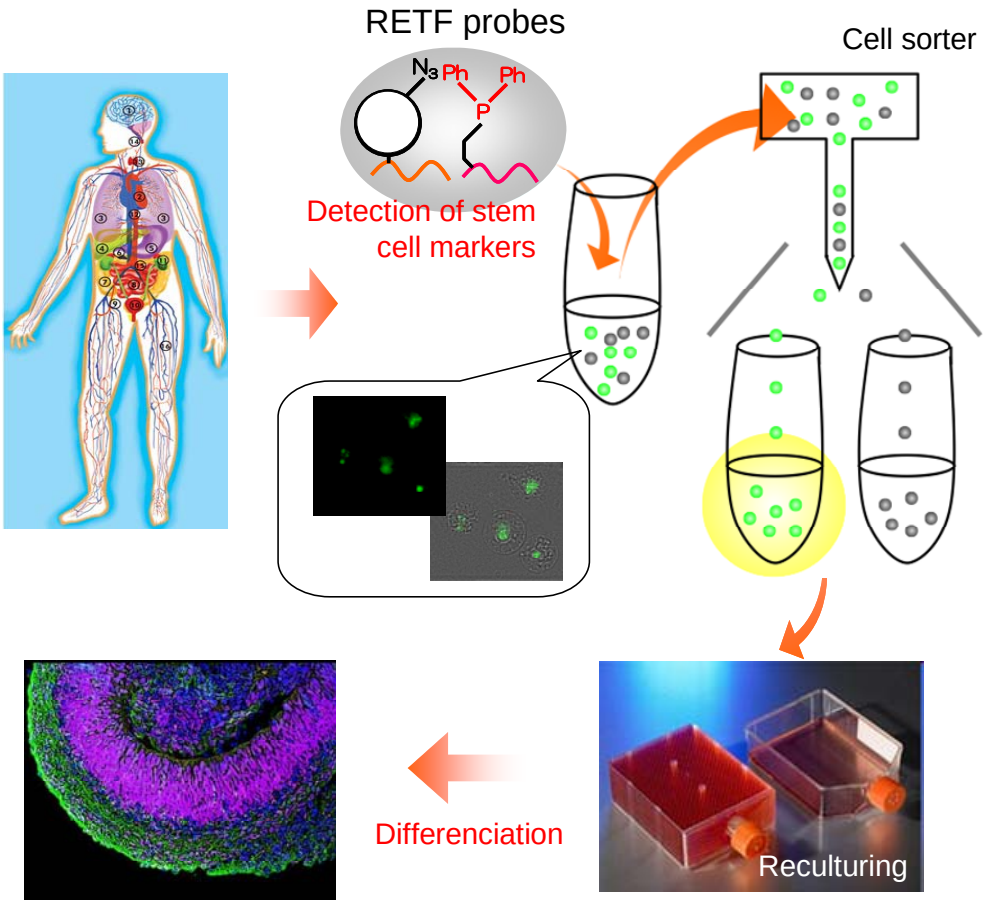

Figure 7.2 Schematic presentation of somatic stem cell separation method based on genetic information using RETF system and cell sorter.

world, and there are limitations to analyze living bacteria with molecular biology. Then biologists and engineer have required the technique for separation of living bacterial cells from environmental conditions. Although some bacterial separation techniques such as electrophoresis, monoclonal antibody, cell chromatography and FISH have been developed, there is no complete method to separate target bacteria specifically from bacterial consortium as living cells. On the other hand, the database of microbial rRNA gene has increased due to the progress of molecular biology methods; therefore we can use much information for separation. In case of the target cells could not be cultured with conventional methods, recultivation could be carried out with the hollow fiber membrane chamber (HFMC) method. Therefore, my strategy could be a powerful tool for the concentration and isolation of environmental microorganisms (Figure 7.1).

The stem cells are considered to be very useful to the regenerated medicine. Recently, many methods are developing for this region such as the induction of differentiation, the propagation of stem cells, and reprogramming to iPS cell. Furthermore, the method for separation between differentiated and undifferentiated cells should be one of the most important topics in this area. For this purpose, many researchers have been searching the genetic or cell surface markers for stem cells; however, no crucial methods were developed until now. There is no doubt that the genetic marker for stem cells due to the continuation of intensive search. On the other hand, there are some reports on stem cells in adipose cells. Therefore, my strategy could be a powerful tool for the separation of somatic stem cells (Figure 7.2).

Acknowledgements

Acknowledgements

I would like to express my profound respect and gratitude to Prof. Satoshi Tsuneda (Waseda University) as my supervisor. I greatly appreciate his continuous support, timely advice, and sincere encouragement.

I would like to express my gratitude to Prof. Kiyotaka Sakai, Prof. Izumi Hirasawa (Waseda University), and Prof. Oliver Seitz (Humboldt-Universität zu Berlin) for valuable suggestions and helpful comments.

I would like to express my heartfelt gratitude to Dr. Hiroshi Abe (RIKEN) for giving me a chance to study in RIKEN in Wako and helpful advice and encouragement throughout the study.

I would like to express my gratitude to Dr. Yoshihito Ito (RIKEN), Dr. Yuhei Inamori (NIES), Dr. Naohiro Noda (AIST), and Dr. Tatsuhiko Hoshino (University of Aarhus) for constructive and useful comments.

I am thankful to Dr. Yasushi Sako and Dr. Kayo Hibino (RIKEN) for technical advices and warm encouragement.

I am very grateful to all the members in the Nanomedical Engineering Laboratory in the RIKEN, particularly Ms. Tomoko Tamai, Ms. Reiko Takeuchi, and Ms. Yaeko Yazaki for secretarial contribution.

I am very grateful to all the members of RIKEN I worked with, particularly Dr. Wang Jin, Dr. Aya Shibata, Dr. Masaya Toda, Dr. Mingzhe Liu, Dr. Akira Wada, Mr. Kazuma

Oki, Mr. Atsushi Nagao, Mr. Atsushi Uchiyama, Ms. Naoko Abe, Ms. Yuko Kondo, Ms. Miwako Uda, Mr. Mitsuru Harada, and Ms. Mika Ito.

I am very grateful to all the members of the Tsuneda Laboratory, particularly Ms. Hiroko Takeno, Dr. Yoshiteru Aoi, Dr. Sachiko Yoshie, Dr. Akihiko Terada, Dr. Takashi Kondo, Dr. Naohiro Kishida, Dr. Toshifumi Osaka, Dr. Takeshi Terahara, Dr. Hidenori Tani, Mr. Ken Adachi, and Mr. Shinya Matsumoto.

I was financially supported by Junior Research Associate (JRA) from RIKEN from 2007 to 2008 and the Research Fellowship for Young Scientists from Japan Society for the Promotion of Science (JSPS) from 2008 to 2009.

Finally, I would like to express my profound gratitude to my family. Without their help and encouragement, I would not be able to complete this thesis.

February 2008

Kazuhiro Furukawa

Appendix

博士論文概要

これまでの生命科学研究の主流は，PCR（Polymerase Chain Reaction）や，シーケンシングによる塩基配列取得などに代表される，試験管内（*in vitro*）での研究が一般的であった。しかしながら，実際の生体内において「何が」「どこで」「どのように」働いているかといった生命現象の根本を理解するには、細胞内（*in vivo*）における現象を解明する必要がある。一方，RNA（Ribonucleic acid）は、現在の生命科学研究の大きなターゲットとなっている生体分子である。触媒作用をもつ RNA 分子であるリボザイムや、二本鎖 RNA が同じ配列を有する mRNA を特異的に分解する現象である RNA 干渉（RNA interference；RNAi）の発見により，RNA が生命の起源であるという RNA ワールド仮説までもが提唱されるようになった。また、ゲノム研究と転写産物の網羅的解析によって，タンパク質をコードしない ncRNA（non-cording RNA）が驚くほど多く転写されていることが明らかになった。これらのことから，生体内における RNA の機能解明は，生命科学研究において重要な課題となっている。しかしながら，近年の光学顕微鏡と蛍光化合物の技術的進歩に伴い検出感度や解像度が向上してきたにもかかわらず、細胞内における RNA 検出においては未だ確立された方法がないのが現状である。特に，生きた細胞内における RNA 検出については，既往の報告は皆無に等しい。

以上の点を踏まえ，本研究では，酵素または蛍光発生分子でラベル化したオリゴ核酸（機能性核酸）を用い，細胞内における新規 RNA 蛍光検出技術を開発した。さらに，本法をヒト生細胞内での RNA の可視化へ応用した。

本論文は 7 章より構成されている。以下に各章の概要を述べる。

第 1 章では，細胞内における RNA 検出法，およびこれらの手法に使用される機能性核酸や蛍光色素等に関する既往の知見および問題点，さらに蛍光発生分子のメカニズムや既往の研究に関して有機化学的な観点から概説し，本研究の意義・目的を明らかにした。

第 2 章では，酵素や抗体を用いてシグナルを増幅する，高感度 FISH（Fluorescence *in situ* hybridization）法を細菌細胞に適用し，その問題点を明らかにした。細胞内における RNA には極めて発現量の低い RNA も存在するため，蛍光シグナルを増幅する必要がある。これまでに様々なシグナル増幅手法が開発されてきたが，いずれの手法も酵素や抗体などの高分子を細胞内に浸透させる必要がある。ところが，細菌細胞の細胞壁の性状は菌種によって大きく異なるため，シグナルを得るための細胞壁消化条件に差異が生じる。したがって，複合微生物系にこのような手法を適用する場合，目的とする細菌群を一括して検出できない可能性がある。そこで，細胞壁消化酵素の種類および濃度を変化させた場合における高感度 FISH の検出結果のばらつきについて検討を行った。様々な属に属する 8 菌種を対象とした。各細菌種の細胞壁を細胞壁消化酵素であるリゾチームおよびアクロモペプチダーゼで消化したのち，全真正細菌をターゲットとする EUB338 プローブを用いて FISH, DIG（Digoxigenin）-FISH, CARD（Catalyzed and Reporter Deposition）-FISH を行った。得られた画像においてプローブ由来のシグナルを発している細胞をカウントし，検出可能な割合を算出した。その結果，菌種によるばらつきを抑え細菌を均一に検出するためには細胞壁を 10mg/ml のリゾ

チームで処理し，CARD-FISH 法で検出することが有効であり，この方法でも検出不可能な一部の細菌においては，アクロモペプチダーゼ処理が有効であることを明らかにした。以上の結果より，細菌種間における検出感度のばらつきを定量的に把握し，高感度 FISH 法の細菌細胞への適用における知見を得ることができた。しかしながら，依然として全ての菌種を一括の条件で検出することは困難であり，さらには細胞壁消化酵素による処理により細胞は損傷し，生細胞検出は不可能であるという問題点が残った。

第 3 章では，前述の問題点を解消するため，酵素などの高分子を用いることなくシグナルを増幅することが可能であり，なおかつ生きた状態の細胞を検出することが可能であると考えられる，標的核酸分子を鋳型とした有機化学反応による核酸の蛍光検出法を開発した。これまでに，標的上での消光基の脱離反応を利用した核酸検出法が報告されているが，水溶液中での加水分解によるバックグラウンド蛍光が非常に大きいのが問題であった。そこで本研究では，さらにシグナル／バックグラウンド比を高めて高感度化を図ることを目的として，標的核酸上での酸化還元反応を引き金として蛍光を発生するシステムを開発した。本システムでは，還元を引き金として蛍光を発するローダミンーアジド誘導体を結合したDNAプローブと，還元剤を結合したDNAプローブを合成し，これらが標的上で隣り合うことによって酸化還元反応を起こし，標的核酸を認識することが可能となる。ローダミンーアジド誘導体とは，ローダミンの片側のアミノ基をアジド基に変換した化合物であり，還元剤と反応することにより，アジドがアミンに還元され，共鳴構造が変化することにより吸収スペクトルが変化する。また，この反応によって還元前と比較して約 2000 倍の緑色蛍光を発した。次に，この蛍光分子を DNA プローブに連結し，還元剤（トリフェニルホスフィンおよびジチオスレイトール）を連結した DNA プローブと標的核酸上で反応させた。その結果，標的核酸上での2つのプローブの化学反応に由来する蛍光シグナルが観察された。一方，標的核酸が存在しない場合においてはほとんど蛍光を発さないことから，本蛍光発生システムは優れたシグナル／バックグラウンド比を持つことがわかった。

第4章では，第3章で述べた化合物と同様のメカニズムで赤色蛍光を発する，ナフソローダミンーアジド誘導体を合成した。ローダミンーアジド誘導体と同様に，この化合物は還元剤との反応で共鳴構造が変化することによって吸収スペクトルが変化し，還元前と比べて約 550 倍の赤色蛍光を発した。また，この化合物は，ローダミンーアジド誘導体と同様に，DNA プローブに連結することにより，標的核酸の検出に用いることが可能であった。このように，波長域の異なる 2 種類の蛍光発生分子の合成に成功し，これらを用いることにより，細胞内における 2 種類の RNA 分子を同時に検出する可能性を示した。

第 5 章では，本システムが，細胞内で有効に機能するかどうかを検討するため，ホルムアルデヒド固定した大腸菌細胞内の rRNA の検出を試みた。プローブ配列の設計は，既往の研究を参考に，アクセシビリティーの高い部位を選択した。実際に大腸菌細胞内にローダミンーアジド誘導体およびトリフェニルホスフィンを結合したプローブを導入したところ，完全相補鎖のプローブを用いた場合に強いシグナルが得られたのに対し，スクランブル配列のプローブについてはシグナルが得られなかったことから，本プローブは細胞内においても有効に働くことがわかった。

第 6 章では，第 3 章から第 5 章で述べた，還元を引き金とする蛍光発生メカニズムをさらに発展させるため，フルオレセインーメチルアジド誘導体を合成した。さらに，これを用いてヒト生細胞内メッセンジャーRNA（mRNA）の検出を行った。フルオレセインーメチルアジド誘導体とは，フルオレセインの水酸基をメチルアジド基で保護した化合物であり，アジド基の還元に続く加水分解によってメチルアジド基が脱保護され，蛍光を発する。この化合物はローダミンーアジド誘導体と異なり，ホスフィン分子との結合によるアザイリドの形成がされないため，ターゲット核酸を触媒とした化学反応の回転が期待できる。実際に，試験管内での反応では，等温条件下（37℃）・4 時間で約 50 回の化学反応の回転が見られ，これによって 50 倍の蛍光シグナルの増幅が観察された。このシグナル増幅は，細胞内において低発現量の RNA を検出する場合に，有効になると考えられた。実際に，ヒト白血病細胞 HL60 の 28S rRNA およびベータアクチン mRNA をターゲットとして，フルオレセインーアジド誘導体およびトリフェニルホスフィンを結合したプローブを導入したところ，それらに対応するシグナルが，フローサイトメトリーおよび蛍光顕微鏡下で観察することが可能であった。本法は，酵素などの高分子を用いることなくシグナルを増幅することが可能であることから，生細胞内における低発現の RNA 検出において，有効な手段である。

第 7 章は本論文の総括である。

以上，本研究では，酵素または蛍光発生分子でラベルしたオリゴ核酸（機能性核酸）を用い，新規 RNA 蛍光検出技術を開発した。さらに，蛍光発生システムの改良により化学反応の回転を起こすことによって，生細胞内での低発現 RNA の可視化にも応用できることを明らかにした。以上のことより，本成果は，今後の RNA 研究およびバイオイメージング技術に大いに寄与することが期待される。さらに，フローサイトメトリー・セルソーターと組み合わせることにより，生細胞の選別技術に応用することも可能であると考えられ，微生物学，分子生物学，再生医療学等，様々な分野への応用が期待される。

研究業績

【論文】

(1)(報文)Kazuhiro Furukawa, Hiroshi Abe, Jin Wang, Miwako Uda, Hiroyuki Koshino, Satoshi Tsuneda, and Yoshihiro Ito: Reduction-triggered red fluorescent probes for dual-color detection of oligonucleotide sequences. ***Org. Biomol. Chem.,*** in press

(2)(報文)Kazuhiro Furukawa, Hiroshi Abe, Jin Wang, Kazuma Oki, Miwako Uda, Satoshi Tsuneda, and Yoshihiro Ito: Fluorogenic probe triggered by reduction for nucleic acid sensing. ***Nucleic Acids Symp Ser.,*** **52**, 352-353 (2008).

(3)(報文)Kazuhiro Furukawa, Hiroshi Abe, Naoko Abe, Mitsuru Harada, Satoshi Tsuneda, and Yoshihiro Ito: Fluorescence generation from tandem repeats of a malachite green RNA aptamer using rolling circle transcription. ***Bioorg. Med. Chem. Lett.***, **18**, 4562-4565 (2008).

(4)(報文)Aya Shibata, Kazuhiro Furukawa, Hiroshi Abe, Satoshi Tsuneda, and Yoshihiro Ito: Rhodamine-based fluorogenic probe for imaging biological thiol. ***Bioorg. Med. Chem. Lett.***, **18**, 2246-2249 (2008).

(5)(報文)Hiroshi Abe, Jin Wang, Kazuhiro Furukawa, Kazuma Oki, Miwako Uda, Satoshi Tsuneda, and Yoshihiro Ito: A reduction triggered fluorescent probe for sensing DNA and RNA. ***Bioconjugate Chem.,*** **19**, 1219-1226 (2008).

(6)(報文)Hiroshi Abe, Yuko Kondo, Hiroshi Jinmei, Naoko Abe, Kazuhiro Furukawa, Atsushi Uchiyama, Satoshi Tsuneda, Kyoko Aikawa, Isamu Matsumoto, and Yoshihiro Ito: Rapid DNA chemical ligation for amplification of RNA and DNA signal. ***Bioconjugate Chem.***, **19**, 327-333 (2008).

(7)(報文)Tatsuhiko Hoshino, Kazuhiro Furukawa, Satoshi Tsuneda, and Yuhei Inamori: RNA microarray for estimating relative abundance of 16S rRNA in microbial communities. ***J. Microbiol. Methods***, **69**, 406-410 (2007).

(8)(報文)Kazuhiro Furukawa, Tatsuhiko Hoshino, Satoshi Tsuneda, and Yuhei Inamori: Comprehensive analysis of cell wall permeabilizing conditions for highly sensitive fluorescence *in situ* hybridization. ***Microbes Environ.***, **21**, 227-234 (2006).

(9)(報文)Kazuhiro Furukawa, Naohiro Noda, Satoshi Tsuneda, Takeshi Saito, Tomoaki Itayama, and Yuhei Inamori: Highly sensitive real-time PCR assay for quantification of toxic cyanobacteria based on microcystin synthetase A gene. ***J. Biosci. Bioeng.***, **102**, 90-96 (2006).

【講演(国際会議)】

(1) Kazuhiro Furukawa, Hiroshi Abe, Satoshi Tsuneda, and Yoshihiro Ito: Reduction-triggered fluorescence probe amplifying nucleic acids signal for the detection of intracellular RNAs. 14th Symposium of Young Asia Biochemical Engineer's Community, Tokyo, Japan, 29-1, Sep., 2008, in press

(2) Kazuhiro Furukawa, Hiroshi Abe, Jin Wang, Kazuma Oki, Miwako Uda, Satoshi Tsuneda, and Yoshihiro Ito: Fluorogenic probe triggered by reduction for nucleic acid sensing. Joint Symposium of 18th International Roundtable on Nucleosides, Nucleotides and Nucleic Acids (IRTXVIII) and 35th International Symposium on Nucleic Acids Chemistry (SNAC), Kyoto, Japan, 8-12, Sep., 2008, 352-353

(3) Kazuhiro Furukawa, Hiroshi Abe, Jin Wang, Kazuma Oki, Miwako Uda, Satoshi Tsuneda, and Yoshihiro Ito: Fluorescence detection of nucleic acids triggered by DNA-templated chemical reaction. 235th ACS National Meeting, New Orleans, LA, 6-10, Apr., 2008, MEDI 60

(4) Kazuhiro Furukawa, Hiroshi Abe, Jin Wang, Kazuma Oki, Miwako Uda, Satoshi Tsuneda, and Yoshihiro Ito: Fluorescence activation system triggered by chemical reaction on nucleic acids., The 2nd International Workshop on Approaches to Single-cell Analysis, Tokyo, Japan, 6-7, Sep., 2007, p 52

(5) Kazuhiro Furukawa, Tatsuhiko Hoshino, Satoshi Tsuneda: Quantitative detection of 16S rRNA in a microbial community using RNA microarray. 12th Symposium of Young Asia Biochemical Engineer's Community, Kaohsiung, Taiwan, 25-27, Nov., 2006, p 20

(6) Kazuhiro Furukawa, Tatsuhiko Hoshino, Satoshi Tsuneda: RNA microarray: a novel quantification method in environmental microbiology. The 4th 21COE International Symposium on "Practical Nano-Chemistry", Tokyo, 11-12, Dec., 2006, p 66

(7) Kazuhiro Furukawa, Tatsuhiko Hoshino, Satoshi Tsuneda, Yuhei Inamori: Optimization of the cell wall permeabilizing conditions for highly sensitive fluorescence *in situ* hybridization. 11th International Symposium on Microbial Ecology, Vienna, Austria, 20-25, Aug., 2006, p A112

(8) Kazuhiro Furukawa, Naohiro Noda, Hiroshi Makino, Satoshi Tsuneda, Akira Hirata, Yuhei Inamori: Microbial Community Analysis of Cyanobacteria Based on Microcystin Synthetase A Gene (*mcyA*). The Third International Symposium for Strategies on Toxic Algae Control in Lakes and Reservoirs for Establishment of International Network, Wuxi, CHINA, 25-28, Oct., 2003

【講演(国内)】

(1)長尾厚志, 古川和寛, 大木一真, 烏田美和子, 青井議輝, 阿部洋, 伊藤嘉浩, 常田聡: 遺伝子情報に基づいた微生物生細胞の特異的分離技術の開発, 第 24 回日本微生物生態学会, 札幌, 2008 年 11 月 25 日-28 日

(2)烏田美和子, 古川和寛, 王瑾, 阿部洋, 常田聡, 伊藤嘉浩: 核酸鋳型反応を用いた遺伝子検出, 第 24 回高分子討論会, 大阪, 2008 年 9 月 24 日-26 日

(3)古川和寛, 阿部洋, 戸田雅也, 常田聡, 伊藤嘉浩: 化学反応を引き金とする蛍光発生分子による細胞内 RNA 検出, 化学工学会第 40 回秋季大会, 仙台, 2008 年 9 月 24 日-26 日

(4)阿部洋, 古川和寛, 王瑾, 大木一真, 烏田美和子, 常田聡, 伊藤嘉浩: 新規蛍光化合物を導入した化学反応プローブによる遺伝子シグナルの増幅, 第 3 回バイオ関連化学合同シンポジウム, 横浜, 2008 年 9 月 18 日-20 日

(5)古川和寛, 阿部洋, 戸田雅也, 常田聡, 伊藤嘉浩: 還元反応を引き金とする蛍光発生分子による遺伝子シグナル増幅システム, 日本ケミカルバイオロジー研究会　第3回年会, 東京, 2007 年 5 月 19 日-20 日

(6)古川和寛, 阿部洋, 戸田雅也, 常田聡, 伊藤嘉浩: 還元反応を引き金とする蛍光発生プローブによる遺伝子シグナルの増幅, 日本化学会第 88 春季大会, 東京, 2008 年 3 月 26 日-30 日

(7)烏田美和子, 古川和寛, 柴田綾, 戸田雅也, 阿部洋, 常田聡, 伊藤嘉浩: 標的遺伝子上で赤色蛍光を発する新規蛍光プローブの合成, 日本化学会第 88 春季大会, 東京, 2008 年 3 月 26 日-30 日

(8)原田充, 阿部奈保子, 古川和寛, 阿部洋, 常田聡, 伊藤嘉浩: 化学修飾したダンベル型ナノサークル RNA を用いた RNA 干渉法の検討, 日本化学会第 88 春季大会, 東京, 2008 年 3 月 26 日-30 日

(9)柴田綾, 阿部洋, 古川和寛, 常田聡, 伊藤嘉浩: 遺伝子情報に基づいた新規分子リリースシステムの構築, 日本化学会第 88 春季大会, 東京, 2008 年 3 月 26 日-30 日

(10)阿部洋, 王瑾, 古川和寛, 烏田美和子, 戸田雅也, 常田聡, 伊藤嘉浩: 新規蛍光化合物の合成と遺伝子検出への応用, 第 22 回生体機能関連化学シンポジウム, 仙台, 2007 年 9 月 28 日-29 日

(11)古川和寛, 阿部洋, 王瑾, 大木一真, 烏田美和子, 常田聡, 伊藤嘉浩: 新規蛍光化合物を用いた遺伝子検出技術の開発, 第 59 回生物工学会大会, 広島, 2007 年 9 月 25 日-27 日

(12)古川和寛, 阿部洋, 王瑾, 大木一真, 烏田美和子, 常田聡, 伊藤嘉浩: 有機化学反応を引き金とする蛍光発生システムの開発と核酸検出への応用, 日本化学会第 10 回バイオテクノロジー部会シンポジウム, 東京, 2007 年 9 月 5 日-6 日

(13)内山敦史、古川和寛、阿部洋、神明博、常田聡、伊藤嘉浩: 化学反応DNAプローブによる遺伝子検出, 日本化学会第 87 春季大会, 大阪, 2007 年 3 月 25 日-28 日

(14)古川和寛, 阿部洋, 常田聡, 伊藤嘉浩: ローリングサークル転写反応を用いた蛍光発生 RNA アプタマーの増幅による核酸検出, 日本化学会第 87 春季大会, 大阪, 2007 年 3 月 25 日-28 日

(15)古川和寛, 星野辰彦, 常田聡: RNA Microarray を用いた環境微生物の定量技術の開発,化学工学会第 38 回秋季大会, 福岡, 2006 年 9 月 15 日-18 日

(16)野田尚宏, 古川和寛, 常田聡, 稲森悠平: 環境中における microcystin 産生藍藻類の定量的解析, 化学工学会第 72 年会, 東京, 2006 年 3 月 30 日

(17)古川和寛, 野田尚宏, 常田聡, 稲森悠平: Microcystin 合成遺伝子を指標とした湖沼における藍藻類の毒素産生能の定量評価, 第 40 回日本水環境学会, 仙台, 2006 年 3 月 15-17 日

(18)古川和寛, 星野辰彦, 常田聡, 稲森悠平: 水処理プロセスに関与する微生物に高感度 FISH を適用するための最適細胞壁消化条件の解析, 日本水処理生物学会第 42 回大会, 静岡, 2005 年 11 月 23 日-25 日

(19)古川和寛, 星野辰彦, 常田聡, 稲森悠平: の細胞壁構造の違いを考慮した高感度 FISH 操作条件の検討, 日本生物工学会平成 17 年度大会, つくば, 2005 年 11 月 15 日-17 日

(20)星野辰彦, 古川和寛, 常田聡, 稲森悠平: 高感度 FISH を様々な細菌に適用する際の細胞膜消化条件の検討, 第 21 回日本微生物生態学会, 福岡, 2005 年 10 月 30 日-11 月 2 日

(21)古川和寛, 星野辰彦, 常田聡, 平田彰, 稲森悠平: 環境微生物の高感度 in situ 検出における問題点, 化学工学会第 37 回秋季大会, 岡山, 2005 年 9 月 15 日-17 日

(22)古川和寛, 星野辰彦, 常田聡, 平田彰, 稲森悠平: 細胞内機能遺伝子の in situ 検出手法の体系化, 化学工学会関東支部 50 周年記念大会, 東京, 2005 年 8 月 4 日-5 日

(23)古川和寛, 星野辰彦, 常田聡, 平田彰, 稲森悠平: 高感度 FISH の水処理生態系への適用における課題, 第 39 回日本水環境学会, 千葉, 2005 年 3 月 17-19 日

(24)古川和寛, 常田聡, 平田彰, 野田尚宏, 稲森悠平: Real-Time PCR 法を用いた有毒藍藻類の迅速定量解析手法の開発, 第 41 回日本水処理生物学会, つくば, 2004 年 11 月 10-12 日

(25)古川和寛, 常田聡, 平田彰, 野田尚宏, 稲森悠平: Real-Time PCR 法を用いた有毒藍藻類の迅速モニタリング技術の開発, 平成 16 年度日本生物工学会, 名古屋, 2004 年 9 月 21-23 日

(26)稲森悠平, 古川和寛, 金子直哉, 野田尚宏, 常田聡, 平田彰: 有毒藍藻類の迅速モニタリング手法の開発ーアオコ発生予測に向けてー, 第 38 回日本水環境学会, 札幌, 2004 年 3 月 17-19 日

(27)稲森悠平, 古川和寛, 金子直哉, 牧野博, 野田尚宏, 常田聡, 平田彰: ミクロシスチン合成遺

伝子に基づく, 湖沼における有毒藍藻類の評価･解析, 第 40 回日本水処理生物学会, 熊本, 2003 年 11 月 19-21 日

【著書･著作物】

（1）長尾厚志，古川和寛，“FISH から FISHing へ　―化学反応プローブを釣り針とした微生物生細胞セレクション―（リサーチ最前線）”，日本微生物生態学会誌，日本微生物生態学会，印刷中

（2）阿部洋，古川和寛，常田聡，伊藤嘉浩，“細胞内遺伝子シグナルの解析”，生物工学，日本生物工学会，268-270, (2008)

（3）阿部洋，古川和寛，常田聡，伊藤嘉浩，“細胞内 RNA 可視化のためのバイオプローブ”，ケミカルバイオロジー，蛋白質核酸酵素 増刊，共立出版，1619-1624, (2007)

（4）阿部洋，古川和寛，常田聡，伊藤嘉浩，“細胞内遺伝子発現検出用の蛍光バイオプローブの設計と合成”，一細胞定量解析の最前線 - ライフサーベイヤ構築に向けて，シーエムシー出版, 135-146, (2006)

【特許】

（1）特願 2007-239234: 阿部洋，伊藤嘉浩，古川和寛: 蛍光発生分子

（2）特願 2007-104938: 阿部洋，古川和寛，伊藤嘉浩，曽家義博，氏内圭一: 核酸の検出方法

（3）特願 2006-341245: 阿部洋，伊藤嘉浩，王瑾，古川和寛: 蛍光発生分子

謝辞

本研究ならびに本論文の作成は，早稲田大学大学院理工学研究科応用化学専攻常田研究室にて行われました。研究を進めるにあたりお世話になった方々へこの場を借りて感謝の意を表します。

本研究を進めるにあたり，終始温かくご指導下さいました早稲田大学理工学研究科生命医科学科常田聡教授に心から深く感謝いたします。

本研究をまとめるにあたり，早稲田大学理工学研究科応用化学科の酒井清孝教授，平沢泉教授，ベルリン・フンボルト大学化学科の Oliver Seitz 教授の諸先生方には，副査の立場から貴重な御教示と御助言を頂きました。厚く御礼申し上げます。

理化学研究所・伊藤ナノ医工学研究室研究員の阿部洋博士には，実質的な研究の進め方から日々の研究活動に至るまで，常に貴重なご指導をいただき，親身になって研究生活を支えて頂きました。謹んで感謝申し上げます。

理化学研究所・伊藤ナノ医工学研究室主任研究員の伊藤嘉浩博士，国立環境研究所・バイオエコエンジニアリング研究室長の稲森悠平博士（現・福島大学教授），産業技術総合研究所生物機能工学研究部門研究員の野田尚宏博士，早稲田大学理工学研究科助手の星野辰彦博士（現・日本学術振興会特別研究員）には，研究に対するフィロソフィーから論文の作成法まで，大変貴重な御指導を頂きました。心より感謝申し上げます。

理化学研究所・佐甲細胞情報研究室の佐甲靖志博士，日比野佳代博士には，蛍光イメージングに関する有意義なご助言と力強い励ましを頂きました。

理化学研究所秘書の玉井智子さん，武内礼子さん，矢崎弥栄子さんをはじめとする伊藤ナノ医工学研究室の皆様には,日々の研究の遂行に当たり,多大なご協力と激励を頂きました。

理化学研究所にて研究生活を共にした，王瑾博士，柴田綾博士，戸田雅也博士，劉明哲博士，和田章博士，大木一真氏，長尾厚志氏，内山敦史氏，原田充氏，阿部奈保子さん，近藤裕子さん，烏田美和子さん，伊藤美香さんには，公私ともに多大なるご助力と励ましを頂きました。

常田研究室秘書の武野弘子さん，青井議輝博士，吉江幸子博士，寺田昭彦博士，近藤貴志博士，岸田直裕博士，大坂利文博士，寺原猛博士，谷英典博士，足立賢氏，松本慎也氏をはじめとする常田研究室の皆様には，日々の研究の遂行に当たり，温かい励ましや，大変有意義な意見を頂きました。

こうした皆様をはじめとする，様々な方々の協力と助力によって本研究を無事成就することができました。改めて心から厚く感謝申し上げます。

尚，本研究の一部は，理化学研究所（ジュニア・リサーチ・アソシエイト）および日本学術振興会（特別研究員 DC2）の支援を受け遂行されました。深く御礼申し上げます。

最後に，常に私の行動を温かく見守り，惜しみなく援助して下さった両親に，心から厚く御礼申し上げます。

2009 年 2 月

古川　和寛